NTNU

Norwegian University of
Science and Technology

Energy Utilization in EDC Cracking

Stine Karlsen

Summary

The exergy losses in the thermal cracking of 1,2-dichloroethane (EDC) have been investigated for the EDC cracker in INEOS' vinyl chloride monomer (VCM) plant at Rafnes in Norway. This process section is the most energy demanding section in the plant, and an overview of the distribution of exergy losses was desired as part of the work for reducing energy consumption.

The investigations were based on the results of established mass and energy balances for the process section in Aspen Plus. Calculations were done in a spreadsheet.

Exergy balances were computed for a base case simulation. Different tests that were developed to investigate different modification's effect on exergy losses.

The total exergy losses in the EDC cracking section were found to be 59.5 MW, or 3362 kJ/kg VCM. The largest exergy losses in the process section were located in the cracker unit. The internal losses in the cracker dominated and accounted for 75 % of all the internal exergy losses in the process section. The rest of the noticeable exergy losses were discovered in the heat exchangers in the top system.

Preheating the EDC feed and the combustion air was found to give the largest reductions in the cracker exergy losses. This test shows a reduction in fuel gas needs of 6.6 %. Reduction in excess combustion air on the other hand showed no noticeable reductions. Fouling in H1406 and unnecessarily large amounts of excess air under normal conditions both result in large increases in exergy losses, and should be avoided if possible.

Preface

This report is the result of the Master Thesis (TKP 4900 Chemical Process Technology). The work has been conducted during the period January to June 2011. The work was carried out in cooperation with INEOS ChlorVinyls Technology & Production Support in Porsgrunn and the Department of Chemical Engineering at NTNU.

I would like to thank my supervisor at NTNU, Magne Hillestad, and my co-supervisor Torbjørn Herder Kaggerud at INEOS for all their help and guidance throughout this project. I would also like to thank Rebecca Williams for her proof writing and social coffee breaks. Finally a special thanks to my little sis who read the entire report even though she only understood bits and pieces.

I declare that this is an independent work according to the exam regulations of the Norwegian University of Science and Technology.

Trondheim, 09.06.2011

Stine Karlsen

List of Symbols

Symbol	Denomination	Description
B	J	Exergy
E	J	Energy
ΔG_f^0	J	Gibbs free energy of formation
g_E	m/s^2	Gravitational acceleration
h	J/mol	Molar enthalpy
I	J	Exergy destruction term
L	mol/s	Liquid molar flow
m	kg/s	Mass flow
P	Pa	Pressure
Q	J	Heat
R	J/mol K	Gas constant
s	J/mol K	Molar entropy
T	K	Temperature
V	mol/s	Gaseous molar flow
W	J	Work
x	-	Molar fraction in liquid phase
y	-	Molar fraction in gas phase
Z	m	Hight
ν	-	Number of a element in a compound

Subscripts		
0		Reference conditions
1,2,3		Specified state
Ch		Chemical
el		Element
i		Property of the i-th component
K		Kinetic
m		Molar
P		Potential
Ph		Physical
Ref		Reference case

Superscript	
Q	Heat exergy
$\cdot$	Flow

Abbreviation	
EDC	Ethane 1,2-dichloride
VCM	Vinyl chloride monomer
HCl	Hydrogen chloride
PVC	Poly vinyl chloride
CWS	Cooling water supply
CWR	Cooling water return
IPS	Intermediate pressure steam
IPC	Intermediate pressure condensate
LPS	Low pressure steam
LPC	Low pressure condensate
HPF	High pressure flushing
RAI	Relative avoided irreversibility
RATI	Relative avoided total irreversibility

Contents

1 Introduction

The chemical industry is facing two challenges concerning their current energy usage. Firstly most energy is supplied by fossil fuels, which is a limited resource steadily increasing in price. Secondly the CO_2 created by this fuel is a known greenhouse gas, and increasingly strict regulations are put on emissions of such gasses. It is therefore beneficial for the industry to work for a reduction in their energy requirements. The exergy method is an acknowledged procedure for investigating the energy utilization in order to discover potentials for improvement.

It was discovered early on that a mere energy analysis based on the first law of thermodynamics did not give enough information about the energy efficiency of a process. The second law needed to be a part of the consideration as well, to determine the quality of the energy lost. An energy analysis will typically show large losses of energy by the discharge of used cooling water to the environment. The exergy analysis will find small losses in the same case, as the temperature of the cooling water is too low to be of any particular use. The concept of exergy has become more and more acknowledge over the years, and is today applied in many different fields of engineering. Sciubba and Wall [2007] gives a comprehensive summary of the history of exergy. Some of the major events are presented below.

The exergy concept had its starting point in the last part of the 19th century when scientists like Carnot, Gibbs and Clapeyron did research which in the end resulted in the formulation of the second law of thermodynamics, and lay the foundation for thermodynamics as a field. Gibbs even recognized the idea of available work. Gouy and Stodola independently developed what later is known as the Gouy-Stodola theorem at the start of the 1900s. During the first part of the 20th century, the different components of the exergy method took shape, and most of the possibilities for use, and the problems with the method, recognised.

In 1953 Rant introduced the word *Exergy* as a proposed name for the concept which earlier had been described by many different names (available, work, useful work, availability etc). Exergy was a development from the Greek words which gave energy its name - *en* and *ergon* which together means "internal work". By exchanging the *en* with *ex* (outwards), the word exergy took form. The use of this expression has spread to most of the scientific world, but still today some use "availability".

At the end of the 1960's most of the theory in exergy was complete, but few attempts had been made at practical application of the method. This changed in the 1970s among other things as a consequence of the oil crisis in 1973. Increased energy efficiency was suddenly a top priority. The remaining limited amount of fossil raw materials and fuels makes this a current problem as well. The development in the field the last four decades has been formidable, and today there is even a journal dedicated merely to exergy.

An important branch of the exergy concept that is worth mentioning, even though it has not been relevant for this project, is thermoeconomics. This is the combination of elements from the exergy method and economic analysis. The concept is, among other things, used to evaluate different process solutions and to do the final optimization of a process. This

is easily done by combining simulation software, which makes modeling and comparing of processes quick and easy, and additional economic models in spreadsheets, as presented in Querol et al. [2011].

In earlier days vinyl chloride monomer (VCM) was produced by reacting acetylene and hydrogen chloride [Blindheim]. China is the only country that still uses this method as they have a large abundance of cheap coal from which they can produce acetylene [pvc.org]. Today most producers use the balanced process producing VCM from ethylene and chlorine via ethane 1,2-dichloride (EDC). A description of this process is given in Section 2. Acording to McPherson et al. [1978] 96 % of the world's production of VCM goes in as raw material for the production of polyvinyl chloride (PVC). PVC is the world's second most used polymer, with polyethylene as number one [Ore and Stori].

INEOS is currently the third largest chemical company in the world and through INEOS ChlorVinyls they are the largest PVC producer in Europe. In 2007 INEOS bought the chemical production at Rafnes and the PVC plant at Herøya, Porsgrunn from Hydro Polymers. The Rafnes site consists of an ethylene plant, a chlorine plant and a VCM plant. Production at Herøya started in 1951 and at Rafnes in 1978. Improvements to the VCM plant were done several times during the 80's and 90' to increase production. Today the VCM factory produces approximately 515 000 tonnes per year. The produced VCM is split between being transported under the Frier fjord to the PVC plant and being shipped out to internal and external costumers.

EDC cracking is the most energy consuming part of the modern VCM process, and any reduction in the energy consumption in this section would give large economical profits. It is therefore of interest to investigate this energy consumption and its distribution over the process section to examine how any reductions can be made. The investigation of the energy efficiency in the EDC cracking section in INEOS' VCM plant at Rafnes is the purpose of this project.

In the project an exergy analysis is preformed on the EDC cracking section. Further test simulations are completed in order to investigate ways to reduce the energy usage in the section. The results from the original exergy analysis are used as a basis for this investigation, and the reduction of exergy losses are checked by exergy analyses of each test. It was decided together with the supervisors to carry out these tests in stead of the pinch analysis. The report starts off with a presentation of the VCM process and the relevant theory for this project. A description of the simulations and calculations follows, together with the results and a discussion of these.

This project is founded on a project completed in the autumn of 2010. In the previous project an Aspen Plus model of the process section was established, and this model is the basis for the exergy analyses in this project. A summary of the previous simulation work is presented in the report, with further details in the Appendices.

2   Process Description

A simple overview of the balanced VCM process is given before a more extensive description of the EDC cracking section at Rafnes is presented. This presentation is the same as the one given in the report for the previous project [Karlsen, 2010], but a thorough process description is found necessary for the proper understanding of the present work.

2.1   An Overview of the Balanced VCM Process

The VCM process at Rafnes is a balanced ethylene process. The feed stock is chlorine, ethane and air. Figure 1 shows the general flow scheme of the process. The process can be divided into five areas: The direct chlorination, the oxychlorination, the purification of EDC, the thermal cracking of EDC and the purification of VCM.
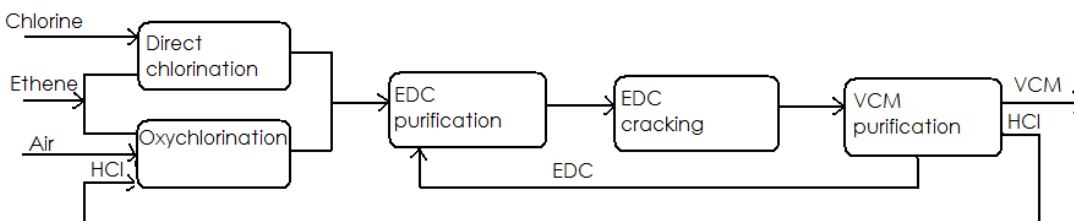
Figure 1: Block diagram for the balanced VCM process

The direct chlorination reaction of ethylene follows Equation 1.

$$\text{Ethene} + \text{Cl}_2 \rightarrow \text{EDC} \tag{1}$$

The oxychloration reaction of ethylene with hydrogen chloride (HCl) and oxygen is shown in Equation 2. Copper chloride is used as catalyst for this reaction [McPherson et al., 1978]. At Rafnes air is the source of oxygen in the process. The HCl is produced as a byproduct in the cracking of EDC.

$$\text{Ethene} + 2\text{HCl} + 0.5\text{O}_2 \rightarrow \text{EDC} + \text{H}_2\text{O} \tag{2}$$
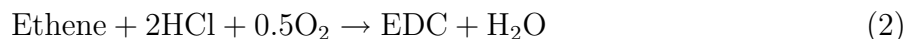
The EDC needs to be purified before the cracking, since impurities will affect the cracking reactions. EDC recycled from the cracking section is also purified before returning to the cracker. After purification, the process stream contains over 99.5 % pure EDC [McPherson et al., 1978]. The main reaction in the thermal cracking of EDC is given by Equation 3.

$$\text{EDC} \rightarrow \text{VCM} + \text{HCl} \tag{3}$$

After the cracking, the unconverted EDC, the product stream is quenched and the produced HCl and the by-products are separated from the VCM. The VCM is purified to product

quality, HCl is fed to the oxychloration reactor and EDC is recycled.

The balanced process has its name from the following concept: The production of HCl in the cracking section is such that it equals the amount needed in the oxychlorination. The result is that the overall mass balance of HCl is zero [McPherson et al., 1978].

2.2   The Cracking Section

The cracking of EDC takes place at approximately 500 ℃ and 20-25 barg, where about 60 % of the EDC is converted [Tarragon]. The products are mainly VCM and HCl, as described by Equation 3, but by-products like butadiene, acetylene, trichloroethane and heavier components are also produced. Coke deposits on the walls of the cracker, giving an increase in pressure drop and a lowering of heat transfer coefficient over time. As a consequence the cracker needs to be decoked every nine to twelve months. The rate of coke formation depends on a number of factors. Most important are temperature, EDC conversion and feed impurities.

The EDC cracking is endothermic. Reaction (3) has a reaction enthalpy of 71 kJ per mol. The heat, which is used to drive the reaction, is supplied by the combustion of fuel gas. At Rafnes, the fuel gas mainly consist of hydrogen (approx. 70 mol%) and methane (approx. 30%).

In the following process description the equipment is assigned a letter and a serial number equal to the equipment names at Rafnes. T, V, F, C, H, P, X indicates tank, vessel, furnace (cracker), column, heat exchanger, pump and refrigerant cycle respectivly.

Battery limit for this project is the storage tank for dry EDC (T2702) at the start and the HCl distillation column (C1501) at the end. EDC from the storage tank is transported to the cracker feed drum (V2704) by a pump, P2703. Both these tanks are at atmospheric pressure. EDC is then pumped up to a pressure of between 25 and 38 barg by feed pump P1405, and a small stream of High Pressure Flushing (HPF) is withdrawn. The HPF is used to flush the bottom valves of the quench towers where heavy by-products have a tendency to clog the valves. The HPF is also injected into the hot side of heat exchangers H1401 and H1406 to help the stream reach its dew point at the inlet.

The rest of the EDC is heated in H1406 by the hot effluent from the top of the quench tower. It is heated up to the cracker inlet temperature and then split into three equal streams entering the parallel crackers (F1401 A,B,C), adiabatic reactors (F1401-AR A,B,C) and quench towers (C1401 A,B,C). The EDC is further split between the two coils of the crackers. The EDC is still liquid when it enters the convection zone at top of the cracker. It is heated to its boiling point by hot flue gas as it passes down through the cracker. It then enters the shock zone where the evaporation takes place. When the gas reaches the bottom of the cracker, it enters the reaction zone which is the hottest zone. The major part of the cracking takes place in this zone. The products exit the cracker and enter the adiabatic reactor where the heat in the gas drives the reaction even further.

The product gas is quenched by cold reflux fluid in the quench towers C1401 A,B,C. The towers contains seven trays which are there to stop coke and other heavy by-products from following the product gas. The gas leaves at the top of the tower and enters the top system. The top system consists of a series of coolers and flash tanks that bring down the temperature of the product gas and starts a coarse separation of the components, taking some load of the following HCl column, C1501.

The gas first passes through cooler H1401 where some of it condenses. The heat from the gas is used to produce low pressure steam at approximately 3 barg. The condensed gas goes to a reflux tank, V1406. The gas enters H1406 where more of the gas will condense as it is used to heat the cracker feed. The condensate is gathered in vessel V1406, while the gas continues through cooler H1402 to flash tank V1401. At high production, reflux fluid can also be supplied from this tank. The reflux is pumped from V1406 to the three quench towers by pump P1404.

The liquid from V1401 enters C1501 at the appropriate tray. The gas is further cooled by H1405 and the two-phase exit stream is separated in flash tank V1404. Both H1402 and H1405 are cooled by cooling water. The liquid from V1404 enters C1501 directly while the gas is first heat exchanged with the HCl feed to the oxychlorination reactor. The pressure in the EDC cracking section is controlled by the pressure in the HCl column.

From the bottom of the quench tower, liquid is taken out in pulses. The liquid flow from each tower equals 3-4 tonnes per hour, and binging coke and other heavy by-products with it. The liquid contains mainly EDC, but also some VCM and HCl. It is desirable to recover VCM and HCl, and the recovery is done in two flash tanks. The pressure is let down 6-7 bar over a valve, and is heated by intermediate pressure steam (IPS) in H1407 before it enters the first tank, V1402. The gas enters C1501, while the pressure in the liquid is let down as far as possible over a second valve before it enter the second flash tank (V1403). The liquid from V1403 is sent to a vacuum column (C1303) in the process section for EDC purification. The gas is condensed by the coolers H1451 and H1404 before it is pumped into C1501 by P1403. H1451 is cooled by cooling water and H1404 is cooled by a refrigerant.

A flow scheme of the process section is given in Figure 2.
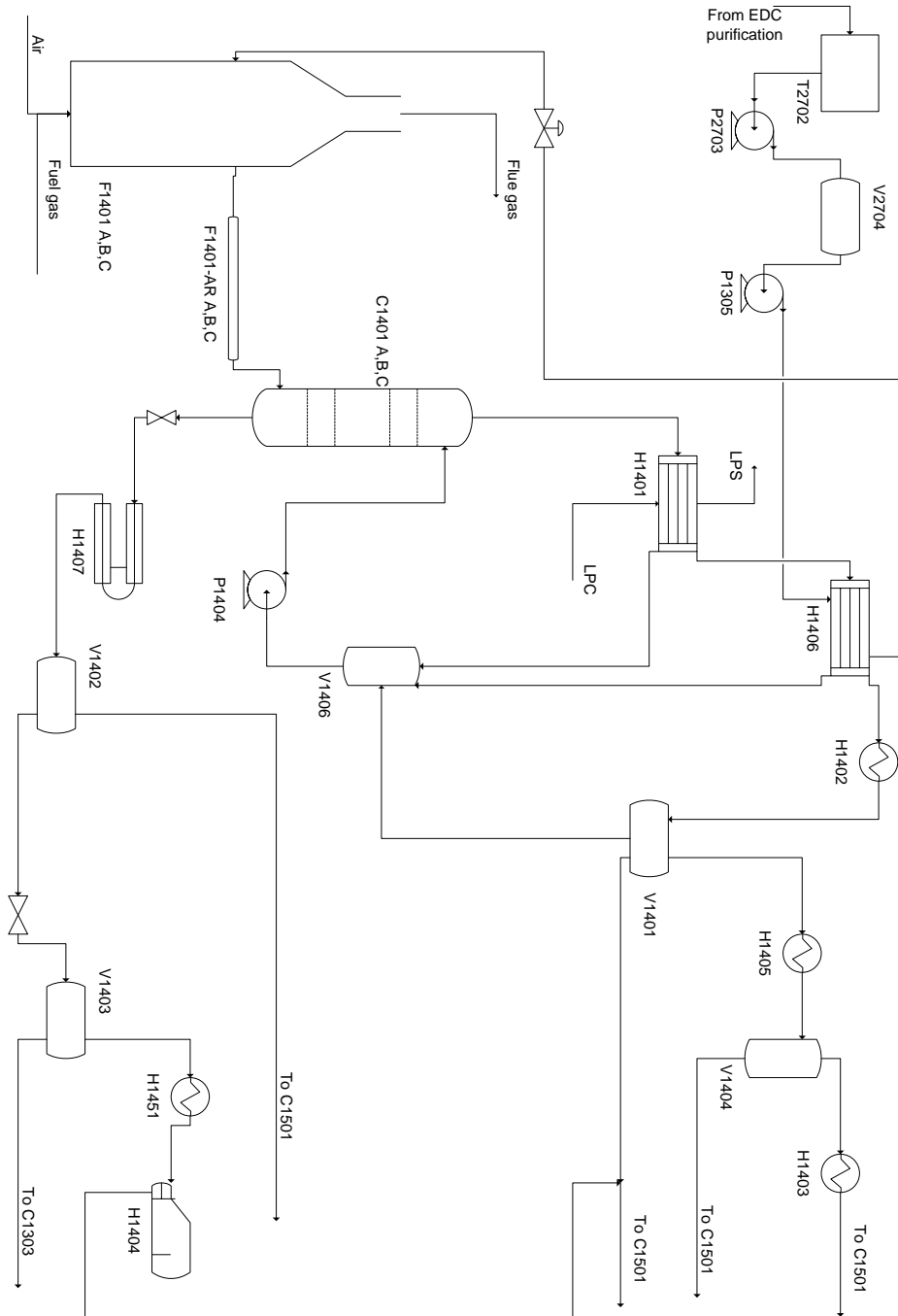
Figure 2: A flow scheme over the EDC cracking section.

3 Theory

3.1 The First and Second Law of Thermodynamics

The first law of thermodynamics is also known as the law of energy conversion. Graveland and Gisolf [1998] expresses it in the following familiar way:

> Energy can neither be destroyed nor created.

This law is the basis for energy balances much used in analysis of chemical processes, and can be expressed in a general form for a system as

$$Q - W = \Delta E \tag{4}$$

where E in most normal cases includes internal, kinetic and potential energy. W denotes work and Q heat. Heat transferred *to* the system and work done *by* the system are defined as positive in this project.

A simple energy balance says little of the quality of the energy in the system, and how the energy changes quality through the system. To include this in the analysis the second law of thermodynamics is needed. The second law has been presented in many different ways, all essentially saying the same. In Kotas [1995] this law is expressed as follows:

> There is an extensive property of a system called entropy, S. The entropy of an isolated system can never decrease.

Auracher [1984] defines the second law in connection to exergy and exergy losses:

> If a process was reversible, the exergy would remain constant; if it was irreversible, some exergy would be consumed and lost forever.

3.2 Irreversibility

The definition of reversibility is a result of the second law. A reversible process is an ideal process were both the process system and its surroundings can be returned to its initial state. All real processes are irreversible to some degree, and as the second definition of the second law expresses; this leads to exergy losses and a less efficient process. The first definition of the second law indicates that all irreversibilties are connected to entropy production. Moran and Shapiro [2010] lists some sources of irreversibility commonly mentioned in connection with exergy losses:

- Heat transfer at a finite temperature difference

- Spontaneous chemical reactions

- Mixing of streams at different state or composition

- Unrestrained expansion of gas or liquid to a lower pressure

3.3   Exergy

Exergy is a method developed to consider the changes in energy quality through a system. The exergy method looks at the difference between the process and a reference environment to see the maximum theoretical useful work obtainable when a system is brought into thermodynamic equilibrium with the environment by means of processes in which it interacts only with the environment [Sciubba and Wall, 2007]. By the definition of the second law, the exergy change through a system can never be negative.

3.3.1   Definitions

As Kotas [1995] writes, the environment is a concept which is peculiar for the exergy method. The environment is assumed to be in perfect thermodynamic equilibrium and among other things operating as a thermal reservoir (a body with very large heat capacity which's temperature will be unaffected by any heat transferred to it). The choice of reference environment has been discussed by many sources, especially in relation to determination of chemical exergy. More about this issue will therefore be presented in Section 3.3.6. The reference environment used for the exergy calculations is often taken as the average temperature (T_0) and pressure (P_0) in the area around the plant.

As presented above, equilibrium is an important part of the exergy method. Two equilibrium states are defined in connection with this method; the environmental state and the dead state. In the environmental state the system is in thermal and mechanical equilibrium with the environment. In the dead state the system is in total equilibrium with the environment, namely thermal, mechanical *and* chemical equilibrium. When in the dead state, no more work can be extracted from the system.

3.3.2   Exergy Balance

The exergy entering an open system can come from three different sources; work (W), heat (B^Q) and stream of matter ($\dot{B}$). Some exergy is destroyed throughout any process, as no real process can be run reversibly. Since exergy is not a conserved size, a destruction term ($\dot{I}$) must be included in the exergy balance. The resulting exergy balance for an open system is give by Equation 5.

$$\sum \dot{B}_{i,in} + \dot{B}^Q = \sum \dot{B}_{i,out} + \dot{W} + \dot{I} \tag{5}$$

According to its definition, exergy is work ($\dot{W}$), thus work is entered directly into Equation 5. $\dot{B}_i$ is the stream exergy in stream i. Transferred heat ($\dot{B}^Q$) is given by Equation 6.

$$\dot{B}^Q = \dot{Q}_r(1 - \frac{T_o}{T_r}) \tag{6}$$

The destruction term can also be calculated from the rate of entropy production, $\dot{S}$, using the Gouy-Stodola theorem, given by Equation 7.

$$\dot{I} = T_0 \dot{S} \tag{7}$$

3.3.3   Stream Exergy

The exergy of a process stream can be further divided. Equation 8 shows the most important terms to consider in a chemical process.

$$\dot{B} = \dot{B}_{Ph} + \dot{B}_{Ch} + \dot{B}_K + \dot{B}_P \tag{8}$$

$\dot{B}_{Ph}$ denotes the physical exergy, $\dot{B}_{Ch}$ the chemical exergy and $\dot{B}_K$ and $\dot{B}_P$ denote the kinetic and potential exergy respectively. Other terms may also be included for more special processes where the system is affected by electromagnetism or other forces.

3.3.4   Kinetic and Potential Exergy

Kinetic and potential exergy are given by Equation 9 and Equation 10 respectively, where $\dot{m}$ is mass, C_0 is velocity, g_E is gravitational acceleration and Z_0 is height above reference level [Kotas, 1995]. Both kinetic and potential energy are ordered forms of energy, and therefore directly convertible to work.

$$\dot{B}_K = \dot{m}\frac{C_0^2}{2} \tag{9}$$

$$\dot{B}_P = \dot{m}g_E Z_0 \tag{10}$$

3.3.5   Physical Exergy

The physical, or thermomechanical, exergy of a stream of matter is the maximum amount of work that theoretically can be extracted from the stream as it is brought to the environmental state (T_0, P_0) by reversible processes which interacts only thermally with the environment. Equation 11 expresses this mathematically. Enthalpy and entropy are denoted by h and s respectively and T is temperature. The subscript zero indicates environmental conditions while other subscript numbers indicates states different from the environmental state.

$$B_{Ph,m} = (h_1 - h_0) - T_0(s_1 - s_0) \tag{11}$$

The change in exergy for a stream passing through a process section is given by Equation 12.

$$B_{Ph,m,2} - B_{Ph,m,1} = (h_2 - h_1) - T_0(s_2 - s_1) \tag{12}$$

The physical exergy can be separated into a thermal and a pressure component, emerging from a division of the reversible process into an isobaric ($B^{\Delta T}$) and an isothermal ($B^{\Delta P}$) sub-process. These two processes are expressed by Equations 13 and 14 [Kotas, 1995]. At isobaric

conditions, the physical exergy will increase again when the temperature passes below the reference temperature, as work is needed to obtain this low temperature. The temperature term of physical exergy is therefore always positive [Szargut, 2005]. This is emphasized as it is relevant for several streams in this project.

$$B_{1,m}^{\Delta T} = \left[-\int_{T_1}^{T_0} \frac{T - T_0}{T} dh \right]_{P_1} \tag{13}$$

$$B_{1,m}^{\Delta P} = T_0(s_0 - s_i) - (h_0 - h_i) \tag{14}$$

3.3.6   Chemical Exergy

The chemical exergy is the maximum amount of work that can be extracted through reversible processes bringing the stream of matter from the environmental state to the dead state by only interacting with the environment thermally and through exchange of chemical components. The calculation of chemical exergy is not as straight forward as for the physical exergy.

Several methods have been presented over the years, and a large part of the differences centers on the definition of the reference environment. The real environment is not in equilibrium since there is a constant supply of energy to the earth from the sun. The determination of equilibrium concentrations of chemical components of the environment is therefore challenging, and different approaches have been developed.

Gallo and Milanez [1990] presents some of the approaches. The main difference is between either defining the environment for each problem or defining a standard environment. There have also been attempts in developing an equilibrium environment containing the atmosphere, the ocean and the earth's crust and by that including all the chemical components on earth and their chemical equilibrium.

The first approach is easy to use as long as all chemical components included in the system exist only in the atmosphere. For a system including components from the ocean or the earth's crust the computations become more challenging. The second approach is therefore the one that seems to be the most employed in the analyses presented in the literature. Szargut [1988] defines a standard environment with specified pressure, temperature and chemical composition. From this system standard chemical exergies for the elements have been tabulated, and the calculation of chemical exergy for chemical components is very simple, as presented by Equation 15. ΔG_f^0 is the Gibbs free energy of formation, ν_{el} is the number of a element in a compound and $B_{el,m}$ is the standard chemical exergy of the element. This is the approach used in this project, and the only one that will be described further.

$$B_{Ch,m} = \Delta G_f^0 + \sum \nu_{el} B_{el,m} \tag{15}$$

Updated values for standard chemical exergies for the elements are given in Rivero and Garfias [2006] for 298.15 K, 101.325 kPa, relative humidity of 0.7, 345 ppm in volume CO_2 and seawater salinity of 35 ‰ (older data can be found in for instance in Szargut [1988] and Kotas [1995]). Air has a chemical exergy of zero by definition. For reference environments at other temperature, pressures and relative humidities the standard chemical exergies can be corrected according to Equation 16 [Ertesvåg, 2007]. For further explanation of Equation 16 the reader is referred to Ertesvåg [2007].

$$B_{Ch,i,m} = B_{Ch,i,m}^{ref} \frac{T_0}{T_{ref}} + \frac{T_{ref} - T_0}{T_{ref}}(-\Delta H^{ref}) + W_1 + W_2 + T_0 R \sum_{j \neq i} \nu_j \ln \frac{X_j^{ref}}{X_j^e} \tag{16}$$

For streams containing a mixture of components and phases, Equation 17 can be used to calculate the chemical exergy of the stream assuming ideal gas [Xiang et al., 2004].

$$B_{Ch,mix} = L \sum x_i B_{Ch,i,m} + V(\sum y_i B_{Ch,i,m} + T_0 R \sum y_i \ln y_i) \tag{17}$$

3.3.7 Exergy Efficiency

The exergy efficiency is defined as the ratio between the usable exergy output from a system and the total exergy input to the system, as shown in Equation 18. The efficiency can also be expressed by the irreversibilities in the system, as in Equation 19.

$$\psi = \frac{\sum\limits_{useful} B_{i,out}}{\sum\limits_{total} B_{i,in}} \tag{18}$$

$$\psi = 1 - \frac{I}{\sum\limits_{total} B_{i,in}} \tag{19}$$

RAI (relative avoided irreversibility) is a concept introduced by Ertesvaåg [2007], and is defined there as the ratio between the difference in internal exergy losses in a reference case and another case, and the total exergy input in the reference case. Equation 20 shows the definition as it is presented in Ertesvaåg [2007], where ψ_{ref} is the exergy efficiency of the reference case.

$$RAI = (1 - \psi_{ref}) - (1 - \psi)\frac{B_{in}}{B_{in,ref}} \tag{20}$$

4 Simulations

This section presents the simulation work which has been completed during this project. As this project partly builds on a project written in the autumn of 2010, a short summary of the resulting process simulation is given in the first part together with a description of the modifications done to make it applicable to this project. The next part presents the test simulations that were done in the project. Two tests look into the effects of the tuning of a parameter in the previous project. Several tests investigate different ways of reducing exergy losses based on literature and creative experiments in Aspen Plus. A couple of tests are performed to indicate the increased losses experienced under poor operating conditions. One final test points out the positive effects of some historical process modifications made in the plant.

4.1 Base Case

During the autumn of 2010, mass and heat balances over the EDC cracking section were established in Aspen Plus in order to investigate the energy consumption in the process section. The simulations were developed using process measurements taken from different stable periods in the plant during the last three years. The periods varied in production and in time elapsed after the last decoking of one of the crackers. One of the periods was appointed the base case. This base case forms the basis of the exergy analyses performed in this project. A summary of the original simulation is given below, while a full description is given in Appendix A.

4.1.1 Simulation Summary

The simulation was developed using Peng-Robinson as the property method, and steady state was a fundamental assumption. Other important assumptions that were made were:

- Parallel units of the same equipment could be treated as one single large unit.

- No feed impurities or byproducts.

- The fuel gas contains only hydrogen and methane.

- The bottom stream from C1401 was assumed continuous, while in reality it is taken out in pulses.

The reaction zone of the cracker and the adiabatic reactor were modeled as conversion reactors, and the conversions were adjusted to get the correct outlet temperature after the adiabatic reactor. The first part of the cracker (heating and vaporization) was modeled by two heaters. The pressure drop over the cracker was fitted to simulation results from a simulation in EDC Crack®. The combustion chamber was simulated by a Gibbs reactor with a specified outlet temperature. The quench tower, C1401, was simulated by RadFrac without condenser or reboiler. To separate the gas and condensate at the end of both H1401 and
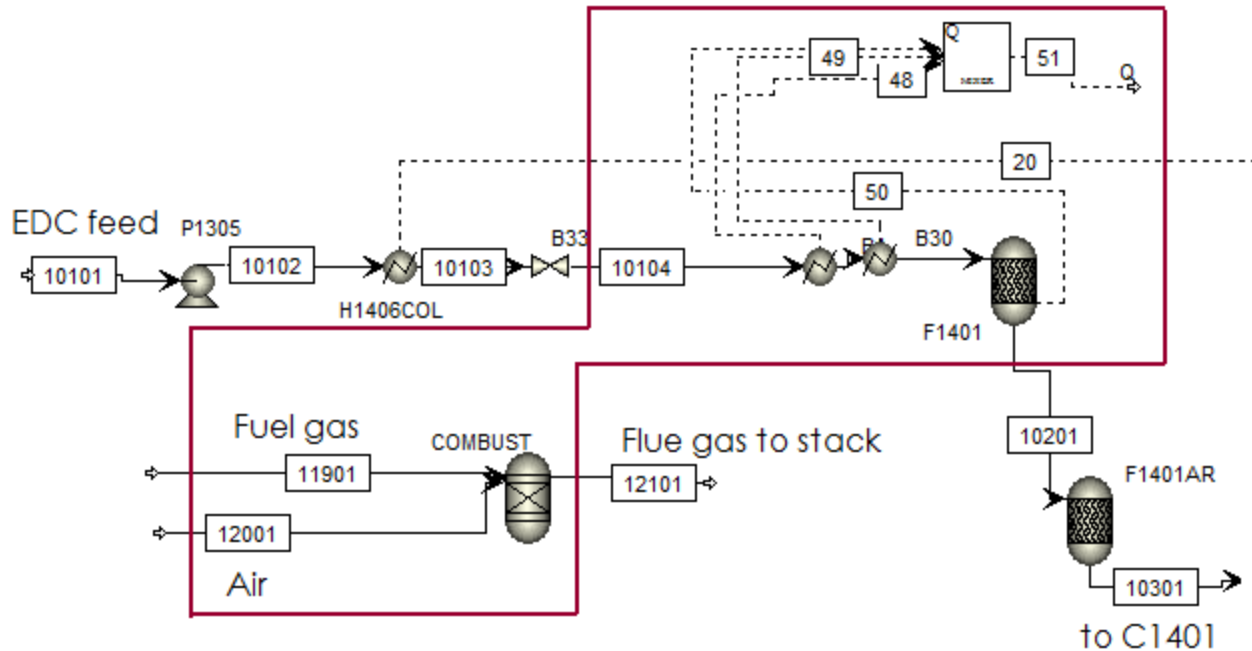
Figure 3: Aspen Plus flowsheet from the feed and cracker system, indicating the control volume around the cracker.

H1406, a flash tank (Flash2) was added to the outlet of each heat exchanger. The connection of the gas equalization line to the gas stream between H1401 and H1406 gave errors in the simulation. This stream is therefore not connected to the rest of the process, giving some small losses of fluid from the reflux loop. The HPF was neglected in the simulation. The rest of the simulation was established using simple heat exchangers, flash tanks, pumps and valves. The major tuning problem in the simulation was the reflux flow to C1401. As a result it was assumed that the flow gauges on the reflux flow were incorrect and the outlet temperature in H1401 was tuned to a higher value to obtain a reasonable bottom flow from C1401. The outlet temperature in H1402 and H1405 was lowered slightly to achieve an appropriate mass distribution in the streams leaving the top system. Figure 3, Figure 4 and Figure 5 show the simulation flowsheet from Aspen Plus. These Figures also indicate the control volume for the cracker, top and bottom system respectively.

4.1.2   Simulation Modifications

To be able to use the base case simulation for the exergy analyses, some additions had to be made to it. This mainly meant modifying many of the heat exchangers, as the type and amount of media being heat exchanged with the process had little importance in the previous project. The existing heaters were kept, and new heaters heating the cooling media (and vice versa) were connected to them by heat streams. By taking this approach, care had to be taken to avoid temperature crossover during the heat exchange.

In H1401 the added heater handled the boiling of low pressure condensate (LPC). Flow mea-
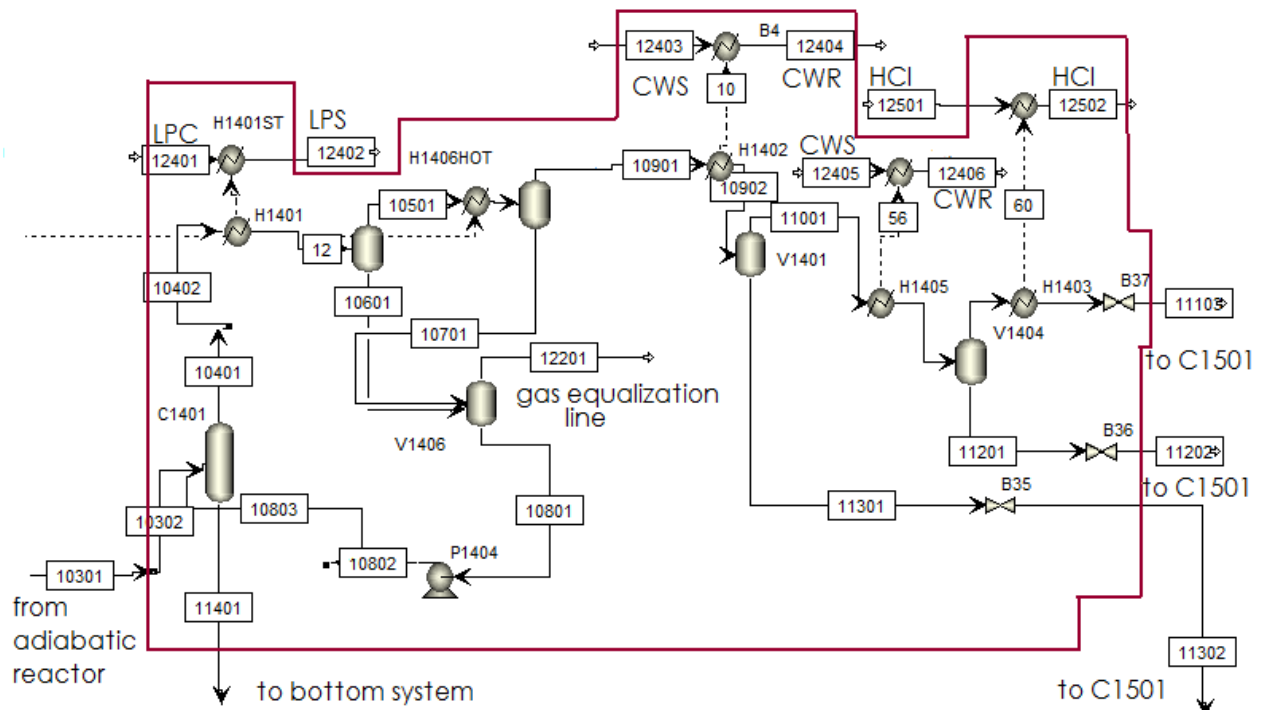
Figure 4: Aspen Plus flowsheet from the top system indicating the control volume around it.
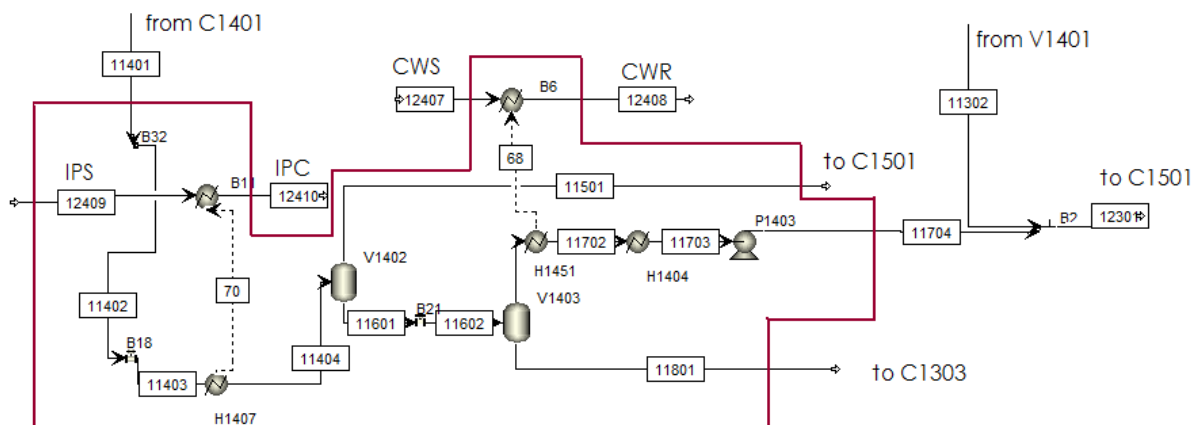
Figure 5: Aspen Plus flowsheet from the bottom system indicating the controle volume around it.

surements exist for both condensate and produced steam together with steam pressure. The simulation was attempted adjusted according to those parameters. Problems arose as the tuning of the outlet temperature on the process side of H1401 implemented during the autumn gave too little heat for the production of the measured amount of steam. Investigations around this problem were done with two tests which are presented in the following section.

At Rafnes two cooling water networks exit, operating at two different temperature intervals. The coldest network supplies cooling water at 8 ℃ to equipment operating at low temperatures. This cooling water is heated up to a maximum of 14 ℃ and subsequently supplied to the next network as cold cooling water to be used in equipment at higher temperatures. In this next network the water is heated to a maximum of 30 ℃ before it is rejected to the environment. As no temperature measurement exist on the cooling water outlets, it is assumed that the heat exchangers reject cooling water at the maximum temperature for the respective cooling water network. In the simulation this assumption was used to adjust the cooling water flow in the heat exchangers. H1405 and H1451 are supplied from the coldest network and H1402 from the warmer.

H1407 is heated by IPS supplied at a known pressure. The flow of steam was adjusted according to the heat requirements on the process side.

In H1403 the process side is heat exchanged with the HCl feed to the oxychloration reactor. Temperature, pressure and flow measurements exist on both sides of the unit, but the use of these data gave temperature crossover due to too high temperature on the outlet HCl. The increase in the HCl flow needed in order to avoid this was too large to be realistic, since the VCM process is a balanced process and only a given amount of HCl produced. It was therefore decided to ignore the crossover.

H1404 is cooled by a refrigerant which also cools other units in the plant (the condenser in the HCl distillation column etc.). When it comes to the distribution of refrigerant to the different equipment, little is known about this system, so it was decided not to simulate both sides of this heat exchanger. As H1404 is part of the bottom system, a very small amount of fluid passes through this unit compared with units in the top system. Knowledge about the exergy losses in this unit is therefore of little importance.

In the plant one of the streams in the top system mixes with one of the streams from the bottom system, before entering the HCl column. This mix was not part of the original simulation, as it had no affect on the results then, but it was added in this project.

The simulation resulting from these modifications constitutes the basis for all the tests and analyses performed during this project. The main analysis of the exergy losses in the EDC process section is completed from the results of this simulation of the base case. Other tests done on the system involve changes to this base case of various magnitudes. The different tests are described in Section 4.2.

4.1.3   Effects of Temperature Tuning on H1401

Problems obtaining the correct production of low pressure steam (LPS) in the simulation of H1401 were mentioned above. The problems arose from the high outlet temperature on the process side of the heat exchanger. This temperature was tuned to a higher than measured value in order to get a sensible flow from the bottom of the quench tower, C1401. It was decided to run two alternative simulations examining the results when the outlet temperature and the steam flow were at their measured values.

In Case 1 the measured steam flow was specified in the simulation, and the outlet temperature on H1401 was adjusted in order to get the corresponding heat flow from the process side.

In Case 2 the measured temperature was specified in the simulation, and the steam flow was adjusted to correspond to the smaller heat flow from the process side.

4.2   Test Simulations

The major part of the exergy losses in the EDC cracking section is expected to occur in the EDC cracker as combustion is a known source of large irreversibilities [Kotas, 1995, Szargut, 1988]. Another noticeable source of exergy losses in the EDC cracking section is assumed to be heat exchangers. Exergy is lost in connection with heat exchangers when: 1) hot process streams are cooled with cooling water which is then discharged into the environment, 2) heat is exchanged at finite temperature differences or 3) pressure drops through the heat exchanger.

The flue gas at the plant is discharged at a temperature between approximately 180 and 210 ℃. This stream still contains a large amount of unutilized energy which originally is supplied by the fuel gas. In most plants this heat source remains unused because of corrosion risks. Water vapor starts to condensate and absorbs sulfuric compounds in the flue gass creating sulfuric acid and thereby a highly corrosive environment. The sulfur is introduced to the system from impurities in the fuel gas. The fuel gas used at Rafnes is composed of hydrogen produced in the chlorine factory and methane which is a byproduct in the ethene factory. The sulfur content in this fuel gas is therefore negligible compared to natural gas, which is a common fuel gas in the process industry. Because of this, the condensation of water vapor should not pose a large risk to the equipment added to the flue gas stream.

The tests completed in this project only evaluate improvements in the cracker and top system of the process section, as the bottom system only manages a minor part of the materials flowing through. Changes in the bottom system caused by small changes in the bottom flow from C1401 during tests are neglected. Notice that no pressure drop has been added to the new heat exchangers in the tests. This is disregarded mainly since most of the heat exchangers are added to the combustion side of the cracker system where the pressure is assumed to be atmospheric in the simulations in the first place. The need for a fan for the combustion air as equipment is added to the flue gas stream has also been neglected in this project. The temperature differences in the additional heat exchangers are set to be 10 ℃

for heat exchange without phase change, and 5 ℃ for those with phase change.

This sections starts off with a closer look at exergy losses in combustion processes and ways to avoid these. A description of all the simulation tests follows next.

4.2.1   About Exergy Losses in Combustion Processes

The EDC cracking is assumed to be the largest source of exergy losses in the process section, therefore combustion processes deserve some closer attention. Knowledge about the distribution of exergy losses throughout the combustion is important to be able to reduce some of these losses by adjustments in the process parameters and the equipment. In the project this knowledge was used in planning the simulations tests in order to discover potentials of improvement in the EDC cracking section.

The combustion process contains not only the spontaneous chemical reaction between fuel and oxidizer, but also transport processes distributing heat, mass and momentum by both convection and diffusion. It is interesting to know which of these processes dominate the exergy losses, as this will indicate the sensible actions to be taken against the losses.

Som and Datta [2008] gives an overview of some of the different studies done on thermodynamic irreversibilities and exergy losses in combustion processes. The article sorts the studies according to fuel (gas, liquid and solid). Studies on gaseous fuels are further divided between laminar and turbulent flow, with turbulent flow being the common case in industrial applications, and premixed and diffusion (non-premixed) flames. The burners in the EDC crackers at Rafnes are premixed burners with turbulent flames burning a mixture of hydrogen and methane. The effects of premixing and turbulence are therefore the most interesting for this project.

One of the studies, Nishida et al. [2002], looked at both premixed and diffusion flames for linear flows for both methane and hydrogen fuel. In the case of the premixed flame, the chemical reaction was found to be the source of the largest losses and heat conduction the second largest. The portion of losses related to chemical reactions where smaller in simulations using methane as fuel compared to the ones using hydrogen, while the opposite was the case for heat conduction. Tests done in the study reveal that reduction of excess combustion air and higher inlet temperature on the feed reduce losses from heat conduction and chemical reactions.

Another relevant study is by Stanciu et al. [2001]. Stanciu et al. [2001] conducted studies on irreversibilities in both laminar and turbulent diffusion flames, simulating methane flames as examples. In the turbulent cases it was concluded that exergy losses caused by the turbulent part of the transport processes (dissipation) were substantially larger than those created by the mean motion field. The largest losses are the thermal turbulent losses, in addition to the losses generated by the chemical reactions. Stanciu et al. [2001] points out that though turbulent flames give large exergy losses through dissipation, it also enhances the mixing of

reactants and thus increasing the reaction rate.

Som and Datta [2008] concludes the review by indentifying different actions that can be taken to reduce exergy losses. The most relevant for this project are preheating of reactants and variations in excess air. Other actions mentioned are oxygen enrichment, fuel-air staging and controlling the jet velocities. These last methods are not suitable for this project, partly because an equilibrium approach is used - in other words only what goes in and what comes out of the control volume is considered under the assumption of both chemical and physical equilibrium - and partly because oxygen is not easy accessible at Rafnes.

4.2.2 Preheating of Combustion Air

Following the conclusions from both Nishida et al. [2002] and Som and Datta [2008], a test where the combustion air was preheated was conducted. This simulation left the process side undisturbed, while the hot flue gas was heat exchanged with the cold combustion air. This reduced the need for fuel gas which was adjusted to get the needed heat for the cracking reactions. The flow of combustion air was automatically adjusted to give the correct excess of air. The outlet temperature on the cold side of the heat exchanger was specified to be 10 ℃ lower than the hot side. The outlet temperature from the combustion chamber was kept at the same value as in the base case. A flowsheet showing the relevant part of the simulation is given in Figure 6.
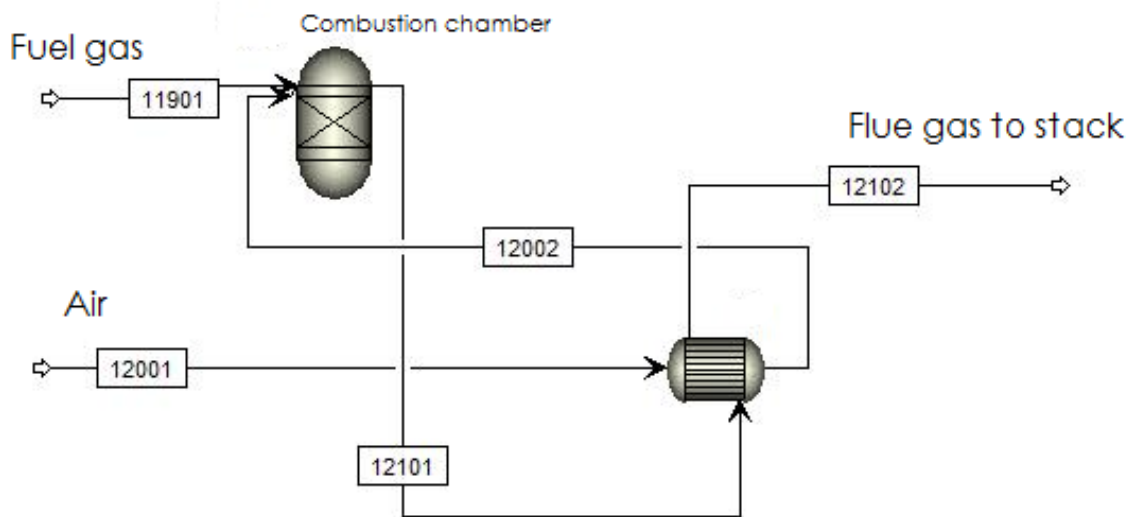
Figure 6: Flowsheet showing the preheating of combustion air.

4.2.3   Production of Low Pressure Steam by the Remaining Heat in the Flue Gas

This test was done to investigate other ways of utilizing some of the remaining heat in the flue gas. A heat exchanger was added to the flue gas, using the heat to produce low pressure steam at the same pressure as in H1401. This was a method used in the early days of the plant, before a series of rebuilds was done in this process section. The warm condensate entering the heat exchanger was assumed to be at its boiling point, and the cold stream vapor fraction was set to 1 at the outlet. The condensate flow was adjusted to give the wanted temperature difference over the heat exchanger. A flowsheet showing the relevant part of the simulation is given in Figure 7.
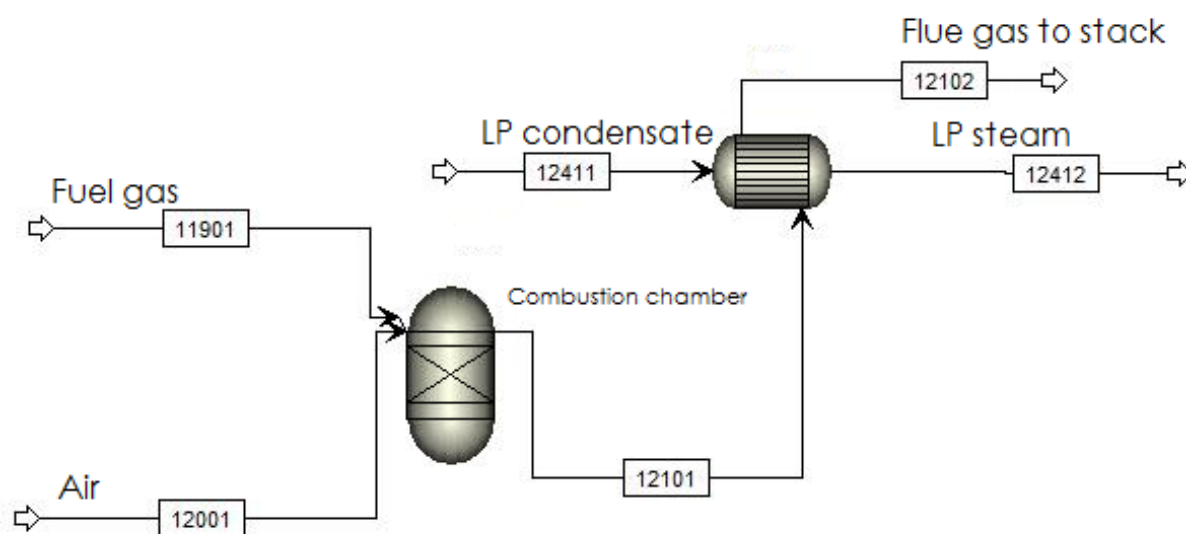
Figure 7: Flowsheet showing the production of low pressure steam from the remaining heat in the flue gas.

4.2.4   Further Heating of EDC Feed to Crackers by Remaining Heat in the Flue Gas

Another way of utilizing the remaining heat in the flue gas is by using it to preheat the EDC feed to the cracker even further after H1406. A heat exchanger was added to the feed stream between H1406 and the valve, as in reality the feed stream is split in the six feed streams for the three crackers after H1406, and the valve is in reality six valves regulating the feed flow after the split. The hot stream outlet temperature was set to 10 ℃ above the cold stream inlet temperature. By preheating the feed even further, the fuel gas demands in the cracker was reduced, and the amount of fuel gas and air was adjusted as in the previous tests. Figure 8 shows the relevant part of the simulation flowsheet.
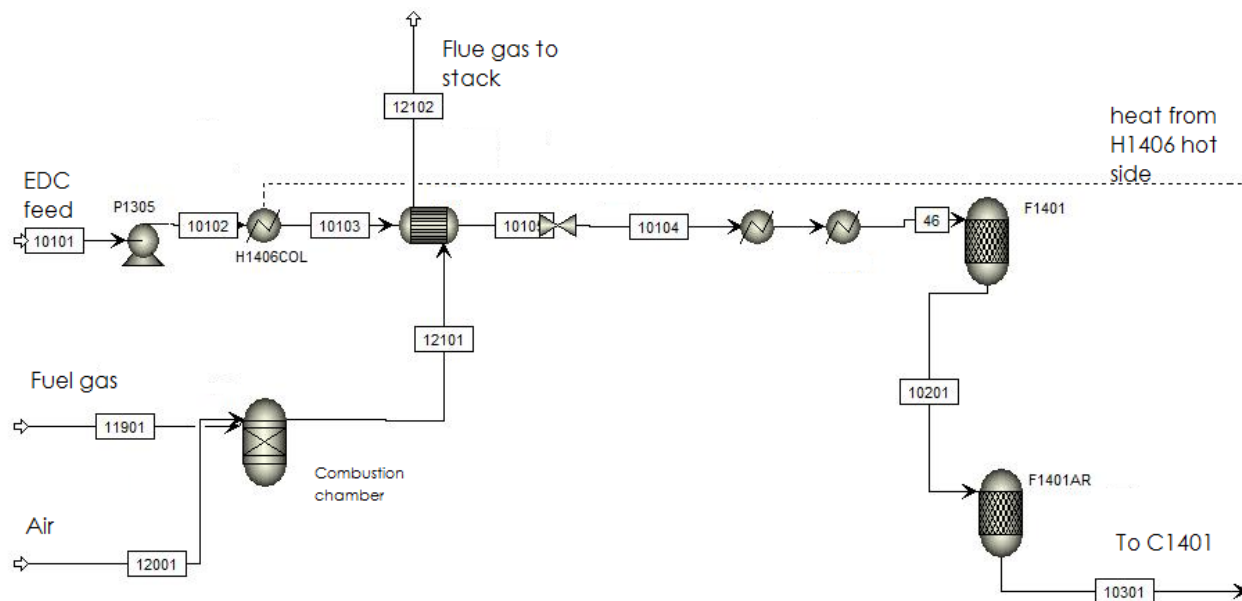
Figure 8: Flowsheet showing the further preheating of EDC feed to the cracker by the remaining heat in the flue gas.

4.2.5   Further Heating of EDC Feed and Combustion Air to Crackers by Remaining Heat in the Flue Gas

After utilizing the flue gas heat as much as possible to preheat the EDC feed, much heat at high temperature is still available. This was used to preheat the combustion air by the addition of a second heat exchanger to the flue gas stream. The outlet temperature on the cold side was specified at 10 °C below the hot stream inlet temperature, and fuel gas and air was adjusted in the usual manner. Figure 9 shows the relevant part of the simulation flowsheet.

4.2.6   Reduction of Excess Air in Combustion

As presented in Som and Datta [2008] the exergy losses in connection with combustion are reduced with the reduction of excess air to the combustion. For the original case from Rafnes, the amount of excess air was already as low as 3.3 vol% O_2 in the flue gas. The possibilities for reductions are therefore small, but a test taking the excess air down to 2.0 vol% O_2 was completed. An adjustment on the amount of air was already added to the original case in order to get the desired amount of excess air. This test was therefore easily accomplished by changing the desired target value in the adjustment setup. In addition the fuel gas flow was adjusted to get the correct heat production in the combustion chamber.
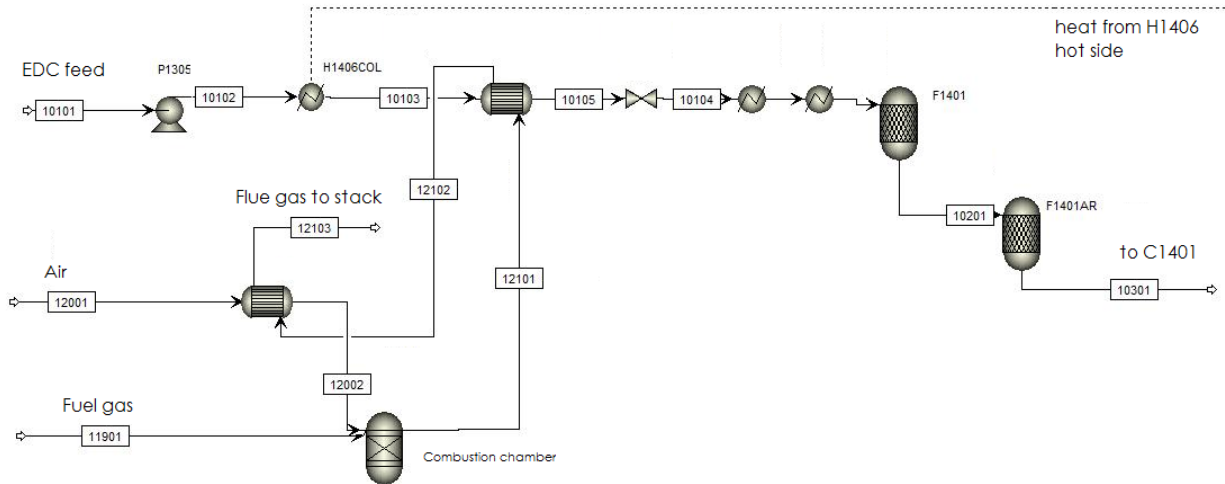
Figure 9: Flowsheet showing the further preheating of EDC feed and combustioin air to the cracker by the remaining heat in the flue gas.

4.2.7 Increase of Excess Air to the Combustion for Cases of Fouling in H1406

In contrast to the simulations employed in this project, the crackers at Rafnes will in reality produce more cracking products than just VCM and HCl. Many of the byproducts are heavy hydrocarbons, giving fouling in the downstream equipment over time. In cases of severe fouling on the hot side of H1406, the heat transfer is reduced and the preheating of EDC feed is less effective. This results in higher heat demands in the cracker, as more of the heating will take place there instead. The amount of flue gas also needs to be increased by increasing the amount of excess air.

In the last part of November 2009, the fouling in H1406 was very bad giving an outlet temperature on the EDC feed of approximately 80 °C. The excess air was set at 6 vol% O_2 at this time. These data were applied in the simulation to investigate the exergy effect on the cracker for this type of situation.

4.2.8 Increase of Excess Air to the Combustion under Normal Operating Conditions

Since the amount of excess air under normal conditions usually is low, it was interesting to investigate the effect of an increased level while the rest of the process section is run as normal. The potential increase of exergy loss and of fuel gas demands might motivate the operators to keep the excess air as low as practically possible. The test was accomplished in the same way as for the reduction of air. The target value was changed to 5 vol% O_2 and the fuel gas was adjusted accordingly.

4.2.9   Further Heating of EDC Feed to Crackers by Removing H1401

Another way of preheating the EDC feed, and thereby reducing the need for fuel gas, is by utilizing the hot top steam from the quench tower even more than today. By removing H1401, the heat that was used to produce low pressure steam can be used to preheat EDC instead. After removing H1401, the outlet temperature of the EDC feed was adjusted to be 10 ℃ lower than the hot top stream from C1401. The outlet temperature on the hot side of H1406 turned out higher than in the original case, giving too little condensate to the reflux tank V1406. To compensate for this, condensate from V1401 was used to get the correct reflux flow. In the simulation a split was added to the condensate stream exiting V1401, and a pump was added on the reflux part of the split to transport the liquid to V1406. Under full production in the plant, condensate from V1401 is supplied to the reflux tank to get enough reflux, and this is done without a pump, so the effects of the added pump in the simulation are neglected. As the condensate from V1401 is colder than the condensate ordinarily coming from H1401 and H1406, the reflux flow was reduced to get a sensible bottom flow from C1401 (9-12 tonnes/hr). The cold reflux also gave a much lower temperature on the top stream from C1401. In this test the gas equalization line was connected to the gas outlet stream from H1406. The fuel gas and air was adjusted in the usual way. A flowsheet showing the relevant part of the simulation is given in Figure 10.
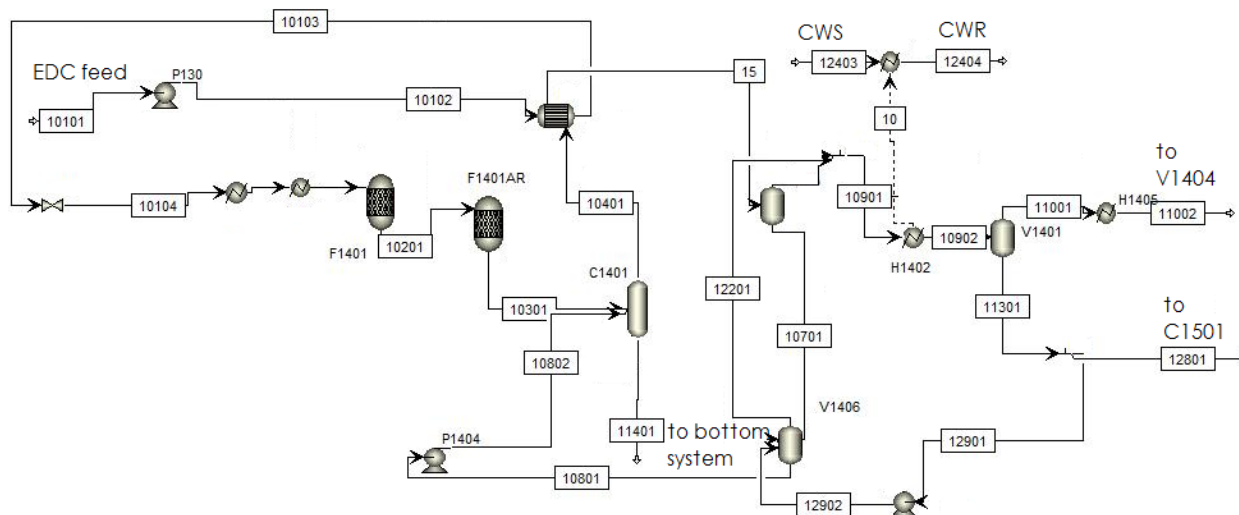
Figure 10: Flowsheet showing the further preheating of EDC feed and combustioin air to the cracker by removing the production of low pressure steam in H1401.

4.2.10   The Effect of Removing H1401 and H1406

When the plant was built in the late 1970s, the top system did not include H1401 and H1406. These heat exchangers were added during a rebuild in 1984, and before that H1402 removed all the heat alone. H1401 and H1406 were removed in a test simulation to investigate the

positive effect they had on the process section when they were added. Many other changes have been done to the process section over the years, but these have been neglected in this test. It would have been practically impossible to recreate the first version of the process section, so only the effect of removing these heat exchangers from a system run as today is looked into. Some of the other changes made to the system over the years that are worth mentioning are the addition of a third cracker unit and the adiabatic reactors, the process integration accomplished by adding H1403, the reduced need for refrigeration in the bottom system by addition of the cooling water cooled H1451, generally a larger production in the plant and increased conversion in the crackers.

By removing H1401 and H1406 from the simulation, all the reflux had to come from the condensate in V1401, and V1406 could be removed from the simulation. A split on the condensate outlet was adjusted to get a sensible bottom flow from C1401. The cooling water to H1402 was adjusted to the correct flow, while the rest of the settings in the simulation were kept as before. A flowsheet showing the relevant part of the simulation is given in Figure 11. Note that this flowsheet only presents the part of the simulation which has been modified, even though the whole top system has been evaluated. When H1406 is removed, the preheating of EDC feed must happen either in a heat exchanger or in the cracker itself with heat coming from an external source. This has not been evaluated in this project.
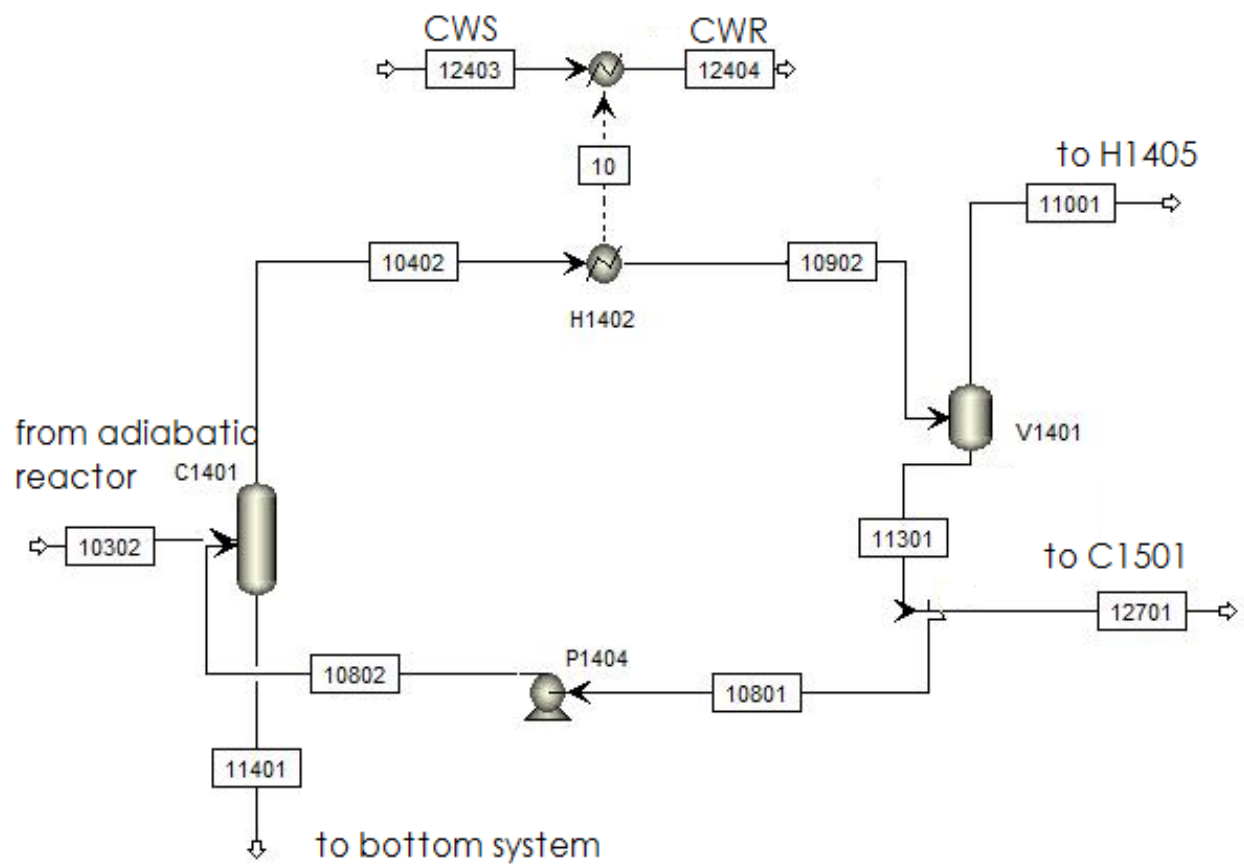
Figure 11: Flowsheet indicating the process without H1401 and H1406.

5 Exergy Calculations

The data needed to calculate the absolute exergy of each stream came mainly from Aspen Plus simulations, and the exergy calculations were completed in an Excel spreadsheet as Aspen Plus itself does not handle exergy. Some additional data were collected from literature. The procedure presented in Querol et al. [2011] was partly followed in the calculations. Below follows a detailed description of the work done and assumption made in determining the exergy content of all the relevant streams.

5.1 Reference Environment

A reference environment had to be defined for the project before any calculations could commence. To determine the suitable temperature, pressure and relative humidity, meteorological data from the period of the base case data (June 2008) was extracted from the database of the Norwegian Meteorological Institute [2008]. The meteorological data was taken from two weather stations in the area around Rafnes (Jomfruland and Geiteryggen) and the data was compared. A reference temperature of 15 ℃ (or 288.15 K), a pressure of 1 atm (or 1.01325 bara) were chosen on the basis of the data. It was also noticed that there was a relative humidity of 0.64

5.2 Reference Values and Stream Names

As Equation 11 in the Theory chapter indicates the reference enthalpy and entropy of a stream is needed in order to calculate its physical exergy. This can be found in Aspen Plus by adding a heat exchanger for every new stream composition in the system and using this composition as the input. The heat exchanger, hereafter referred to as the composition exchanger, is specified to operate at the reference conditions, giving the values for h_0 and s_0 in the outlet stream results. Figure 12 displays the composition exchangers for the base case. Note that h_0 and s_0 had to be recalculated in the tests for the streams that changed composition due to modifications in the simulation.

Querol et al. [2011] identifies each stream with a five digit number. The first three digits are identical for all streams with the same composition, while the two last digits give a unique number to each stream. The same naming procedure was applied in these simulations. In this project, the first three digits also became the name of the composition exchangers. The composition name for the stream was attempted given in a logical, increasing manner through the simulations, but in some of the more extensive simulations a low number might be followed by a much larger one in a couple of cases (like 10501 followed by 12701). The stream names are shown in the Aspen Plus flowsheets over the base case in Figure 3, Figure 4 and Figure 5. Notice that streams which have been added extra in the simulation in order to simulate e.g. the cracker system and the gas liquid separation in H1401 and H1406, but do not exist in the plant, have not been named in this fashion.
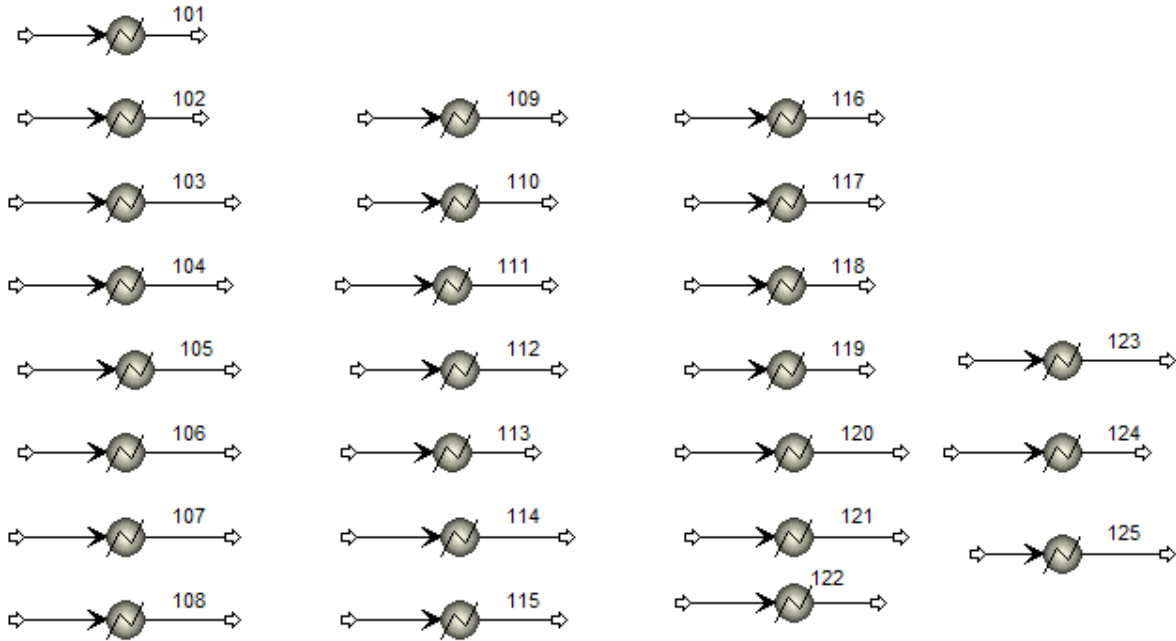
Figure 12: The composition exchangers in Aspen Plus.

Both data at reference conditions for the calculation of physical exergy and the composition at reference conditions needed in the calculation of chemical exergy were found using the composition exchangers.

5.3   Exergy Calculations

In the Theory chapter the most ordinary exergy terms were presented. In this project the kinetic and potential exergy has been neglected. According to Kotas [1995], the potential exergy is negligible for most gas streams. The kinetic and potential exergy has been entirely omitted in many sources, such as Wølneberg and Ertesvåg [2008], Araújo et al. [2007], Hinderink et al. [1996a,b], Graveland and Gisolf [1998], Doldersum [1998], Wang and Zheng [2008], Modarresi et al. [2010], Querol et al. [2011], Szargut [2005]. Some of these sources mention that these terms are small compared to the other exergy terms, while others do not mention them at all. The absolute exergy has been calculated for all the relevant streams in the simulations. The physical and chemical exergy was calculated separately and added to get the absolute value.

5.3.1   Physical Exergy

The physical exergy is a simple value to calculate since data can be collected from simulation software like Aspen Plus. As described in the previous section, the reference enthalpy and entropy were obtained from the composition exchangers. The enthalpy and entropy of the stream itself, h_1 and s_1, was collected directly from the stream results in the simulation

together with the molar flow. The physical exergy was calculated according to Equation 11.

5.3.2   Chemical Exergy

Before the chemical exergy of the streams could be calculated, the standard chemical exergy for all the components had to be decided. Equation 15 was used to calculate the standard chemical exergy. Gibbs energies was taken from Haynes [2011] while the standard chemical exergy of the elements came from Rivero and Garfias [2006]. The data are given in Table 1 and Table 2.

The Gibbs free energy used in the calculations of standard chemical exergies have a reference pressure of 1 bar in Haynes [2011], while the tabulated standard exergies for the elements are given at 1 atm. This difference has been assumed negligible as the error in doing so is miniscule. No standard chemical exergy was calculated for VCM or HCl in liquid phase because information about the Gibbs free energy of formation for this phase is lacking. When necessary the standard chemical exergy for the components in gas phase was used. The calculated standard chemical exergies for the components are given in Table 3.

Table 1: Standard free energy of formation (T_0=298.15 K, P_0=1 bar) Haynes [2011].

Chemical compound	$\Delta_f G_0$ [kJ/mol]
Methane	-50.5
CO_2	-394.4
Water (g)	-228.6
Water (l)	-237.1
EDC (g)	-70.8
EDC (l)	-73.8
HCl	-95.3
VCM	53.6

Table 2: Standard chemical exergy for the elements (T_0=298.15 K, P_0=101.325 Pa, RH=0.7) Rivero and Garfias [2006].

Chemical element	E_{Ch} [kJ/mol]
Carbon	410.27
Hydrogen (H_2)	236.12
Chlorine (Cl_2)	123.7
Nitrogen (N_2)	0.67
Oxygen (O_2)	3.92

Table 3: Calculated standard chemical exergy for the chemical compounds.

Chemical compound	E_{Ch} [kJ/mol]
Methane	832.01
CO_2	19.79
Water (g)	9.48
Water (l)	0.98
EDC (g)	1345.68
EDC (l)	1342.68
HCl	84.61
VCM	1290.17
H_2	236.12
N_2	0.67
O_2	3.92

The reference temperature used in the exergy analyses is ten degrees lower than the reference temperature in the tables giving the standard chemical exergies for the elements [Rivero and Garfias, 2006] applied in the analyses. This deviation could have been corrected in accordance with Equation 16, but as the investigations done by Ertesvåg [2007] show that the temperature dependence of most hydrocarbons are weak in the relevant temperature span, this correction was not done. The behavior of chlorinated alkanes and alkenes is not investigated in Ertesvåg [2007], but it is assumed a similar behavior as for pure alkanes/alkenes. The same is done in the case of hydrogen chloride. The assumption is made since other uncertainties, especially in the Aspen Plus simulations which are based on plant measurements, are likely to be much larger than the error by not doing the correction.

The relative humidity of the reference environment is also 6 percentage points lower than for the tabulated standard chemical exergies. This not been corrected for, as the results in Ertesvåg [2007] indicates very small errors for the difference in relative humidity at the relevant temperature.

Most of the streams in the process simulation are mixed streams. The majority also contain both gas and liquid phase at the reference conditions. The composition of the different streams had to be known in order to use Equation 17 in the calculation. As mentioned above the outlet data from the composition exchangers were used to determine this. A detailed description of this procedure is given in Appendix B. Notice that in the calculations of the gas and liquid phase composition in mixed streams the gas and liquid was assumed to behave ideal. In the calculation of chemical exergy for mixtures, the mixtures have been treated as ideal.

5.4   Exergy Balances

Equation 5 was used to calculate the internal losses in the process and the individual equipment. It was assumed no heat loss to the environment through the walls of the equipment.

The pump duty calculated by Aspen Plus is used directly in the balance equation without any correction by a pump efficiency. The estimated work is therefore the minimum requirement for the pumps.

The internal losses are caused by irreversibilities which only to a certain degree can be counteracted. The internal losses can be divided into what Kotas [1995] defines as avoidable and intrinsic irreversibilities, namely irreversibilities that can be avoided by changes to the process parameters and equipment within economical, technological and physical limits and irreversibilities which are inevitable within these limits. The division into these two categories calls for complicated calculations and this is partly handled by thermoeconomics. It is mentioned here as a reminder that not all irreversibilities can be eliminated.

Following Hinderink et al. [1996b] external and total exergy losses are also included in this project. External losses have been defined here as the exergy lost through useless streams leaving the system boundary. Useless streams include exit cooling water and flue gas. Notice that steam condensate is defined as a useful stream in this project on the basis of its high temperature and the fact that the condensate is recycled back to the boiler. Total exergy is the sum of both internal and external losses.

All other process streams exiting the system are defined as useful streams as they enter other equipment for further processing. The fuel gas, condensate and steam entering the system have been treated as the other process steams, not as import exergy as in Hinderink et al. [1996b]. No penalty is therefore given for the exergy needed to produce some of these streams, as the main objective of this project is to look at exergy losses within the process section. The reduction of fuel gas as part of the simulation tests, on the other hand, are emphasized in the results.

In the simulation tests mostly small parts of the process is modified. An exergy balance over the whole process section is therefore not necessary for most of the tests. The process section has therefore been divided into three subsystems: the cracker system, the top system and the bottom system. The control volumes for the subsystems are indicated in the Aspen Plus flowsheets of the base case in Figure 3, Figure 4 and Figure 5.

5.5   RAI and RATI

In order to relate the results of each test to the total exergy input to the cracker in the base case, RAI and RATI (relative avoided total irreversibility) was calculated. For this project RAI has been calculated as shown in Equation 21.

$$RAI = \frac{I_{\text{basecase}} - I_{\text{test}}}{\sum\limits_{total} B_{\text{i,in,basecase}}} \tag{21}$$

A similar efficiency was developed for the total exergy losses. The expression for RATI is

given in Equation 22.

$$RATI = \frac{I_{\text{total,basecase}} - I_{\text{total,test}}}{\sum\limits_{total} B_{\text{i,in,basecase}}} \tag{22}$$

5.6   Cracker Efficiency

At Rafnes the cracker efficiency is calculated from online data for each of the three crackers. The efficiency is given by Equation 23.

$$\eta = \frac{(\text{Fired heat - heat loss})}{\text{Fired heat}} \tag{23}$$

Heat is lost in the flue gas and through the cracker walls. The heat lost through the cracker walls is assumed constant both in the online calculations and in this project. This loss looks, by the difference in energy needs in the cracker and energy utilized in the combustion chamber in the base case simulation, to be approximately 2 %. The heat loss in the flue gas is the only heat loss included in the online calculations of the efficiency. The amount of flue gas is calculated and used to calculate the heat. The heat calculation does not consider the condensation heat from the water in the flue gas.

In the tests in this project the condensation heat is utilized in several of the tests. The estimation of the energy loss in the flue gas therefore includes the condensation of the remaining water vapor. In all the relevant simulations a heat exchanger has been added to the flue gas, cooling it down to the reference temperature of 15 ℃. The heat duty of this heat exchanger is considered to be the heat loss in the cracker efficiency. The fired heat is calculated from the flow and composition of the fuel gas together with the lower heating value of hydrogen and methane, as shown in Appendix E. By using this calculation approach, the efficiency is considerably lower than the one calculated online at Rafnes, which usually is approximately 0.9-0.92 [Kaggerud]. By calculating the efficiency for the base case as well as for the tests, the results should still show sensible trends for the effect of the tests.

6   Results

The exergy content in all the relevant streams in the process section where calculated and the results were used to examine the overall exergy balance of the section. The losses in the section were examined in more detail by balances over the major equipment. All the resulting exergy losses are reported as kJ/kg VCM, based on a production of 1530 tonnes VCM per day.

6.1   Stream Results

The calculation results for physical, chemical and total exergy for the streams in the base case are presented in Table 4, Table 5 and Table 6 for the feed and cracker, the top and the bottom system respectively. The calculated stream results for the other simulations are given in Appendix C and the stream results from Aspen Plus are given in Appendix F. The total exergy results in the tables look incorrect as the numbers have been rounded off after being summed up. The chemical exergy dominates the total exergy results, making the total exergy very dependent on the composition of the streams. The physical exergy varies a lot, but being a smaller term than the chemical exergy, its influence on the total exergy is minor. Note that the physical exergy in streams 10101, 11901 and 12001 is zero as the streams are at reference temperature and pressure, while the chemical exergy in 12001 (combustion air) is zero as a matter of definition.

Table 4: Calculated physical, chemical and total exergy loss per kg VCM for the simulated process streams in the feed and cracker system.

Stream	Physical exergy [kJ/kg VCM]	Chemical exergy [kJ/kg VCM]	Total exergy [kJ/kg VCM]
10101	0	36113	36113
10102	6	36113	36119
10103	75	36113	36188
10104	74	36113	36187
10201	911	36516	37426
10301	837	36568	37405
10302	279	12189	12468
11901	0	3186	3186
12001	0	0	0
12101	97	46	143

Table 5: Calculated physical, chemical and total exergy loss per kg VCM for the simulated process streams in the top system.

Stream	Physical exergy [kJ/kg VCM]	Chemical exergy [kJ/kg VCM]	Total exergy [kJ/kg VCM]
10401	267	26767	27034
10402	801	80301	81102
10501	487	50524	51011
10601	88	29776	29864
10701	38	17173	17211
10801	123	46718	46841
10802	123	46718	46842
10803	41	46718	46759
10901	318	33352	33670
10902	158	33352	33510
11001	101	6539	6640
11002	94	6539	6633
11101	74	3243	3317
11102	73	3243	3316
11103	72	3243	3315
11201	17	3299	3316
11202	17	3299	3316
11301	51	26822	26874
11302	51	26822	26873
12201	2	231	233
12401	41	16	57
12402	247	16	264
12403	6	512	518
12404	22	512	535
12405	3	171	174
12406	2	171	173
12501	96	1362	1458
12502	94	1362	1457

Table 6: Calculated physical, chemical and total exergy loss per kg VCM for the simulated process streams in the bottom system.

Stream	Physical exergy [kJ/kg VCM]	Chemical exergy [kJ/kg VCM]	Total exergy [kJ/kg VCM]
11401	4	996	1000
11402	12	2987	2999
11403	11	2987	2999
11404	14	2987	3001
11501	5	539	544
11601	9	2448	2457
11602	6	2448	2454
11701	5	939	944
11702	0	939	939
11703	0	939	940
11704	0	939	940
11801	1	1508	1510
12407	1	60	61
12408	1	60	60
12409	3	0	3
12410	0	0	1

6.2   Total Exergy Balance

The stream results used for calculating the total balance over the process section, and the balance results, are given in Table 7. In Table 8 the exergy balance over the top system is given.

Table 7: Total exergy balance over the EDC cracking section.

In Streams	[kW]	[kJ/kg VCM]	Out Useful streams	[kW]	[kJ/kg VCM]
10101	639206	36113	11103	58673	3315
11901	56388	3186	11202	58698	3316
12001	0	0	11501	9634	544
12401	1015	57	11801	26724	1510
12409	55	3	12301	492250	27811
12403	9165	518	12402	4667	264
12405	3076	174	12410	12	1
12407	1077	61	12502	25781	1457
12501	25812	1458			
sum	735793	41570	sum	676438	38217
Work			Useless streams	[kW]	[kJ/kg VCM]
P1305	140	7.9	12101	2528	143
P1404	9	0.5	12404	9464	535
P1403	4	0.2	12406	3054	173
		8.6	12408	1069	60
sum	153		sum	16116	910
Total exergy in	735946	41579			
Total balance				59508	3362
Internal balance				43393	2452

Table 8: Total exergy balance over the top system in the EDC cracking section.

In	[kJ/kg VCM]	Out	[kJ/kg VCM]
Stream exergy	39612	Useful stream exergy	38224
Work (pumps)	8	Useless stream exergy	707
Internal exergy losses	689	Total exergy losses	1397

6.2.1   Exergy Losses in the Major Equipment

The losses in all the major equipment are given in Table 9 ranked after magnitude of internal exergy losses. The equipment not present in this table had even lower exergy losses and the results are only presented in Appendix D. Notice that the crackers, adiabatic reactors and the quench towers (C1401) are still evaluated as one large unit each instead of three in parallel. The exergy losses in the EDC cracker are one order of magnitude larger than in the

rest of the equipment, making these the most pronounced losses. This is also illustrated in Figure 13 for the internal exergy losses. The large losses in the cracker unit corresponds to what was assumed in the development of the different simulation tests.

Table 9: Exergy balance over the major equipment in the EDC cracking section.

Unit	Internal exergy loss [kJ/kg VCM]	External exergy loss [kJ/kg VCM]	Total exergy loss [kJ/kg VCM]
Cracker	1804	143	1947
C1401	146	0	146
H1402	143	17	678
H1406	61	0	61
Adiabaic reactor	22	0	22
H1401	20	0	20
H1405	8	-1*	181
H1451	5	60	66

*The negative results occur since the cooling water has a lower temperature than the reference temperature, hence giving it a higher stream exergy at the inlet temperature 8 ℃ than at the exit temperature 14 ℃.
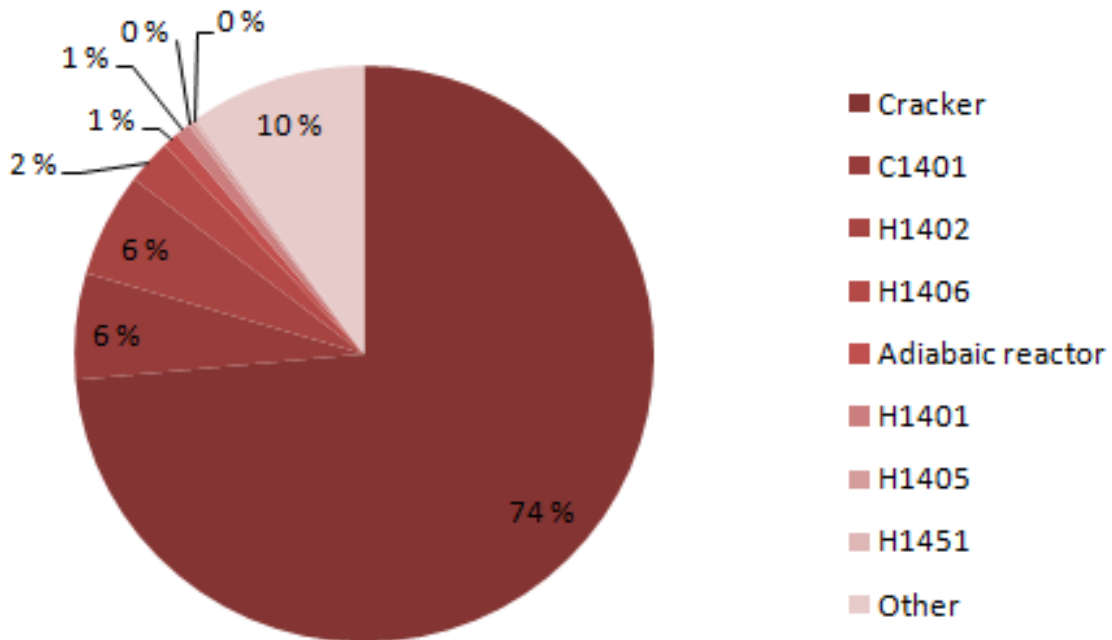
Figure 13: The distribution of the internal exergy losses between the major equipment.

6.3   Investigation of Effects of Temperature Tuning in H1401

The first case was the adjustment of the exit temperature to give the measured amount of produced low pressure steam. The results of this case is given in Table 10. The second case was the adjustment of the condensate feed to H1401 to get the measured exit temperature on the process side of the heat exchanger. The results of this case are given in Table 11. A comparison of the internal losses in the equipment in the two cases and the original case is shown in Figure 14, and a comparison of the exergy losses over the top system for the three cases is shown in Figure 15. As can be seen from Figure 14, the exergy results are fairly equal for all equipment except H1402, where the differences are large. The results in Figure 15 reflects the results from Figure 14 as the total losses show the largest variations indicating large variations in the external losses. Table 12 shows the comparison of some key measurements from the real plant and the three simulation cases. Simulation results from the cases are presented in Appendices F.2 and F.3.

Table 10: Exergy balance over the first tuning case.

Unit	Internal exergy loss [kJ/kgVCM]	Total exergy loss [kJ/kgVCM]
C1401	150	150
H1406	55	55
H1402	100	510
H1401	18	18
H1405	13	9
H1403	2	2

Table 11: Exergy balance over the second tuning case.

Unit	Internal exergy loss [kJ/kgVCM]	Total exergy loss [kJ/kgVCM]
C1401	148	148
H1406	59	59
H1402	122	611
H1401	19	19
H1405	10	208
H1403	1	1
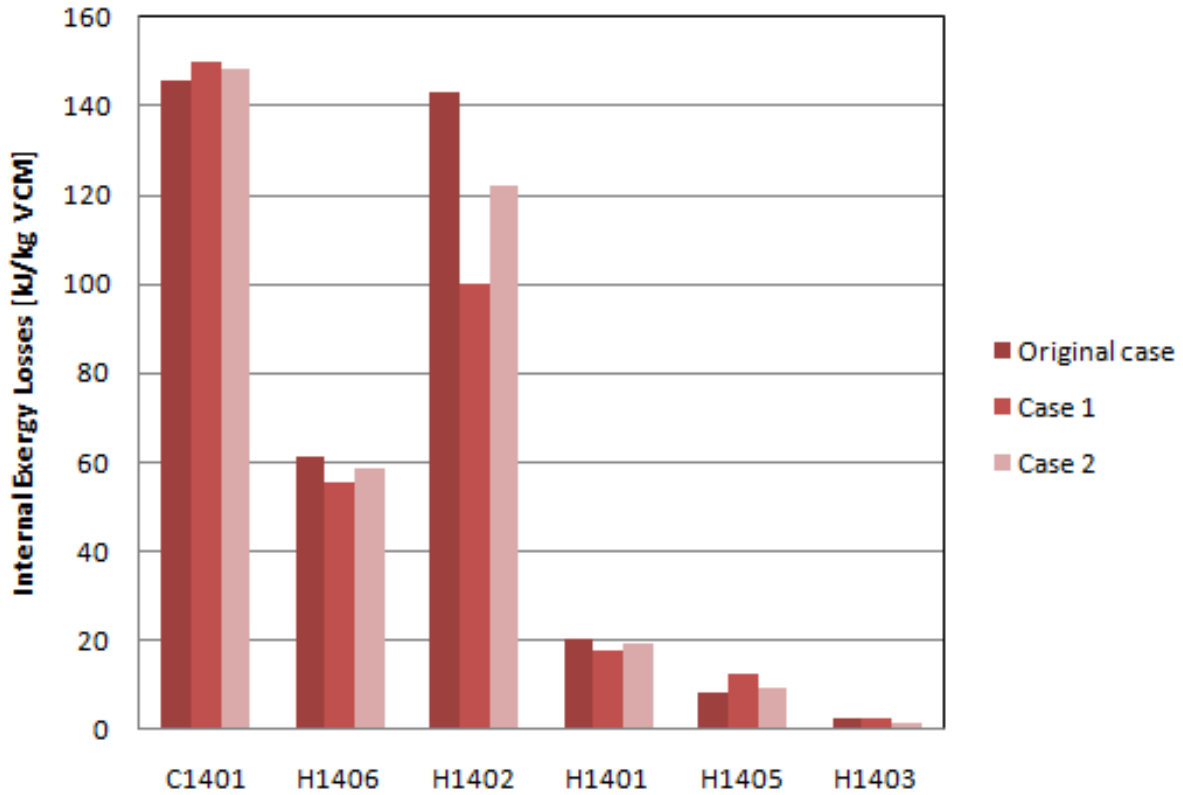
Figure 14: A comparison of the internal losses in major equipment in the original case and the two tuning cases.

Table 12: A comparison of some key measurements from the real plant and the three simulation cases.

Measurement	Real	Base Case	Case 1	Case 2
Bottom stream C1401 [tonnes/hr]	9-12	13.7	32.8	23.4
Top stream V1404 [tonnes/hr]	27.5	29	30.9	30
Bottom stream V1404 [tonnes/hr]	13.7	13.8	19.4	16.3
Bottom stream V1401 [tonnes/hr]	116.6	112.1	85.3	98.8
Outlet temperature H1401 [℃]	156.5	159.5	153	156.5
Top stream temperature C1401 [℃]	177.8	176.5	174.2	175.5
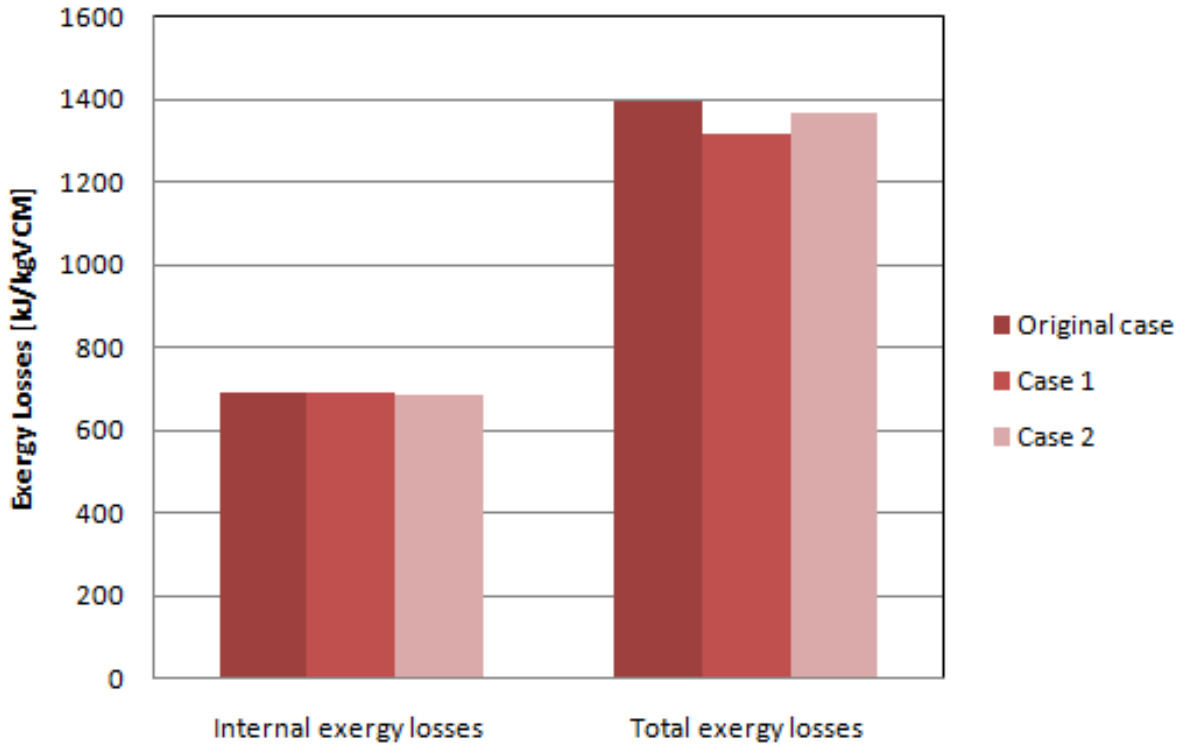
Figure 15: Comparison of exergy losses in the top system for the original case and the two tuning cases.

6.4   Tests for Reduction of Exergy Losses

As was seen in Section 6.2.1 the largest exergy losses occur in connection with the EDC cracker. Several tests were conducted in order to investigate ways for reducing these large losses. In addition the rest of the process section was examined for potential reductions of exergy loss.

6.4.1   Preheating of Combustion Air

The results of preheating the combustion air with the remaining heat in the flue gas are shown in Table 13 and Table 14. In this test the changes only affect the cracker system; hence an exergy balance is only established for this unit by defining a control volume including the new heat exchanger.

Table 13: Exergy results in cracker for preheated combustion air.

Internal exergy loss [kJ/kg VCM]	Total exergy loss [kJ/kg VCM]	Reduction in internal loss [kJ/kg VCM]	Reduction in total loss [kJ/kg VCM]
1658	1746	145	200

Table 14: Fuel gas results in cracker for preheated combustion air.

Flow [tonne/hr]	Flow original case [tonne/hr]	Reduction [tonne/hr]	Reduction [%]
2.83	3.02	0.19	6.3

6.4.2   Production of Low Pressure Steam by the Remaining Heat in the Flue Gas

The results of producing low pressure steam by heat from hot flue gas are shown in Table 15. They indicate that the internal losses will increase insignificantly and that the total losses will be reduced slightly. In this test the changes only affect the cracker system; hence an exergy balance is only established for this unit by defining a control volume including the new heat exchanger and the condensate and steam streams that enter and exit it.

Table 15: Exergy results in cracker for production of low pressure steam by the remaining heat in the flue gas.

Internal exergy loss [kJ/kg VCM]	Total exergy loss [kJ/kg VCM]	Reduction in internal loss [kJ/kg VCM]	Reduction in total loss [kJ/kg VCM]
1805	1935	-2	11

6.4.3   Further Heating of EDC Feed to Crackers by Remaining Heat in the Flue Gas

The results of utilizing the remaining heat in the flue gas to preheat the EDC feed to the cracker are shown in Table 16 and Table 17. In this test the changes only affect the cracker system; hence an exergy balance is only established for this unit by defining a control volume including the new heat exchanger and the valve. Notice that the valve is excluded from many other cracker balances, but the effects of including it is negligible.

Table 16: Exergy results in cracker for further heating of EDC feed by remaining heat in the flue gas.

Internal exergy loss [kJ/kg VCM]	Total exergy loss [kJ/kg VCM]	Reduction in internal loss [kJ/kg VCM]	Reduction in total loss [kJ/kg VCM]
1763	1884	41	63

Table 17: Fuel gas results in cracker for further heating of EDC feed by remaining heat in the flue gas.

Flow [tonne/hr]	Flow original case [tonne/hr]	Reduction [tonne/hr]	Reduction [%]
2.96	3.02	0.06	2.0

6.4.4   Further Heating of EDC Feed and Combustion Air to Crackers by Remaining Heat in the Flue Gas

The remaining heat in the flue gas was also attempted utilized to preheat both the EDC feed and the combustion air. The results are given in Table 18 and Table 19. In this test the changes only affect the cracker system; hence an exergy balance is only established for this unit by defining a control volume which also includes the two new heat exchangers and the valve. Notice that the valve is excluded from many other cracker balances, but the effects of including it is negligibly small.

Table 18: Exergy results in cracker for further heating of EDC feed and combustion air to crackers by remaining heat in the flue gas.

Internal exergy loss [kJ/kg VCM]	Total exergy loss [kJ/kg VCM]	Reduction in internal loss [kJ/kg VCM]	Reduction in total loss [kJ/kg VCM]
1650	1736	154	210

Table 19: Fuel gas results in cracker for further heating of EDC feed and combustion air to crackers by remaining heat in the flue gas.

Flow [tonne/hr]	Flow original case [tonne/hr]	Reduction [tonne/hr]	Reduction [%]
2.82	3.02	0.2	6.6

6.4.5 Reduction of Excess Air in Combustion

The excess of air was reduced to 2 mol% oxygen, resulting in a minuscule reduction of fuel gas and no noticeable change in exergy losses. The results are given in Tables 20 and 21. In this test the changes only affect the cracker system; hence an exergy balance is established only for this unit.

Table 20: Exergy results in cracker for reduction of excess air in combustion

Internal exergy loss [kJ/kg VCM]	Total exergy loss [kJ/kg VCM]	Reduction in internal loss [kJ/kg VCM]	Reduction in total loss [kJ/kg VCM]
1804	1947	0	0

Table 21: Fuel gas results in cracker for reduction of excess air in combustion.

Flow [tonne/hr]	Flow original case [tonne/hr]	Reduction [tonne/hr]	Reduction [%]
3.01	3.02	0.01	0.3

6.4.6 Increase of Excess Air to the Combustion for Cases of Fouling in H1406

The results of increased air at extensive fouling in H1406 are given in Table 22 and Table 23, indicating both increased exergy losses and fuel gas needs. In this test the changes affect the whole system, but as mentioned in Section 4.2.7 only the cracker system was evaluated; hence an exergy balance is established only for this unit.

Table 22: Exergy results in cracker for increase of excess air to the combustion for cases of fouling in H1406

Internal exergy loss [kJ/kg VCM]	Total exergy loss [kJ/kg VCM]	Reduction in internal loss [kJ/kg VCM]	Reduction in total loss [kJ/kg VCM]
2018	2174	-214	-227

Table 23: Fuel gas results in cracker for increase of excess air to the combustion for cases of fouling in H1406.

Flow [tonne/hr]	Flow original case [tonne/hr]	Reduction [tonne/hr]	Reduction [%]
3.28	3.02	-0.26	-8.6

6.4.7   Increase of Excess Air to the Combustion under Normal Operating Conditions

The punishment for increased excess air in the combustion under normal operating conditions was investigated for a case with 5 vol% excess oxygen. The results are given in Table 24 and Table 25, indicating both increased exergy losses and fuel gas needs. In this test the changes only affect the cracker system; hence an exergy balance is established only for this unit.

Table 24: Exergy results in cracker for increase of excess air to the combustion under normal operating conditions.

Internal exergy loss [kJ/kg VCM]	Total exergy loss [kJ/kg VCM]	Reduction in internal loss [kJ/kg VCM]	Reduction in total loss [kJ/kg VCM]
1834	1978	-30	-32

Table 25: Fuel gas results in cracker for increase of excess air to the combustion under normal operating conditions.

Flow [tonne/hr]	Flow original case [tonne/hr]	Reduction [tonne/hr]	Reduction [%]
3.05	3.02	-0.03	-1.0

6.4.8   Further Heating of EDC Feed to Crackers by Removing H1401

The results of the exergy balances over major equipment are given in Table 26, the total exergy balances over the top system are given in Table 27 and the fuel results for the cracker are given in Table 28. The results indicate reduced internal losses, increased total losses, reduced fuel gas needs and varied results for the different equipment. The whole top system, in addition to the cracker, is affected by this test. Balances over all the relevant units were performed together with a total balance over the top system.

Table 26: Exergy results in all the major equipment for further heating of EDC feed to crackers by removing H1401.

Unit	Internal exergy loss [kJ/kg VCM]	Total exergy loss [kJ/kg VCM]	Reduction in internal loss [kJ/kg VCM]	Reduction in total loss [kJ/kg VCM]
Cracker	1733	1871	71	76
C1401	179	178	-33	-32
H1406	66	70	-5	-9
H1402	276	1256	-133	-578
H1405	8	175	0	6
H1403	3	3	0	0

Table 27: Exergy balance over the top system for further heating of EDC feed to crackers by removing H1401.

In	[kJ/kg VCM]	Out	[kJ/kg VCM]
Stream exergy	39986	Useful stream exergy	38186
Work (pumps)	8	Useless stream exergy	1152
Sum	39994		39338
Internal exergy losses	656	Total exergy losses	1808
Reduction in internal losses	34	Reduction in total losses	-411

Table 28: Fuel gas results in cracker for further heating of EDC feed to crackers by removing H1401.

Flow [tonne/hr]	Flow original case [tonne/hr]	Reduction [tonne/hr]	Reduction [%]
2.92	3.02	0.1	3.3

6.5   The Effect of Removing H1401 and H1406

The effect of removing H1401 and H1406, leaving only H1402 to cool down the top stream from C1401 was tested. The total balances and equipment balances are given in Tables 29 and 30 respectively. Notice the extreme total losses experienced in H1402 because of external losses in this case. The test affects the top system. Balances were established for the relevant units and the top system as a whole.

Table 29: Exergy balances over the the top system for the effect of removing H1401 and H1406.

In	[kJ/kg VCM]	Out	[kJ/kg VCM]
Stream exergy	43093	Useful stream exergy	40869,3
Work (pumps)	1	Useless stream exergy	1585,3
Sum	43093		42454,6
Internal exergy losses	639	Total exergy losses	2224
Reduction in internal losses	51	Reduction in total losses	-827

Table 30: Exergy results in the equipment for the effect of removing H1401 and H1406.

Unit	Internal exergy loss [kJ/kg VCM]	Total exergy loss [kJ/kg VCM]	Reduction in internal loss [kJ/kg VCM]	Reduction in total loss [kJ/kg VCM]
C1401	236	236	-90	-90
H1402	393	1815	-250	-1137
H1405	7	171	1	10
Total reduction			-339	-1217

6.6   Test Comparison

In Table 31 and Table 33 the effects of the tests are presented sorted after their reduction of total exergy losses in the cracker unit and percentage reduction of fuel gas needs in the cracker respectively. The results of the calculations of RAI and RATI are given in percent in Table 32.

Table 31: The effects of the tests sorted after their reduction of total exergy losses in the cracker.

Test	Internal [kJ/kg VCM]	Total [kJ/kg VCM]	Reduction in internal loss [kJ/kg VCM]	Reduction in total loss [kJ/kg VCM]
Fouling H1406	2018	2174	-214	-227
Inc. excess air	1834	1978	-30	-32
Red. excess air	1804	1947	0	0
LP steam prod	1805	1935	-2	11
Preheat feed	1763	1884	41	63
No H1401	1733	1871	71	76
Preheat air	1658	1746	145	200
Preheat feed + air	1650	1736	154	210

Table 32: RAI and RATI presented in percent for the test cases.

	RAI %	RATI %
Fouling H1406	-0,54	-0,58
Inc. Excess air norm	-0,08	-0,08
Red. excess air	0,00	0,00
LP steam prod	0,00	0,03
Preheat feed	0,10	0,16
No H1401	0,18	0,19
Preheat air	0,37	0,51
Preheat feed + air	0,39	0,53

Table 33: The effects of the tests sorted after their percentage reduction of fuel gas needs in the cracker.

Test	Flow [tonne/hr]	Flow original case [tonne/hr]	Reduction [tonne/hr]	Reduction [%]
Fouling H1406	3.28	3.02	-0.26	-8.6
Inc. Excess air norm	3.05	3.02	-0.03	-1.0
Red. excess air	3.01	3.02	0.01	0.3
Preheat feed	2.96	3.02	0.06	2.0
No H1401	2.92	3.02	0.10	3.3
Preheat air	2.83	3.02	0.19	6.3
Preheat feed + air	2.82	3.02	0.20	6.6

6.7   Cracker Efficiency

The cracker efficiency for the original case and the different tests are presented in Figure 16 in ascending order.

	Fouling H1406	Inc. Excess air norm	No H1401	Original case	Red. excess air	LP steam prod	Preheat feed	Preheat air	Preheat feed + air
Efficiency	0,772	0,777	0,784	0,784	0,788	0,795	0,801	0,845	0,847
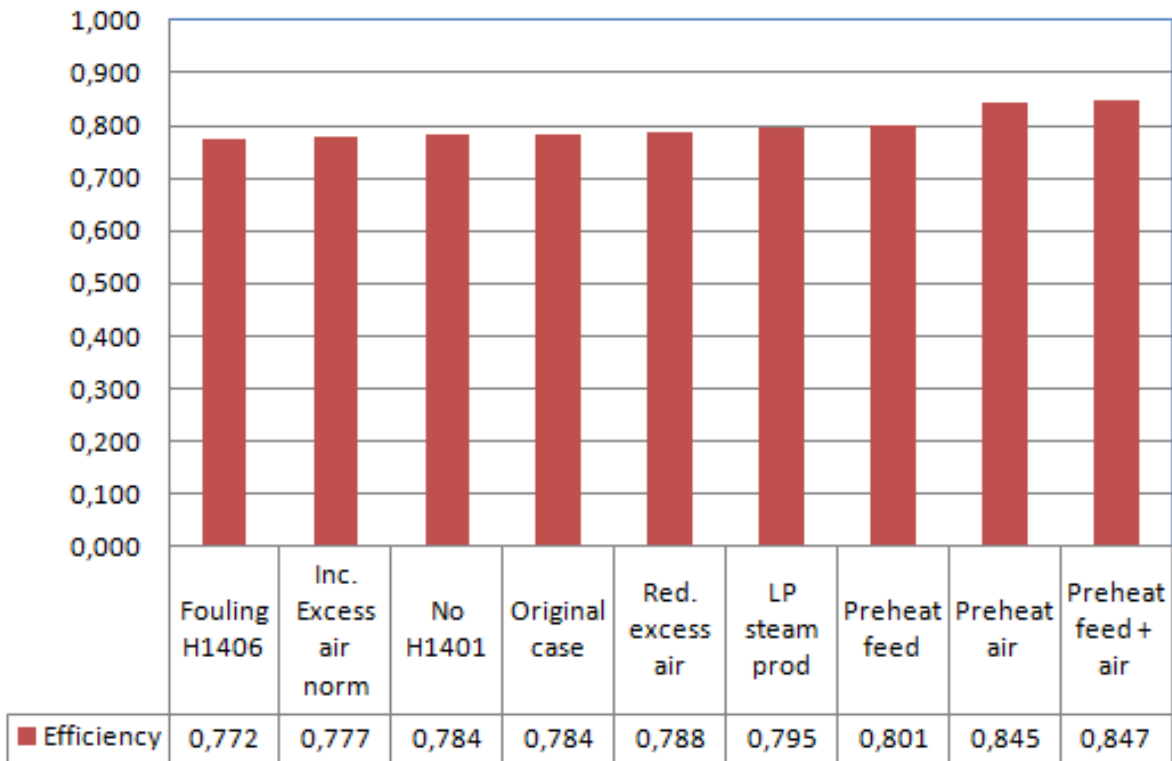
Figure 16: Cracker efficiency for the original case and the test cases.

7 Discussion

7.1 Exergy Calculations

7.1.1 Calculation of Physical Exergy

The choice of property method for the simulations in this project was discussed extensively in Karlsen [2010]. This choice was found to have a minor effect on the enthalpy and entropy results for a constant stream (approximately 1 % deviation in the physical exergy in the exit stream from the adiabatic reactor for both IDEAL and NRTL property methods). The different property methods have a much larger influence on the gas liquid equilibrium, and thereby the distribution of matter in the streams following a separation unit. The physical exergy for these types of streams can differ greatly with the property method. Peng-Robinson was found to give reasonably good results compared to the others which were tested in Karlsen [2010]. The physical exergy results are therefore thought to be representative for the plant.

7.1.2 Calculation of Chemical Exergy

The chemical exergy is also affected by the distribution of matter in the streams, but as for the physical exergy the results are thought to be good, and no further discussing will be performed here.

Several assumptions were made during the calculation of chemical exergy. The standard chemical exergy for the components were not corrected for different reference temperature and relative humidity. Standard chemical exergy was not calculated for the liquid phase of VCM and HCl, so the gas phase exergy was used when necessary. Ideal gas was assumed when determining the composition of gas and liquid phase in a stream at reference temperature and pressure, and the same was assumed when the chemical exergy of a mixed stream was calculated. As the results in Section 6.1 shows, the chemical exergy is the dominant term in the total exergy of the streams. Any serious errors caused by any of the assumptions mentioned above could affect the results noticeably. Note that any errors in the chemical exergy will cancel each other for balances over ordinary heat exchangers where only the temperature and pressure changes and not the composition.

The choice of not correcting the standard chemical exergies for deviating reference temperature and relative humidity was argued for in Section 5.3.2 as a minor error compared to errors in simulation results. The Gibbs free energy of formation for the other components were found in literature, but liquid phase VCM and HCl were not presented. The standard chemical exergy for VCM and HCl in liquid phase was thus not calculated. As the amount of HCl in particular, but also VCM, in liquid phase at reference conditions are minor. Hence these data were thought to be unimportant for the final results. According to the tabulated standard chemical exergy in Kotas [1995], the difference between standard chemical exergy for liquid and gas phase for a hydrocarbon is minor anyway.

The assumption of ideal gas is a common assumption to make, and very few sources deals with any other forms for calculation the exergy of a mixed stream. Xiang et al. [2004] con-

siders water vapor as ideal as long as its mole fraction is below 0.1. This is the case for the only stream containing water in this project - the flue gas from the cracker.

Table 12 shows some of the difference in real and simulated values, and these inaccuracies are thought to influence the results of the analyses much more than the errors resulting from the assumptions described above.

7.2   Base Case with Modifications - Simulation and Exergy Results

7.2.1   Base Case Simulation with Modifications

The simulation of the original base case was discussed at length in Karlsen [2010]. This discussion will therefore only include the parts of the simulation which are added during this project.

It was chosen to add cooling/heating media by adding an extra heater beside the first and connect the two with a heat stream. This could also have been solved by replacing the heater with a heat exchanger (HeatX), but the results would have been the same, since care was taken to avoid temperature crossover.

In one case though, the temperature crossover was not avoided. As described earlier, the HCl flow to the heat exchanger H1403 could not be adjusted as much as was necessary to avoid the crossover. Another solution could have been to adjust the flows in the top system by tuning outlet temperatures in the heat exchangers prior to H1403, but these temperatures had already been adjusted in the previous project to get the best possible distribution of flows. The crossover was therefore overlooked, as the results from this heat exchanger were thought to be relatively unimportant compared to the larger units in the process section.

The flow of cooling water in the heat exchangers was tuned according to the maximum cooling water return (CWR) temperature for the relevant cooling water network. This was found to be the only possible way to decide the cooling water flows, as there are no temperature measurements on the CWR from each heat exchanger. It is possible that the exit temperature is lower in some heat exchangers, resulting in a larger cooling water flow than what is simulated. As the irreversibilities in a heat exchanger increases with the temperature difference between the hot and cold side, the internal exergy losses calculated in this project are the minimum internal exergy losses that can be found at these operating conditions. Reductions in CWR temperature, at constant inlet and outlet temperature on the process side, will increase the internal exergy losses. It is also worth to notice that this also means that by using the warmest heat exchanger network where it is possible in the plant, the internal exergy losses are lower compared to what they would have been by using the coldest network.

7.2.2 Exergy Results for the Base Case

The total exergy loss of 59.51 MW corresponds nicely with a similar study done by Graveland and Gisolf [1998] which showed an exergy loss of 62.3 MW for the EDC cracking section in the plant under consideration. That study was for a production of 68.75 tonne VCM/hr, while this project looks at a production of 63.72 tonne VCM/hr. Notice that the configuration of the process section investigated in Graveland and Gisolf [1998], and its similarity with the same section at Rafnes, is unknown.

The distribution of the losses throughout the process section also turned out as expected. The major losses in the cracker are backed by results in Hinderink et al. [1996b] for similar equipment - a steam reformer in the production of synthesis gas. The exergy losses in the cracker are mainly of the internal type. Utilizing the heat in the flue gas to heat any random cold stream is therefore not very effective, as it only will reduce the quite minor external losses. The most useful application of this stream is in the preheating of reactants to the cracker; an action which reduced both the external and the internal losses in the unit. The rest of the equipment that contribute to large internal losses are all heat exchangers gathered in the top system, but these losses are just one fourth of the total internal losses as seen in Figure 13. The choice to focus mainly on the cracker system is therefore justifiable. The losses in the heat exchangers in the top system are in the same order of magnitude as the reboiler and condenser in Araújo et al. [2007], indicating that these results also are reasonable. The internal losses in the heat exchangers are difficult to avoid as this mainly would mean to reduce the temperature difference in the exchanger.

7.3 Temperature Tuning in H1401 - Simulations and Exergy Results

7.3.1 Simulation Results

The tuning of the outlet temperature in H1401 which was executed in the previous project was evaluated by two cases in this project. The background for this experiment was that the heat transferred in H1401 was not enough to produce the measured amount of low pressure steam. To reach this steam production (22.2 tonnes/hr) the outlet temperature in H1401 had to be reduced to 153 ℃, while at the measured outlet temperature (156.5 ℃) only 20.5 tonnes/hr steam was produced. The outlet temperature in the base case (159.5 ℃) gave a even lower steam production of 19.3 tonnes/hr. Still it was found that the other simulation results from Case one and two corresponds more poorly with the rest of the real process, indicating that the original case is the best simulation of the three cases. This is illustrated by the presented measurement comparisons in Table 12. The distribution of flow in the different streams was worse in the test cases than in the base case. The bottom flow from C1401 was unrealistically high in both cases, and the distribution of flow in the top system was a poorer match to the measured values than the one in the base case. It is still curious that both the low pressure condensate (LPC) and low pressure steam (LPS) flow measurements show the exact same value, indicating that the flow gauges probably cannot be too erroneous either.

7.3.2   Exergy Results

Figure 14 indicated that the largest differences in internal exergy losses for the three different simulations could be found in H1402, with the largest losses experiences in the base case. Figure 15 showed largest total exergy losses in the base case. This makes sense since H1406 removes a predefined amount of heat from the stream. H1402 will therefore in cases of higher outlet temperatures from H1401 remove a larger quantity of heat from the stream at a higher inlet temperature than in cases of lower outlet temperature in H1401. There are, in other words, both an increased temperature difference in the heat exchanger, giving larger internal losses, and a larger cooling water flow increasing the total losses. Even though the original case was tuned to give results corresponding as close as possible to the real plant, this test has shown that there are large insecurities in the results for H1402. The results also indicate that if any error exists in the exergy losses in H1402, they are lightly to be overestimated.

7.4   Tests done to Reduce Exergy Losses

Among the tests which are compared in Table 31, the six last tests on the list are the ones done seeking to reduce the exergy losses and hereby, among other things, reduce the fuel consumption in the cracker as seen in Table 33. As mentioned earlier in the report, these tests do not consider the potential need for a fan in the cracker system in order to utilize the flue gas. This is something that needs to be addressed if these results are to be considered further for any practical applications. Comments on the simulation of the tests are only given where it is found necessary.

In the context of utilizing the heat in the flue gas, a point to notice is the distribution of flue gas in different stacks. Cracker A and B share the same stack, while Cracker C has two stacks. The flue gas could e.g. either be collected into on single stream before any heat exchange, or the flue gas from the different stacks could be used to heat different streams. The latter solution would potentially result in several heat exchangers, while the former would give only one. The former solution would therefore probably lead to lower investment costs, allowing for a rebuild of the stack system, than the latter. Also notice the possibility of combining some of the tests to increase reductions in exergy losses further; e.g. the heat in the flue gas can be utilized at the same time as the amount of excess air is reduced. These are possibilities that have not been investigated in this project.

The reduction of combustion air did not give any noticeable results as the air was reduced from 3.3 to 2.0 vol% oxygen. It is known from literature that larger reductions would have given positive results.

The production of low pressure steam from some of the heat in the flue gas did not give any large improvements to the exergy losses either, as this measure only affects the external losses from the cracker. The internal exergy losses are actually increased, probably due to adding a heat exchanger to the system. The total exergy losses are nevertheless reduced, since the external losses from the flue gas are reduced by almost 10 %. It is also worth remembering

that the low pressure steam is a useful product which can be utilized in other parts of the plant.

The preheating of EDC feed to the cracker gives reduction in both internal and total exergy, resulting in an apparent reduction in fuel gas need of 2 %.

In the simulations where H1401 was removed to give larger heat transfer in H1406, some changes had to be made to the process. The most important change was that some of the reflux fluid had to be taken from V1401, as not enough was condensed in H1406. The changes were done without changing the set point in any of the equipment not directly affected by these changes. Whether these process values would have stayed unaffected in a real process has not been evaluated. By removing H1401 and using the heat to preheat the cracker feed instead, the exergy losses in the cracker were reduced. The losses in the top system on the other hand were increased. This means that the heat in the high temperature streams leaving H1406 in the top system is left unutilized, while the fuel gas needs in the cracker are reduced noticeably. It is a matter of evaluation which losses are preferred in this case. Cooling water at low temperature is abundant in the area the plant is located, making it a quite cheap resource. The fuel gas on the other hand is partly a non-renewable hydrocarbon and partly an energy carrier with an energy demanding production. In addition the VCM plant has a heat surplus in the form of net production of intermediate pressure steam in the oxychlorination reactor. All these factors, and more, need to be taken into consideration when deciding whether this is a sensible process solution or not.

Preheating the combustion air is one of the tests giving the largest reduction in exergy losses and fuel gas needs. The amount of air going into the combustion chamber at ambient temperature in the base case is vast, and heating it by over 150 ℃ has a great effect on the exergy efficiency in the unit. An advantage with this solution is that it most likely leaves the rest of the process section unaffected, both at ordinary operation and during start-up and shut down.

The test giving the best results is the preheating of both combustion air and EDC feed which gives a reduction in fuel gas needs of 6.6 %. The difference between this solution and only preheating the combustion air is small and would probably not justify investing in two heat exchangers instead of just one.

Though some of the tests show large reductions in exergy losses in the cracker, RAI and RATI indicate that these reductions are small compared to the exergy entering the cracker. At best they reach approximately 0.4 and 0.5 respectively. It is still thought that it is the economical evaluation of the tests which is important for their relevance.

The cracker efficiency is seen to be noticeably improved in the last to tests mentioned, compared to the base case. This shows a better utilization of the heat delivered by the fuel gas, than in today's plant. The increase in excess air because of fouling in H1406 or at normal operation conditions is not seen to have the same corresponding negative effect. For the case of fouling this can be explained by the fact that the extra heat supplied to the cracker is used to do the heating not accomplished in H1406, so no extra heat is actually lost with the flue

gas. For the increase in excess air under normal conditions, the increase in fuel gas is not that severe compared to the fouling case, so the effect on the cracker efficiency will be small even though the extra heat added is lost again with the flue gas.

7.5   Tests Illustrating Increased Exergy Losses

Several tests were done to illustrate both the punishment in form of increased exergy losses and fuel gas needs as the plant is run in a less than optimal way, and to see the effect of process integration in the top system of the process section. Table 31 summarizes the results for the two first tests - the cases of severe fouling in H1406 with resulting increase in excess air to the combustion chamber and the increase of excess air at normal operation conditions.

The fouling in H1406 as simulated in the relevant test is so severe that according to the results obtained in this project, the fuel gas needs be increased with 8.6 %. This is more than any reduction experienced in any of the other tests in the project. Large savings can naturally be done by avoiding this kind of operating conditions in the process section. The rest of the process section was not analyzed for this kind of scenario, so the effect on the rest of the equipment is unknown.

It is shown in a test that by increasing the excess air to the combustion chamber at otherwise normal operating conditions the exergy losses in the cracker, and thereby the need for fuel gas, are increased. Any unnecessary increase like this should evidently be avoided.

The test where both H1401 and H1406 were removed showed a very large increase in both internal and especially total losses in H1402. It is evident that the process integrations accomplished by adding H1401 and H1406 to the top system have done much to reduce the exergy losses in this part of the process section. Since the preheating of the EDC feed was not considered in this simulation, the extra energy needs in the feed system as a result of not having H1406 has not been evaluated. But the simulated heat duty in H1406 of over 7000 kW in the base case emphasizes the positive effect this heat integration has on the energy efficiency in the process section. It is still important to remember that the simulated process is far from similar to the one at the time before H1401 and H1406 was added to the plant. It has already been mentioned that the rest of the simulated process was kept as in the base case, and the simulation was only adjusted to the degree that in converged. This test has therefore only been done for illustrative purposes, and is to be look upon as a qualitative study as the numerical results are without any practical meaning.

8 Concluding Remarks

The total exergy losses in the EDC cracking section were 59.5 MW or 3362 kJ/kg VCM. The largest exergy losses in the process section were found in the cracker unit. The internal losses in the cracker were dominating and accounted for 75 % of all the internal exergy losses in the process section. The rest of the noticeable losses were discovered in the heat exchangers in the top system.

Preheating the EDC feed and the combustion air was found to give the largest reductions in the cracker exergy losses. This test show a reduction in fuel gas needs of 6.6 %. Reduction in excess combustion air on the other hand showed no noticeable reductions.

Fouling in H1406 and unnecessarily large amounts of excess air under normal conditions both result in large increases in exergy losses, and should be avoided if possible.

The uncertainties in the investigations results mainly from insecurities in the simulation.

References

A. C. B. Araújo, L. G. S. Vasconcelos, M. F. Fossy, and R. P. Brito. Exergetic and economic analysis of an industrial distillation column. *Brazilian Journal of Chemical Engineering*, 24(3):461–469, 2007.

AspenTech. Aspen Plus Help. The help file included in Aspen Plus 2006.5.

H. Auracher. Fundamental aspects of exergy application to the analysis and optimization of energy processes. *Heat Recovery Systems*, 4(5):323–327, 1984.

G. Aylward and T. Findlay. *SI Chemical Data.* John Wiley & Sons Australi, Ltd, 2002. 202 pages.

F. Benyahia. Flowsheeting Packages: Reliable or Fictitious Frocess Models? *Chemical Engineering Research and Design*, 78(6):840–844, 2000.

F. Bezzo, R. Bernardi, G. Cremonese, M. Finco, and M. Barolo. Using Process Simulators for Steady-state and Dynamic Plant Analysis: An Industrial Case Study. *Chemical Engineering Research and Design*, 82(4):499–512, 2004.

U. Blindheim. vinylklorid. `http://www.snl.no/vinylklorid`. Store norske leksikon (05.12.2010).

E. C. Carlson. Don't Gamble with Physical Properties for Simulations . *Chemical Engineering Progress*, 92(10):35–46, 1996.

A. C. Dimian and C. S. Bildea. *Chemical Proscess Design; Computer-Aided Studies.* Wiley-VCH, 1 edition, 2008. 508 pages.

A. Doldersum. Exergy analysis proves viability of process modifications. *Energy Conversion and Management*, 39(16-18):1781–1789, 1998.

I. S. Ertesvaåg. Exergetic comparison of efficiency indicators for combined heat and power (chp). *Energy*, 32(11):2038–2050, 2007.

I. S. Ertesvåg. Sensitivity of chemical exergy for atmospheric gases and gaseous fuels to variations in ambient conditions. *Energy Conversion and Management*, 48(7):1983–1995, 2007.

W. L. R. Gallo and L. F. Milanez. Choice of a reference state for exergetic analysis. *Energy*, 15(2):113–121, 1990.

A. J. G. G. Graveland and E. Gisolf. Exergy analysis: An efficient tool for process optimization and understanding. demonstrated on the vinyl-chloride plant of akzo nobel. *Computers and Chemical Engineering*, 22(SUPPL.1):S545–S552, 1998.

B. P. Guedes, M. F. Feitosa, L. S. Vasconcelos, A. B. Arautjo, and R. P. Brito. Sensitivity and Dynamic Behavior Analysis of an Industrial Azeotropic Distillation Column. *Separation and Purification Technology*, 56(3):270–277, 2007.

W. M. Haynes. *CRC handbook of chemistry and physics.* CRC Press/Taylor and Francis, Boca Raton, Fla., 91 edition, 2011.

A. P. Hinderink, F. P. J. M. Kerkhof, A. B. K. Lie, J. De Swaan Arons, and H. J. Van Der Kooi. Exergy analysis with a flowsheeting simulator - i. theory; calculating exergies of material streams. *Chemical Engineering Science*, 51(20):4693–4700, 1996a.

A. P. Hinderink, F. P. J. M. Kerkhof, A. B. K. Lie, J. De Swaan Arons, and H. J. Van Der Kooi. Exergy analysis with a flowsheeting simulator - ii. application; synthesis gas production from natural gas. *Chemical Engineering Science*, 51(20):4701–4715, 1996b.

Norwegian Meteorological Institute. eklima. `http://eklima.met.no/`, 2008. Meteorological data from Geiteryggen and Jomfruland for june 2008, extracted 07.03.2011.

T. H. Kaggerud. Basis for online calculation of edc cracker efficiency. a.

T. H. Kaggerud. INEOS Scandinavia Technology & Production Support - Personal correspondance, b.

T. H. Kaggerud. By-products Rafnes. a presentation at INEOS, 2010.

S. Karlsen. Energy utilization in edc cracking. Technical report, NTNU, 2010.

T. J. Kotas. *The exergy method of thermal plant analysis.* Krieger, Malabar, Fla., 1995. Opptrykk. Opprinnelig utg.: London : Butterworths, 1985.

R. W. McPherson, Ch. M. Starks, and G. J. Fryar. VINYL CHLORIDE MONOMER. . . WHAT YOU SHOULD KNOW. *Hydrocarbon Process*, 58(3):75–88, 1978.

A. Modarresi, W. Wukovits, D. Foglia, and A. Friedl. Effect of process integration on the exergy balance of a two-stage process for fermentative hydrogen production. *Journal of Cleaner Production*, 18(SUPPL. 1):S63–S71, 2010.

M. J. Moran and H. N. Shapiro. *Fundamentals of engineering thermodynamics.* Wiley, Hoboken, N.J., 6 edition, 2010.

K. Nishida, T. Takagi, and S. Kinoshita. Analysis of entropy generation and exergy loss during combustion. *Proceedings of the Combustion Institute*, 29(1):869–874, 2002.

S. Ore and Aa. Stori. polyvinylklorid. `http://www.snl.no/polyvinylklorid`. Store norske leksikon (05.12.2010).

Perry. *Chemical Engineers' Handbook.* McGraw-Hill, 1973.

pvc.org. Vinyl chloride monomer (vcm) production. `http://www.pvc.org/What-is-PVC/How-is-PVC-made/Vinyl-Chloride-Monomer-VCM-Production`. pvc.org (05.12.2010).

E. Querol, B. Gonzalez-Regueral, A. Ramos, and J. L. Perez-Benedito. Novel application for exergy and thermoeconomic analysis of processes simulated with aspen plusÂő. *Energy*, 36(2):964–974, 2011.

R. Rivero and M. Garfias. Standard chemical exergy of elements updated. *Energy*, 31(15): 3310–3326, 2006.

E. Sciubba and G. Wall. A brief commented history of exergy from the beginnings to 2004. *International Journal of Thermodynamics*, 10(1):1–26, 2007.

S. K. Som and A. Datta. Thermodynamic irreversibilities and exergy balance in combustion processes. *Progress in Energy and Combustion Science*, 34(3):351–376, 2008.

D. Stanciu, D. Isvoranu, M. Marinescu, and Y. Gogus. Second law analysis of diffusion flames. *International Journal of Applied Thermodynamics*, 4(1):1–18, 2001.

J. Szargut. *Exergy analysis of thermal, chemical, and metallurgical processes / Jan Szargut, David R. Morris, Frank R. Steward.* Hemisphere, New York, 1988.

J. Szargut. *Exergy method: technical and ecological applications.* WIT Press, Southampton, 2005.

Tarragon. Operational data from the EDC cracking section extrackted from Tarragon and PHD, INEOS Porsgrunn.

Z. Wang and D. Zheng. Exergy analysis and retrofitting of natural gas-based acetylene process. *Chinese Journal of Chemical Engineering*, 16(5):812–818, 2008.

P. W. Wølneberg and I. S. Ertesvåg. Alternatives for power supply to natural-gas export compressors combined with heat production evaluated with respect to exergy utilization and co2 emissions. *Energy Conversion and Management*, 49(12):3531–3540, 2008.

J. Y. Xiang, M. Cali, and M. Santarelli. Calculation for physical and chemical exergy of flows in systems elaborating mixed-phase flows and a case study in an irsofc plant. *International Journal of Energy Research*, 28(2):101–115, 2004.

Appendices

A   Simulation

Below is the description of the development of the simulation in Aspen Plus. The text is the same as was presented in Karlsen [2010].

A.1   The Choice of Property Method

Commercial simulation software like Aspen Plus are very powerful tools in the development of mass and energy balances for chemical processes. The challenge lies in giving the software the appropriate kinetic and thermodynamic data. The software will give you an output no matter how unsuitable the chosen or entered data is. This can lead to misinterpretations of the systems and its properties, and resulting in large errors. In Benyahia [2000] different property methods have been used in a simulation of a VCM factory, and the results have been compared. Large differences appear between the different thermodynamic models, and the article acts as an illustrative example of the importance of the correct choice of a physical property method.

The choice of the most suitable property method for the simulation of the EDC cracking section was researched before the simulation was established in Aspen Plus. Especially two variables seemed to be important for the choice of property method - the HCl being a polar component and the pressure being moderately high. Literature describing other simulations of different process sections in VCM plants was used to limit down the relevant methods. Dimian and Bildea [2008] describe the simulation of an entire VCM plant, and it is stated that for simple flash separations SR-POLAR should be applied while for distillation NRTL-RK is more appropriate. SR-POLAR is an extension of the Soave-Redlich-Kwong (SRK) equation of state (EOS) which can be applied to both highly polar and non-polar components [AspenTech]. NRTL-RK uses an activity coefficient method in the liquid phase and the Redlich-Kwong EOS in the vapour phase [AspenTech]. AspenTech itself recommends either Peng-Robinson or SRK EOS in simulations of VCM plants. Guedes et al. [2007] and Bezzo et al. [2004] indicat that NRTL-RK could be a good choice, but [Bezzo et al., 2004] points out that at higher pressure calls for an EOS. Also notice that it is a distillation that is simulated in Guedes et al. [2007], while no such extensive separations are done in the cracking section. By making use of the navigation trees for selection of physical property method in Carlson [1996] the result is also some extended variant of Peng-Robinson or SRK because of the high pressures. At INEOS there is already experience with Peng-Robinson in VCM simulation, so this was chosen as the property method for the project simulations.

In his article Benyahia [2000] concludes with a couple of recommendations for obtaining reliable simulations:

- "Always use plant data whenever available."

- "Always run your simulations with at least two "suitable" thermodynamic property methods. You will find areas of your process where extra caution must be exercised."

With that in mind, the base case simulation will also be run using SR-POLAR and NRTL-RK, and the results will be compared. The first point will be automatically followed as the simulation is to be established for an already existing process.

A.2   Simulation Periods and Base Case

In the detailed project assignment, it was suggested that sensitivity analyses should include load and time on stream. Time on stream is connected to the periodic decoking of the crackers, which is done every nine to twelve months. This sensitivity analysis would examine potential changes in energy requirements as a result of the time elapsed since last decoking. The other sensitivity analysis would look at changes in energy requirements as a function of the load.

To carry out these analyses, data[Tarragon] was extracted from several different time periods when the plant was running steadily. These data was then averaged over the whole respective period. The periods of different loads are given in Table 34 with the loads indicated as tonnes VCM produced per day. The periods for the time on stream analysis are given in Table 35 together with number of months since last decoking of cracker F-1401B. The chosen periods are from two different "coking periods" for cracker B as it was difficult to find a sufficient number of stable periods at full load within just one "coking period". Notice that P7 and P13 are the same period. Simulations were established in Aspen Plus for all these periods, twelve in total. To be able to compare the different simulations P8 was chosen base case after recommendation from INEOS.

Table 34: Simulation periods for different loads

Period Name	Dates [dd.mm.yyyy tt:mm]	Load [tonne VCM/day]
P1	17.01.2009 01:00 23.01.2009 19:00	885
P2	28.01.2010 01:00 31.01.2010 19:00	1032
P3	19.12.2009 01:00 24.12.2009 19:00	1101
P4	11.12.2008 01:00 16.12.2008 13:00	1207
P5	25.12.2008 01:00 31.12.2008 19:00	1305
P6	21.09.2010 02:00 27.09.2010 08:00	1413
P7	11.10.2010 02:00 19.10.2010 02:00	1546

A periode from the time right before a decoking was also included intially, but this turned out to be too unstable to be used. The sensitivity analysis of time on stream is therefore lacking any results from the last months of a "coking period". The analysis can with advantage be improved at a later time.

A.3   Assumptions

When the mass and energy balances for the system were establish, some assumptions were made. This section gives a summary of these assumptions.

Table 35: Simulation periods for different time on stream

Period Name	Dates [dd.mm.yyyy tt:mm]	Month on Stream
P8	20.06.2008 02:00 23.06.2008 08:00	0
P9	18.07.2008 02:00 24.07.2008 02:00	1
P10	12.08.2010 02:00 16.08.2010 20:00	3
P11	28.10.2008 01:00 02.11.2008 01:00	4
P12	09.11.2008 01:00 16.11.2008 01:00	5
P13	11.10.2010 02:00 19.10.2010 02:00	5

At the plant there are three crackers, adiabatic reactors and quench towers in parallel. In the simulation, these three parallels have been lumped together into one single stream, containing only three units. This is done since the size of the units have no influence on the way they are simulated. This assumption was modified with the size regulation of C-1401 described in the following section. It is assumed that the temperature, pressure and analyses can be averaged over the three parallel streams, and that the total flow is the sum of all three parallels. Some of the measurements exist for both of the coils inside each cracker. In those cases it has been averaged over all six measurements.

Three of the heat exchangers in the process section consist of two or more units in parallel. These heat exchangers are H-1402 A and B, H-1405 A and B and H1407 A, B and C. In H-1402 only A is used. For the other two, all of the units are used. It is assumed that they can be lumped together into two large heat exchangers. This is done since the desired results from the heat exchangers is the energy input/output at given inlet and exit temperatures, and this result independent of the geometry of the heat exchangers.

There is no measurement of the pressure drop over most of the heat exchangers in the system. Where no measurements or other information exist, it is assumed a pressure drop of 0.1 bar.

In H-1401 it is assumed that the low pressure condensate is at its boiling point when entering the heat exchanger.

No temperature measurements exist after H-1451. The exit temperature is assumed to be 30°C [Kaggerud, b].

The cracker feed in the plant contains some impurities. These impurities are mainly benzene and trichloroethene at maximum amounts of 5000 ppm per component. It is assumed that these impurities can be neglected. A test simulation completed in this project for a feed stream with impurities indicates that this assumption gives an error of less than 1 % in the cracker.

A lot of different by-products are produced during the thermal cracking of EDC. It is assumed that the by-product formation can be neglected. Calculations done earlier at INEOS indicate that the by-product distribution is 0.058 tonnes per hour of light elements and 0.805 tonnes

per hour of heavy elements [Kaggerud, 2010]. Acetylene was used to model the light elements and 1,1,2-trichloroethane to model the heavy elements. The resulting by-product reactions are given by Equations 24 and 25. For this simulation test Cl_2 has been taken in as an impurity in the feed. Note that the amount of Cl_2 needed in order to simulate Reaction 25 not represents true conditions in the EDC cracker at Rafnes. The real amount of Cl_2 has not been investigated. A test simulation including by-product formation was completed during this project, and the results indicated an error of less than 1 % in the cracker when the by-products are neglected. During the simulation it was assumed that all by-product formation happened in the cracker, and none in the adiabatic reactor.

$$VCM \rightarrow C_2H_2 + HCl \tag{24}$$

$$VCM + Cl_2 \rightarrow 1, 1, 2 - \text{trichloroethane} \tag{25}$$

The contributions from pump P-2703, pumping EDC from the dry EDC storage tank T-2702 to the furnace feed drum V-2704, is neglected. This pump transports the EDC, but gives no noticeable increase in pressure. The work done by it is therefore a lot less than most of the other pumps in the system.

As mentioned in the process description in Section 2.2 the fuel gas in the plant contains mainly hydrogen and methane. In reality it also contains small amounts of ethane (approx. 1-2 mol%), but this has been neglected.

The bottom stream from C-1401 is in reality taken out in pulses. For the sake of a steady state simulation it has been assumed to be a constant flow.

The EDC stream taken out as HPF is neglected. The feed stream in the simulation is adjusted to be of the same size as the total feed to the crackers.

A.4   Simulating in Aspen Plus

The system contains two reactors, the cracker (F-1401) and the following adiabatic reactor (F-1401-AR). They have been simulated as stoichiometric reactors where Reaction 3 is specified at given conversions of EDC. F-1401 was in addition specified with an outlet temperature together with a pressure drop. F-1401-AR, being an adiabatic reactor, was specified with a pressure drop and zero heat duty. A total conversion is calculated online in the plant for both the reactors together. When dividing the conversion between the two reactors, it was initially guessed that F-1401-AR had a constant conversion of five percentage points, and that the rest of the conversion took place in F-1401. This was information supplied by INEOS.

As both preheating and vaporization of EDC also takes place in F-1401, this unit was split into three separate units - two heat exchangers and a stoichiometric reactor, as already mentioned. This was done in order to examine the distribution of energy requirements in the cracker, between the convective zone (preheating), the shock zone (vaporization) and the

reaction zone. In the plant there is a measurement of the pressure drop over the reactors. At INEOS they have in addition used EDC Crack® to simulate the pressure drop over the convection and shock zone in the cracker at full load. EDC Crack® is a commercial simulation software which predicts the cracking of EDC. The simulated pressure drops were specified in the two heat exchangers in base case P8, while the rest of the total pressure drop was assigned to the reactor F-1401. Since F-1401-AR only is a simple, insulated pipe, it was assumed to be without any noticeable pressure drop. The other simulated periods had different total pressure drops than the base case. For these periods the pressure drops in the heat exchangers were weighted against the pressure drops in the base case.

F-1401 is heated by combustion of fuel gas. The fuel gas chamber was simulated with a Gibbs reactor. Fuel gas and air (79 mol% nitrogen and 21 mol% oxygen) entered as feed. The composition of the fuel gas is not constant over time, so it was calculated from density measurements for each period with the assumption of ideal gas. Each cracker has flow gauges on the fuel gas feed, but these measurements are converted into an energy flow and only displayed in megawatt. To get a mass flow of fuel gas, this energy flow was converted back with the use of the already calculated fuel gas composition and the lower heating value of methane and hydrogen. In the Gibbs reactor, outlet pressure and heat duty was specified. To get the correct outlet temperature, a design spec was added. This design spec manipulated the heat duty of the reactor. To get the measured excess of air in the combustion, a second design spec was added which manipulated the feed flow of air. The cracker and the fuel gas chamber were not connected in any way in the simulation, but the results from both where compared.

The quench tower, C-1401, has been simulated using RadFrac with no condenser or reboiler and five theoretical stages. The feed gas was fed under the bottom tray and the reflux was fed on the top tray. The pressure in the top of the column was specified. It was thought that the large mass flow through the column might influence the convergence of the column. It was therefore added a manipulator to all the inlet and exit streams which divided or multiplied them with three, reducing the size of the column to its actual plant size.

In both H-1401 and H-1406 heat is exchanged between two process media. The hot exit gas is used for vaporizing and heating low pressure condensate and cracker feed respectively. These heat exchangers have been simulated by two simple exchangers each, coupled by a heat stream. This is a standard trick in Aspen Plus, as the two-stream heat exchanger tends to be difficult to work with. There is a third integrated heat exchanger in the system, H-1403, but since the cold side of this is not important for the project, it has been simulated as a standard cooler.

H-1401 and H-1406 are similar in another way too. Gas is condensed in both, and the condensate is separated from the gas and sent to V-1406 to be used as reflux in C-1401. To achieve this separation in Aspen Plus, a flash tank (Flash2) was added after both the heat exchangers. This is done with the assumption that gas and liquid are at equilibrium at the heat exchanger outlet.

V-1406 is the reflux tank and it is simulated as a Flash2. In the plant this vessel has a gas

equalization line that enters the top system between H-1401 and H-1406. An implementation of this was also tried in the simulation, but as the reflux system already was part of a loop, it turned out to be hard to make it converge together with the additional small loop. The gas outlet from V-1406 is therefore not connected to the rest of the process. The gas stream exiting is smaller than one tonne for most of the periods, so the error in doing this is negligible.

The rest of the simulation was established using simple heat exchangers, flash tanks, pumps and valves. The simulation flow scheme is shown in Figures 17 and 18.

A.5   Tuning of the Simulations

The guess that five percentage point of conversion takes place in F-1401-AR turned out to be a conservative guess. The simulated outlet temperature after F-1401-AR was too high for this to be correct. The distribution of the total conversion was tuned for each period to obtain the correct outlet temperature. The resulting conversion in F-1401-AR varied between seven and eight percentage points.

The major tuning problem in the simulation turned out to be the reflux flow to C-1401. The simulated reflux flow was far from large enough, even though all the temperatures around the reflux loop were at, or very close to, the measured values. It was informed early on in the project that the flow gauge on the reflux going to C-1401 C was showing a quantity that was too large. This measurement was therefore left out. Instead the flow measurements from tower A and B was averaged, and the averaged sum was multiplied by three to get an estimated reflux quantity. Still the simulated reflux flow was too small. Adjustments in temperatures and pressures in heat exchangers in the loop did not have the wanted effect, as an increase in reflux flow also gave lower reflux temperature with the result of a too large liquid stream from C-1401 entering the bottom system. After consulting INEOS it was decided that all three flow gauges on the reflux streams probably indicated too large values. The simulation was then tuned to get the most correct temperatures in the loop and a bottom stream from C-1401 in the desired area of 9-12 tonnes per hour (with an absolute maximum of 15 tonnes per hour). This was done by manipulating the outlet temperature in H-1401. This temperature had to be increased in all periods.

In the bottom system there were problems with the outlet temperature in H-1407. The online temperature measurements on the outlet streams have not been working in any of the periods simulated, so the measured temperature in the following flash tank, V-1402, has been used in the simulations instead. This turned out to give cooling instead of heating in H-1407, which is not the case in reality. The measurement had to be defect as the temperature also gave a gas flow out of V-1402 which was too small. It was assumed that the flow measurement on the gas stream was more accurate, and the outlet temperature in H-1407 was tuned to get the correct gas flow. A problem with this measurement is that it is affected by the pulsing stream enter the bottom system, so the average value can not be employed. Investigation of the measured values indicates a flow of 2 tonnes/hr, and this has been used in the tuning of the periods. This way heating was obtained in H-1407 in all the periods.

In the top system, the distribution of gas and liquid in the flash tanks (V-1401 and V-1404) was far from the measured flow values. The liquid flow from V-1401 was typically 10 tonnes per hour too low and the gas flow entering C-1501 was too large. A more correct distribution was obtained by lowering the outlet temperature in H-1402 down to approximately 60 ℃. An even better distribution was obtained by also lowering the outlet temperature in H-1405 by a couple of degrees.
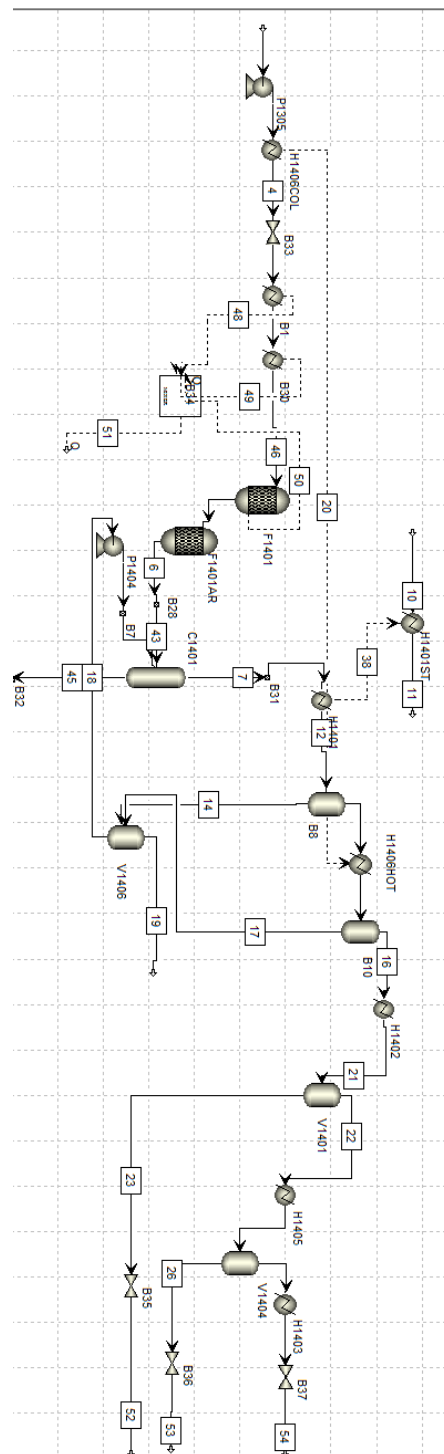
Figure 17: Flow scheme showing the simulation of the cracking and the top system in the EDC cracking section
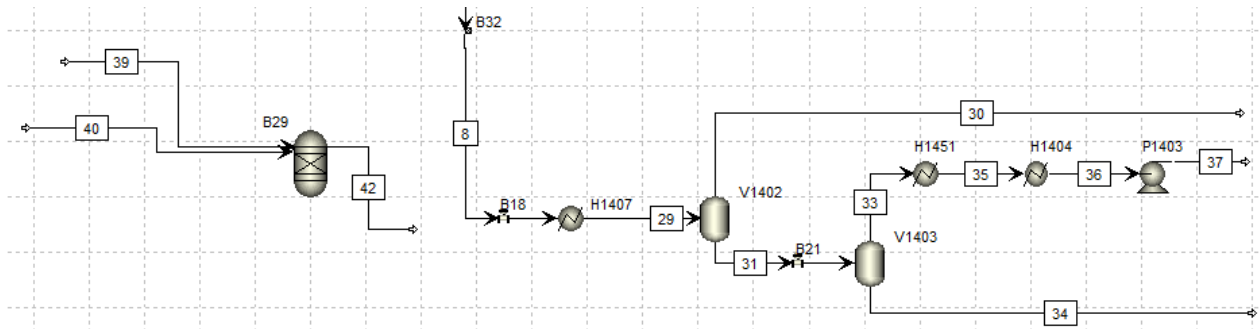
Figure 18: Flow scheme showing the simulation of the combustion chamber and the bottom system.

B Calculation of Stream Composition

The composition of the liquid og gas phase of a mixed stream needed to be found in order for the chemical exergy of the stream to be calculate. Aspen Plus reported the total composition of the stream, the liquid fraction and the vapor pressure of the components. Ideal gas was assumed in the calculation.

The total flow of liquid was found from the liquid fraction and the total mole flow. The total flow of gas was the difference between the total flow and the liquid flow. The composition of the gas phase was calculated from the vapor pressure like in Equation 26.

$$y_i = \frac{p_i}{P_{tot}} \tag{26}$$

The composition of the liquid phase was found from Equation 27

$$x_i = \frac{n_{tot,i} - n_{gas,i} y_i}{n_{liquid}} \tag{27}$$

C Stream Results from the Different Tests

In this appendix the results from the stream calculations in all the tests are given. Only the streams that changed during the test calculation were recalculated.

Table 36: Pre-heating of air for combustion.

Stream	Physical exergy [W]	Chemical exergy [W]	Total exergy [kW]
11901	0	52840172	52840
12001	0	0	0
12102	803928	750061	1554
10104	1310160	639204565	640515
10201	16124029	646324699	662449

Table 37: Production of low pressure steam by the remaining heat in the flue gas.

Stream	Physical exergy [W]	Chemical exergy [W]	Total exergy [kW]
12102	1500871	800439	2301
12411	32259	15111	47
12412	228192	15111	243
11901	0	56387749	56388
12001	0	0	0
10104	1310160	639204565	640515
10201	16124029	646324699	662449

Table 38: Further heating of EDC feed to crackers by remaining heat in the flue gas

Stream	Physical exergy [W]	Chemical exergy [W]	Total exergy [kW]
11901	0	55267454	55267
12001	0	0	0
12102	1360259	784515	2145
10103	1318665	639204565	640523
10201	16124029	646324699	662449

Table 39: Further heating of EDC feed and air to crackers by remaining heat in the flue gas

Stream	Physical exergy [W]	Chemical exergy [W]	Total exergy [kW]
11901	0	52653456	52653
12001	0	0	0
12103	781195	747326	1529
10103	1318665	639204565	640523
10201	16124029	646324699	662449

Table 40: Reduction of excess air to the combustion.

Stream	Physical exergy [W]	Chemical exergy [W]	Total exergy [kW]
11901	0	56387752	56388
12001	0	0	0
12101	1687429	832053	2519
10104	1310160	639204565	640515
10201	16124029	646324699	662449

Table 41: Increase of excess air to the combustion fouling H1406

Stream	Physical exergy [W]	Chemical exergy [W]	Total exergy [kW]
12101	1954850	809825	2765
10104	476872	639204565	639681
11901	0	61242318	61242
10201	16124029	646324699	662449

Table 42: Increase of excess air to the combustion, normal conditions

Stream	Physical exergy [W]	Chemical exergy [W]	Total exergy [kW]
12101	1782699	771636	2554
11901	0	56947889	56948
10104	1310160	639204565	640515
10201	16124029	646324699	662449

Table 43: Further heating of EDC feed to crackers by removing H1401

Stream	Physical exergy [W]	Chemical exergy [W]	Total exergy [kW]
10103	1811056	639204565	641016
10104	1802336	639204565	641007
10402	12654688	1341186251	1353841
10701	1035828	395112354	396148
10801	1098078	729882012	730980
10802	1103299	729882012	730985
10901	8926922	974915393	983842
10902	3496667	974915393	978412
11001	1727592	109426013	111154
11002	1611759	109426013	111038
11101	1275133	55617387	56893
11102	1261827	55617387	56879
11103	1239384	55617387	56857
11201	280827	53866215	54147
11202	280264	53866215	54146
11301	1642894	865683655	867327
11402	139536	35893578	36033
11901	0	54520597	54521
12101	1662490	773915	2436
12201	314170	28840760	29155
12403	180839	16621693	16803
12404	718991	16621693	17341
12405	54206	3022126	3076
12406	32689	3022126	3055
12501	1703387	24108296	25812
12502	1671499	24108296	25780
12701	8739171	946078156	954817
12801	952879	502096516	503049
12802	948113	502096516	503045
12901	690015	363587139	364277
12902	690267	363587139	364277
10201	16124029	646324699	662449
10301	14810632	647250874	662062
10102	102792	639204565	639307

Table 44: The effect of removing H1401 and H1406

Stream	Physical exergy [W]	Chemical exergy [W]	Total exergy [kW]
10301	14810632	647250874	662062
10402	11930856	1309158457	1321089
10801	1439251	701884102	703323
10802	1437915	701884102	703322
10902	4253116	1309158456	1313412
11001	1639484	99211326	100851
11301	2481465	1210145010	1212626
11402	155283	39963275	40119
12403	263039	24177007	24440
12404	981511	24177007	25159
12405	51496	2871020	2923
12406	31115	2871020	2902
12501	989667	72324889	73315
12502	956549	72324889	73281
12701	1042215	508260901	509303
12702	1033101	508260901	509294
11103	1147826	49011373	50159
11202	281336	50251232	50533
11002	1530298	99211326	100742
11101	1196834	49011373	50208
11102	1184570	49011373	50196

D Exergy Balances for all Equipment in the Process Section

Table 45: Internal exergy losses in flash tanks

Unit	Exergy loss [kJ/kg VCM]
V1401	-3,7
V1404	-0,1
V1406	0,6
V1402	0,2
V1403	0,2

Table 46: Internal and total exergy losses in all the heat exchangers in the process section.

Unit	Internal exergy loss [kJ/kgVCM]	Total exergy loss [kJ/kgVCM]
H1406	61	61
H1402	143	678
H1401	20	20
H1405	8	181
H1403	3	3
H1407	0	1
H1451	5	66
H1404	0	0

Table 47: Exergy losses in all the valves in the process section.

Unit	Exergy loss [kJ/kg VCM]
Valve B33	0,5
Valve B18	0,2
Valve B21	2,1
Valve B37	1,2
Valve B36	0,0
Valve B35	0,2

Table 48: Internal and total exergy losses in miscellaneous equipment in the process section.

Unit	Internal exergy loss [kJ/kgVCM]	Total exergy loss [kJ/kgVCM]
C1401	146	1947
Cracker	1804	146
Adiabatic reactor	22	22

E   Energy Content in Fuel Gas

During the autumn project the fuel gas compositions was calculated for the base case. It was found to compose of 71 % hydrogen and 29 % methane. The energy in the fuel gas was calculated for all the tests from the simulated fuel gas flow, the composition of the gas, the molar mass of hydrogen and methane [Aylward and Findlay, 2002] and the lower heating value of hydrogen, methane and propane. The lower heating value ($H_{burn,i}$) is 57,80 kcal/mol and 191,80 kcal/mol for hydrogen and methane respectively [Perry, 1973]. Table 49 gived the simulated fuel gas flows. Equations 28, 29, 30 and 31 were used in the calculations. Table 50 gives the results.

Table 49: Fuel gas needs in the different simulations.

	Fuel gas flow [tonne/hr]
Fouling H1406	3,28
Inc. Excess air norm	3,05
No H1401	2,92
Original case	3,02
Red. excess air	3,01
LP steam prod	3,02
Preheat feed	2,96
Preheat air	2,83
Preheat feed + air	2,82

$$M = (x_{H_2}M_{H_2} + x_{Me}M_{Me}) \tag{28}$$

$$H'_{burn} = (x_{H_2}H_{burn,H_2}) + (x_{Me}H_{burn,Me}) \tag{29}$$

$$H_{burn} = \frac{H'_{burn}}{M}1000 \tag{30}$$

$$E_{tot} = H_{burn}F_{fuelgas} \tag{31}$$

Table 50: Energy in fuel gas.

	Total fuel gas heat [MW]
Fouling H1406	60,8
Inc. Excess air norm	56,5
No H1401	54,1
Original case	55,9
Red. excess air	55,8
LP steam prod	55,9
Preheat feed	54,8
Preheat air	52,4
Preheat feed + air	52,2

F   Calculation Results from Aspen Plus

In this appendix the stream results from the simulations in Aspen Plus are given. Only the relevant streams are presented for the test simulations, while results from all streams are given for the base case.

F.1   Base Case Simulation

Table 51: Stream results from base case.

Stream	10101	10102	10103	10104	10201
Liquid Fraction	1	1	1	1	0
Vapor Fraction	0	0	0	0	1
Enthalpy [J/kmol]	-166736500	-166442400	-151591900	-151591900	-30010410
Entropy [J/kmol K]	-291149,9	-290870,3	-248196,3	-248134,3	-22847,96
Mole Flow [kmol/s]	0,48	0,48	0,48	0,48	0,73
Temperature [°C]	18,4	19,54	133	133,05	498,5
Pressure [barg]	0	27,2	27,1	24,3	19
Mole Fraction					
EDC	1	1	1	1	0,31
VCM	0	0	0	0	0,34
HCL	0	0	0	0	0,34

Table 52: Stream results from base case.

Stream	10301	10302	10401	10402	10501
Liquid Fraction	0	0	0	0	0
Vapor Fraction	1	1	1	1	1
Enthalpy [J/kmol]	-28691430	-28691430	-67903370	-67903370	-57520460
Entropy [J/kmol K]	-19798,34	-19798,34	-93605,54	-93605,54	-73618,62
Mole Flow [kmol/s]	0,76	0,25	0,46	1,37	0,96
Temperature [°C]	461,78	461,78	176,51	176,51	159,5
Pressure [barg]	19	19	19	19	18,6
Mole Fraction					
EDC	0,25	0,25	0,49	0,49	0,35
VCM	0,37	0,37	0,29	0,29	0,34
HCL	0,37	0,37	0,23	0,23	0,31

Table 53: Stream results from base case.

Stream	10601	10701	10801	10802	10803
Liquid Fraction	1	1	1	1	1
Vapor Fraction	0	0	0	0	0
Enthalpy [J/kmol]	-119814900	-112913700	-117711500	-117698200	-117698500
Entropy [J/kmol K]	-202526,9	-197448,4	-201510,7	-201503,1	-201503,3
Mole Flow [kmol/s]	0,41	0,24	0,65	0,65	0,22
Temperature [℃]	159,5	138,02	151,05	151,15	151,15
Pressure [barg]	18,6	17,9	17,9	19	19
Mole Fraction					
EDC	0,81	0,74	0,79	0,79	0,79
VCM	0,15	0,2	0,17	0,17	0,17
HCL	0,04	0,06	0,04	0,04	0,04

Table 54: Stream results from base case.

Stream	10901	10902	11001	11002	11101
Liquid Fraction	0	0,63	0	0,27	0
Vapor Fraction	1	0,37	1	0,73	1
Enthalpy [J/kmol]	-48752610	-66134320	-59118550	-64697480	-72441510
Entropy [J/kmol K]	-55011,95	-101593,5	-24687,8	-42439,97	-22012,86
Mole Flow [kmol/s]	0,71	0,71	0,27	0,27	0,2
Temperature [℃]	138,02	60	60	28	28
Pressure [barg]	17,9	17,8	17,79	17,69	17,69
Mole Fraction					
EDC	0,22	0,22	0,01	0,01	0
VCM	0,39	0,39	0,28	0,28	0,17
HCL	0,39	0,39	0,71	0,71	0,83

Table 55: Stream results from base case.

Stream	11102	11103	11201	11202	11301
Liquid Fraction	0,15	0,14	1	0,98	1
Vapor Fraction	0,85	0,86	0	0,02	0
Enthalpy [J/kmol]	-75038710	-75038540	-43222650	-43222610	-70317330
Entropy [J/kmol K]	-30781,63	-30411,52	-99091,8	-99064,7	-147459,8
Mole Flow [kmol/s]	0,2	0,2	0,07	0,07	0,45
Temperature [℃]	16,9	14,85	28	25,59	60
Pressure [barg]	17,59	16,5	17,69	16,5	17,79
Mole Fraction					
EDC	0	0	0,05	0,05	0,34
VCM	0,17	0,17	0,57	0,57	0,46
HCL	0,83	0,83	0,39	0,39	0,2

Table 56: Stream results from base case.

Stream	11302	11401	11402	11403	11404
Liquid Fraction	0,98	1	1	0,9	0,8
Vapor Fraction	0,02	0	0	0,1	0,2
Enthalpy [J/kmol]	-70317110	-127358800	-127358800	-127358800	-124382700
Entropy [J/kmol K]	-147427,9	-208078,9	-208078,9	-207803,7	-201113,8
Mole Flow [kmol/s]	0,45	0,01	0,04	0,04	0,04
Temperature [℃]	57,77	182,43	182,43	169,25	175
Pressure [barg]	16,5	19	19	12,6	12,5
Mole Fraction					
EDC	0,34	0,88	0,88	0,88	0,88
VCM	0,46	0,09	0,09	0,09	0,09
HCL	0,2	0,03	0,03	0,03	0,03

Table 57: Stream results from base case.

Stream	11501	11601	11602	11701	11702
Liquid Fraction	0	1	0,61	0	1
Vapor Fraction	1	0	0,39	1	0
Enthalpy [J/kmol]	-82300920	-134590700	-134590700	-102397500	-141951500
Entropy [J/kmol K]	-123671,2	-219899,3	-215859,9	-147403,6	-260739,3
Mole Flow [kmol/s]	0,01	0,03	0,03	0,01	0,01
Temperature [℃]	175	175	93,66	93,66	15,6
Pressure [barg]	12,5	12,5	0,5	0,5	0,4
Mole Fraction					
EDC	0,69	0,93	0,93	0,84	0,84
VCM	0,22	0,06	0,06	0,14	0,14
HCL	0,1	0,01	0,01	0,02	0,02

Table 58: Stream results from base case.

Stream	11704	11703	11801	11901	12001
Liquid Fraction	1	1	1	0	0
Vapor Fraction	0	0	0	1	1
Enthalpy [J/kmol]	-143430800	-143739100	-155142900	-21920230	-300378,2
Entropy [J/kmol K]	-266307,4	-267103,6	-259562,7	-19423,77	3253,43
Mole Flow [kmol/s]	0,01	0,01	0,02	0,14	0,74
Temperature [℃]	1,86	-0,3	93,66	15	15
Pressure [barg]	12,5	0,3	0,5	0	0
Mole Fraction					
EDC	0,84	0,84	0,99	0	0
VCM	0,14	0,14	0,01	0	0
HCL	0,02	0,02	0	0	0
CO2	0	0	0	0	0
N2	0	0	0	0	0,79
METHANE	0	0	0	0,29	0
H2	0	0	0	0,71	0

Table 59: Stream results from base case.

Stream	12101	12201	12301	12401	12402
Liquid Fraction	0	0	0,94	1	0,01
Vapor Fraction	1	1	0,06	0	0,99
Enthalpy [J/kmol]	-65654930	-53313140	-72334270	-276241200	-237981200
Entropy [J/kmol K]	10542,1	-66518,25	-150401,4	-136396,5	-46198,1
Mole Flow [kmol/s]	0,83	0	0,46	0,3	0,3
Temperature [℃]	180,8	151,05	49,94	151,24	150,48
Pressure [barg]	0	17,9	12,5	3,9	3,8
Mole Fraction					
EDC	0	0,3	0,35	0	0
VCM	0	0,37	0,45	0	0
HCL	0	0,33	0,2	0	0
CO2	0,05	0	0	0	0
N2	0,71	0	0	0	0
WATER	0,21	0	0	1	1
O2	0,033	0	0	0	0

Table 60: Stream results from base case.

Stream	12403	12404	12405	12406	12407
Liquid Fraction	1	1	1	1	1
Vapor Fraction	0	0	0	0	0
Enthalpy [J/kmol]	-288625700	-287282600	-289115500	-288632300	-289115500
Entropy [J/kmol K]	-170972	-166423,2	-172695,7	-170994,2	-172695,7
Mole Flow [kmol/s]	9,25	9,25	3,08	3,08	1,08
Temperature [℃]	14	30,48	8	13,92	8
Pressure [barg]	5	4,9	5	4,9	5
Mole Fraction					
WATER	1	1	1	1	1

Table 61: Stream results from base case.

Stream	12408	12409	12410	12501	12502
Liquid Fraction	1	0	1	0	0
Vapor Fraction	0	1	0	1	1
Enthalpy [J/kmol]	-288649900	-237192600	-275339200	-94512510	-92723190
Entropy [J/kmol K]	-171055,5	-49210,52	-134281,7	-18290,66	-11701,63
Mole Flow [kmol/s]	1,08	0	0	0,28	0,28
Temperature [℃]	13,71	175,26	173,29	-24,8	28,99
Pressure [barg]	4,9	7,84	7,74	11,7	11,6
Mole Fraction					
HCL	0	0	0	1	1
WATER	1	1	1	0	0

F.2   Tuning of H1401 - Case 1

Table 62: Stream results from tuning of H1401 - Case 1.

Stream	10401	10402	10501	10601	10701
Liquid Fraction	0	0	0	1	1
Vapor Fraction	1	1	1	0	0
Enthalpy [J/kmol]	-65074350	-65074350	-52960910	-116771600	-106632500
Entropy [J/kmol K]	-90592	-90592	-67152,52	-200117,7	-192077,3
Mole Flow [kmol/s]	0,45	1,35	0,89	0,46	0,24
Temperature [°C]	174,16	174,16	153	153	126,9
Pressure [barg]	19	19	18,6	18,6	17,9
Mole Fraction					
EDC	0,46	0,46	0,3	0,78	0,69
VCM	0,3	0,3	0,37	0,17	0,25
HCL	0,23	0,23	0,33	0,04	0,06

Table 63: Stream results from tuning of H1401 - Case 1.

Stream	10801	10802	10803	10901	10902
Liquid Fraction	1	1	1	0	0,53
Vapor Fraction	0	0	0	1	0,47
Enthalpy [J/kmol]	-113860600	-113847600	-113848000	-44341390	-58564120
Entropy [J/kmol K]	-198418,1	-198410,6	-198410,9	-47734,18	-86573,58
Mole Flow [kmol/s]	0,69	0,69	0,23	0,66	0,66
Temperature [°C]	143,57	143,67	143,67	126,9	60
Pressure [barg]	17,9	19	19	17,9	17,8
Mole Fraction					
EDC	0,75	0,75	0,75	0,16	0,16
VCM	0,2	0,2	0,2	0,42	0,42
HCL	0,05	0,05	0,05	0,42	0,42

Table 64: Stream results from tuning of H1401 - Case 1.

Stream	11001	11002	11101	11102	11103
Liquid Fraction	0	0,32	0	0,16	0,15
Vapor Fraction	1	0,68	1	0,84	0,85
Enthalpy [J/kmol]	-55335160	-61815980	-71901370	-74650260	-74650070
Entropy [J/kmol K]	-25922,11	-46536,09	-22194,35	-31472,96	-31106,05
Mole Flow [kmol/s]	0,31	0,31	0,21	0,21	0,21
Temperature [°C]	60	28	28	16,9	14,84
Pressure [barg]	17,8	17,7	17,7	17,6	16,5
Mole Fraction					
EDC	0,01	0,01	0	0	0
VCM	0,31	0,31	0,18	0,18	0,18
HCL	0,68	0,68	0,82	0,82	0,82

Table 65: Stream results from tuning of H1401 - Case 1.

Stream	11201	11202	11301	11302	11402
Liquid Fraction	1	0,98	1	0,98	1
Vapor Fraction	0	0,02	0	0,02	0
Enthalpy [J/kmol]	-40815140	-40815110	-61423190	-61423110	-127349900
Entropy [J/kmol K]	-97219,55	-97192,41	-140291,1	-140259,6	-208072
Mole Flow [kmol/s]	0,1	0,1	0,35	0,35	0,1
Temperature [°C]	28	25,57	60	57,69	182,42
Pressure [barg]	17,7	16,5	17,8	16,5	19
Mole Fraction					
EDC	0,03	0,03	0,29	0,29	0,88
VCM	0,58	0,58	0,51	0,51	0,09
HCL	0,39	0,39	0,2	0,2	0,03

Table 66: Stream results from tuning of H1401 - Case 1.

Stream	11901	12001	12101	12301	12401
Liquid Fraction	0	0	0	0,96	1
Vapor Fraction	1	1	1	0,04	0
Enthalpy [J/kmol]	-21924730	-315814,9	-65654930	-68011140	-276241200
Entropy [J/kmol K]	-28222,76	-5280,85	10542,1	-149783,4	-136396,5
Mole Flow [kmol/s]	0,14	0,74	0,83	0,38	0,34
Temperature [°C]	15	15	180,8	49,66	151,24
Pressure [barg]	1,9	1,8	0	12,5	3,9
Mole Fraction					
EDC	0	0	0	0,34	0
VCM	0	0	0	0,48	0
HCL	0	0	0	0,18	0
CO2	0	0	0,05	0	0
N2	0	0,79	0,71	0	0
METHANE	0,29	0	0	0	0
H2	0,71	0	0	0	0
WATER	0	0	0,21	0	1

Table 67: Stream results from tuning of H1401 - Case 1.

Stream	12402	12403	12404	12405	12406
Liquid Fraction	0,01	1	1	1	1
Vapor Fraction	0,99	0	0	0	0
Enthalpy [J/kmol]	-238023300	-288625700	-287308100	-289115500	-288596600
Entropy [J/kmol K]	-46297,38	-170972	-166507	-172695,7	-170869,9
Mole Flow [kmol/s]	0,34	7,09	7,09	3,85	3,85
Temperature [°C]	150,48	14	30,17	8	14,36
Pressure [barg]	3,8	5	4,9	5	4,9
Mole Fraction					
WATER	1	1	1	1	1

F.3   Tuning of H1401 - Case 2

Table 68: Stream results from tuning of H1401 - Case 2.

Stream	10401	10402	10501	10601	10701
Liquid Fraction	0	0	0	1	1
Vapor Fraction	1	1	1	0	0
Enthalpy [J/kmol]	-66640520	-66640520	-55388920	-118462400	-110188500
Entropy [J/kmol K]	-92240,82	-92240,82	-70530,25	-201459,3	-195141,6
Mole Flow [kmol/s]	0,45	1,36	0,92	0,44	0,24
Temperature [°C]	175,46	175,46	156,5	156,5	132,91
Pressure [barg]	19	19	18,6	18,6	17,9
Mole Fraction					
EDC	0,48	0,48	0,33	0,8	0,72
VCM	0,29	0,29	0,36	0,16	0,22
HCL	0,23	0,23	0,32	0,04	0,06

Table 69: Stream results from tuning of H1401 - Case 2.

Stream	10801	10802	10803	10901	10902
Liquid Fraction	1	1	1	0	0,58
Vapor Fraction	0	0	0	1	0,42
Enthalpy [J/kmol]	-116018700	-116005500	-116005700	-46603280	-62488990
Entropy [J/kmol K]	-200157,7	-200150,2	-200150,3	-51433,68	-94381,4
Mole Flow [kmol/s]	0,67	0,67	0,22	0,69	0,69
Temperature [°C]	147,62	147,72	147,72	132,91	60
Pressure [barg]	17,9	19	19	17,9	17,8
Mole Fraction					
EDC	0,77	0,77	0,77	0,19	0,19
VCM	0,18	0,18	0,18	0,4	0,4
HCL	0,05	0,05	0,05	0,41	0,41

Table 70: Stream results from tuning of H1401 - Case 2.

Stream	11001	11002	11101	11102	11103
Liquid Fraction	0	0,29	0	0,15	0,15
Vapor Fraction	1	0,71	1	0,85	0,85
Enthalpy [J/kmol]	-57355950	-63348590	-72165660	-74840130	-74839950
Entropy [J/kmol K]	-25258,07	-44325,27	-22104,98	-31133,56	-30765,36
Mole Flow [kmol/s]	0,29	0,29	0,2	0,2	0,2
Temperature [°C]	60	28	28	16,9	14,85
Pressure [barg]	17,79	17,69	17,7	17,6	16,5
Mole Fraction					
EDC	0,01	0,01	0	0	0
VCM	0,29	0,29	0,17	0,17	0,17
HCL	0,7	0,7	0,82	0,82	0,82

Table 71: Stream results from tuning of H1401 - Case 2.

Stream	11201	11202	11301	11302	11401	11402
Liquid Fraction	1	0,98	1	0,98	1	1
Vapor Fraction	0	0,02	0	0,02	0	0
Enthalpy [J/kmol]	-41997830	-41997790	-66181080	-66180900	-127354900	-127354900
Entropy [J/kmol K]	-98138,51	-98111,42	-144115,9	-144084,2	-208075,8	-208075,8
Mole Flow [kmol/s]	0,08	0,08	0,4	0,4	0,02	0,07
Temperature [°C]	28	25,58	60	57,74	182,42	182,42
Pressure [barg]	17,7	16,5	17,79	16,5	19	19
Mole Fraction						
EDC	0,04	0,04	0,32	0,32	0,88	0,88
VCM	0,57	0,57	0,48	0,48	0,09	0,09
HCL	0,39	0,39	0,2	0,2	0,03	0,03

Table 72: Stream results from tuning of H1401 - Case 2.

Stream	12301	12401	12402
Liquid Fraction	0,95	1	0
Vapor Fraction	0,05	0	1
Enthalpy [J/kmol]	-70161350	-276241200	-237809900
Entropy [J/kmol K]	-149947,4	-136396,5	-45794,11
Mole Flow [kmol/s]	0,42	0,32	0,32
Temperature [°C]	49,8	151,24	150,48
Pressure [barg]	12,5	3,9	3,8
Mole Fraction			
EDC	0,34	0	0
VCM	0,46	0	0
HCL	0,19	0	0
WATER	0	1	1

F.4 Preheating of Combustion Air

Table 73: Stream results from preheating of combustion air.

Stream	11901	12001	12002	12101	12102
Liquid Fraction	0	0	0	0	0,01
Vapor Fraction	1	1	1	1	0,99
Enthalpy [J/kmol]	-21920230	-300378,2	4252501	-65680470	-69747780
Entropy [J/kmol K]	-19423,77	3253,43	15890,41	10486,83	-74,86
Mole Flow [kmol/s]	0,13	0,7	0,7	0,78	0,78
Temperature [°C]	15	15	170	180	63,42
Pressure [barg]	0	0	0	0	0
Mole Fraction					
METHANE	0,29	0	0	0	0
H2	0,71	0	0	0	0
N2	0	0,79	0,79	0,71	0,71
O2	0	0,21	0,21	0,03	0,03
CO2	0	0	0	0,05	0,05
WATER	0	0	0	0,21	0,21

F.5 Production of Low Pressure Steam

Table 74: Stream results from production of low pressure steam.

Stream	11901	12001	12101	12102	12411	12412
Liquid Fraction	0	0	0	0	1	0
Vapor Fraction	1	1	1	1	0	1
Enthalpy [J/kmol]	-21920230	-300378,2	-65683860	-66412400	-277188500	-237787800
Entropy [J/kmol K]	-19423,77	3253,43	10486,34	8835,79	-138503,7	-45865,08
Mole Flow [kmol/s]	0,14	0,74	0,83	0,83	0,02	0,02
Temperature [°C]	15	15	180	156,67	152,17	152,17
Pressure [barg]	0	0	0	0	3,9	3,9
Mole Fraction						
METHANE	0,29	0	0	0	0	0
H2	0,71	0	0	0	0	0
N2	0	0	0,21	0,21	1	1
O2	0	0	0,05	0,05	0	0
CO2	0	0,21	0,03	0,03	0	0
WATER	0	0,79	0,71	0,71	0	0

F.6   Preheating EDC Feed

Table 75: Stream results from preheating EDC feed.

Stream	10103	10104	10105
Liquid Fraction	1	1	1
Vapor Fraction	0	0	0
Enthalpy [J/kmol]	-151591900	-149610700	-149610700
Entropy [J/kmol K]	-248196,3	-243337,1	-243398,6
Mole Flow [kmol/s]	0,48	0,48	0,48
Temperature [℃]	133	146,61	146,58
Pressure [barg]	27,1	24,3	27,1
Mole Fraction			
EDC	1	1	1

F.7   Preheating EDC Feed and Combustion Air

Table 76: Stream results from preheating EDC feed and combustion air.

Stream	10103	10104	10105	11901	12001
Liquid Fraction	1	1	1	0	0
Vapor Fraction	0	0	0	1	1
Enthalpy [J/kmol]	-151591900	-149704000	-149704000	-21920230	-300378,2
Entropy [J/kmol K]	-248196,3	-243559,6	-243621,1	-19423,77	3253,43
Mole Flow [kmol/s]	0,48	0,48	0,48	0,13	0,7
Temperature [℃]	133	145,98	145,95	15	15
Pressure [barg]	27,1	24,3	27,1	0	0
Mole Fraction					
EDC	1	1	1	0	0
METHANE	0	0	0	0,29	0
H2	0	0	0	0,71	0
N2	0	0	0	0	0,79
O2	0	0	0	0	0,21

Table 77: Stream results from preheating EDC feed and combustion air.

Stream	12002	12101	12102	12103
Liquid Fraction	0	0	0	0,01
Vapor Fraction	1	1	1	0,99
Enthalpy [J/kmol]	3159217	-65665280	-66819150	-69909850
Entropy [J/kmol K]	13314,32	10489	7832,8	-599,68
Mole Flow [kmol/s]	0,7	0,78	0,78	0,78
Temperature [°C]	133	180	143	63,1
Pressure [barg]	0	0	0	0
Mole Fraction				
N2	0,79	0,71	0,71	0,71
O2	0,21	0,03	0,03	0,03
CO2	0	0,05	0,05	0,05
WATER	0	0,21	0,21	0,21

F.8   Reduction of Air

Table 78: Stream results from reduction of air

Stream	11901	12001	12101
Liquid Fraction	0	0	0
Vapor Fraction	1	1	1
Enthalpy [J/kmol]	-21920230	-300378,2	-70789900
Entropy [J/kmol K]	-19423,77	3253,43	9777,74
Mole Flow [kmol/s]	0,14	0,69	0,77
Temperature [°C]	15	15	180,8
Pressure [barg]	0	0	0
Mole Fraction			
METHANE	0,29	0	0
H2	0,71	0	0
N2	0	0,79	0,7
O2	0	0,21	0,02
CO2	0	0	0,05
WATER	0	0	0,23

F.9   Increase in Excess Air, Fouling H1406

Table 79: Stream results from increase in excess air, fouling H1406

Stream	11901	12001	12101	10103	10104	10102
Liquid Fraction	0	0	0	1	1	1
Vapor Fraction	1	1	1	0	0	0
Enthalpy [J/kmol]	-21920230	-300378,2	-54940980	-158862200	-158862200	-166442400
Entropy [J/kmol K]	-19423,77	3253,43	11971,5	-267356,9	-267290,9	-290870,3
Mole Flow [kmol/s]	0,15	0,97	1,07	0,48	0,48	0,48
Temperature [°C]	15	15	180,8	80	80,1	19,54
Pressure [barg]	0	0	0	27,1	24,3	27,2
Mole Fraction						
EDC	0	0	0	1	1	1
METHANE	0,29	0	0	0	0	0
H2	0,71	0	0	0	0	0
N2	0	0,79	0,72	0	0	0
O2	0	0,21	0,06	0	0	0
CO2	0	0	0,04	0	0	0
WATER	0	0	0,18	0	0	0

F.10   Increase in Excess Air, Normal Conditions

Table 80: Stream results from increase in excess air, normal conditions.

Stream	11901	12001	12101
Liquid Fraction	0	0	0
Vapor Fraction	1	1	1
Enthalpy [J/kmol]	-21920230	-300378,2	-58909960
Entropy [J/kmol K]	-19423,77	3253,43	11463,83
Mole Flow [kmol/s]	0,14	0,84	0,93
Temperature [°C]	15	15	180,8
Pressure [barg]	0	0	0
Mole Fraction			
METHANE	0,29	0	0
H2	0,71	0	0
N2	0	0,79	0,71
O2	0	0,21	0,05
CO2	0	0	0,04
WATER	0	0	0,19

F.11   Preheat of EDC Feed by Removing H1401

Table 81: Stream results from preheat of EDC feed by removing H1401.

Stream	10103	10104	10401	10402	10701
Liquid Fraction	1	1	0	0	1
Vapor Fraction	0	0	1	1	0
Enthalpy [J/kmol]	-148255000	-148255100	-56650850	-56650860	-112984600
Entropy [J/kmol K]	-240205,4	-240142	-80402,85	-80402,88	-196850,3
Mole Flow [kmol/s]	0,48	0,48	0,45	1,34	0,31
Temperature [°C]	155,66	155,67	165,66	165,66	150,6
Pressure [barg]	27,2	24,3	19	19	19
Mole Fraction					
EDC	1	1	0,39	0,39	0,76
VCM	0	0	0,36	0,36	0,2
HCL	0	0	0,26	0,26	0,04

Table 82: Stream results from preheat of EDC feed by removing H1401.

Stream	10801	10802	10803	10901	10902
Liquid Fraction	1	1	1	0	0,76
Vapor Fraction	0	0	0	1	0,24
Enthalpy [J/kmol]	-94769180	-94758410	-94758410	-48042850	-69123630
Entropy [J/kmol K]	-179799,6	-179792	-179792	-63210,46	-118858,3
Mole Flow [kmol/s]	0,61	0,61	0,2	1,08	1,08
Temperature [°C]	101,16	101,24	101,24	147,7	60
Pressure [barg]	18	19	19	18	17,9
Mole Fraction					
EDC	0,58	0,58	0,58	0,27	0,27
VCM	0,32	0,32	0,32	0,4	0,4
HCL	0,1	0,1	0,1	0,33	0,33

Table 83: Stream results from preheat of EDC feed by removing H1401.

Stream	11001	11002	11101	11102	11103
Liquid Fraction	0	0,25	0	0,14	0,14
Vapor Fraction	1	0,75	1	0,86	0,86
Enthalpy [J/kmol]	-60009820	-65420460	-72728220	-75289130	-75288970
Entropy [J/kmol K]	-24440,4	-41656,8	-21974,91	-30621,79	-30216,02
Mole Flow [kmol/s]	0,26	0,26	0,19	0,19	0,19
Temperature [°C]	60	28	28	16,9	14,65
Pressure [barg]	17,9	17,8	17,8	17,7	16,5
Mole Fraction					
EDC	0,01	0,01	0	0	0
VCM	0,27	0,27	0,17	0,17	0,17
HCL	0,72	0,72	0,83	0,83	0,83

Table 84: Stream results from preheat of EDC feed by removing H1401.

Stream	11201	11202	11301	11401	11402
Liquid Fraction	1	0,98	1	1	1
Vapor Fraction	0	0,02	0	0	0
Enthalpy [J/kmol]	-44013540	-44013490	-71990900	-127341700	-127341700
Entropy [J/kmol K]	-99317,33	-99287,5	-148560,9	-208065,7	-208065,7
Mole Flow [kmol/s]	0,07	0,07	0,82	0,01	0,03
Temperature [°C]	28	25,38	60	182,4	182,4
Pressure [barg]	17,8	16,5	17,9	19	19
Mole Fraction					
EDC	0,05	0,05	0,35	0,88	0,88
VCM	0,56	0,56	0,45	0,09	0,09
HCL	0,39	0,39	0,21	0,03	0,03

Table 85: Stream results from preheat of EDC feed by removing H1401.

Stream	11901	12001	12101	12301	12403
Liquid Fraction	0	0	0	0,93	1
Vapor Fraction	1	1	1	0,07	0
Enthalpy [J/kmol]	-21920230	-300378,2	-65654370	-73263660	-288625700
Entropy [J/kmol K]	-19423,77	3253,43	10542,17	-150366,1	-170972
Mole Flow [kmol/s]	0,13	0,72	0,81	0,48	16,96
Temperature [°C]	15	15	180,8	49,83	14
Pressure [barg]	0	0	0	12,5	5
Mole Fraction					
EDC	0	0	0	0,36	0
VCM	0	0	0	0,44	0
HCL	0	0	0	0,2	0
H2	0,71	0	0	0	0
METHANE	0,29	0	0	0	0
N2	0	0,79	0,71	0	0
O2	0	0,21	0,03	0	0
CO2	0	0	0,05	0	0
WATER	0	0	0,21	0	1

Table 86: Stream results from preheat of EDC feed by removing H1401.

Stream	12404	12405	12406	12701	12801
Liquid Fraction	1	1	1	0	1
Vapor Fraction	0	0	0	1	0
Enthalpy [J/kmol]	-287288100	-289115500	-288663700	-48131590	-71990900
Entropy [J/kmol K]	-166441,2	-172695,7	-171103,4	-64885,09	-148560,9
Mole Flow [kmol/s]	16,96	3,08	3,08	1,03	0,47
Temperature [°C]	30,41	8	13,54	150,6	60
Pressure [barg]	4,9	5	4,9	19	17,9
Mole Fraction					
EDC	0	0	0	0,28	0,35
VCM	0	0	0	0,4	0,45
HCL	0	0	0	0,32	0,21
WATER	1	1	1	0	0

Table 87: Stream results from preheat of EDC feed by removing H1401.

Stream	12802	12901	12902
Liquid Fraction	0,98	1	1
Vapor Fraction	0,02	0	0
Enthalpy [J/kmol]	-71990660	-71990900	-71989890
Entropy [J/kmol K]	-148526,1	-148560,9	-148559,9
Mole Flow [kmol/s]	0,47	0,34	0,34
Temperature [℃]	57,6	60	60,01
Pressure [barg]	16,5	17,9	18
Mole Fraction			
EDC	0,35	0,35	0,35
VCM	0,45	0,45	0,45
HCL	0,21	0,21	0,21

F.12   The Process Section Without H1401 and H1406

Table 88: Stream results from the process section without H1401 and H1406.

Stream	10401	10501	10402	10801	10802
Liquid Fraction	0	0	0	1	1
Vapor Fraction	1	1	1	0	0
Enthalpy [J/kmol]	-46885200	-44931520	-46885200	-71025590	-71027140
Entropy [J/kmol K]	-65673,48	-63175,93	-65673,48	-145364,1	-145362,7
Mole Flow [kmol/s]	0,47	1,41	1,4	0,67	0,67
Temperature [℃]	151,09	159,5	151,09	60	59,99
Pressure [barg]	19	18,6	19	18,9	18,6
Mole Fraction					
EDC	0,28	0,27	0,28	0,33	0,33
VCM	0,42	0,42	0,42	0,45	0,45
HCL	0,31	0,31	0,31	0,22	0,22

Table 89: Stream results from the process section without H1401 and H1406.

Stream	10803	10902	11001	11002	11101
Liquid Fraction	1	0,83	0	0,26	0
Vapor Fraction	0	0,17	1	0,74	1
Enthalpy [J/kmol]	-71025900	-69341790	-61203400	-66671920	-74099560
Entropy [J/kmol K]	-145363,6	-124629,3	-24411,14	-41814,84	-22051,02
Mole Flow [kmol/s]	0,22	1,4	0,24	0,24	0,18
Temperature [℃]	60,01	60	60	28	28
Pressure [barg]	19	18,9	18,9	18,8	18,8
Mole Fraction					
EDC	0,33	0,28	0,01	0,01	0
VCM	0,45	0,42	0,26	0,26	0,16
HCL	0,22	0,31	0,73	0,73	0,84

Table 90: Stream results from the process section without H1401 and H1406.

Stream	11102	11103	11201	11202	11301
Liquid Fraction	0,15	0,14	1	0,97	1
Vapor Fraction	0,85	0,86	0	0,03	0
Enthalpy [J/kmol]	-76674290	-76674130	-45887650	-45887600	-71025590
Entropy [J/kmol K]	-30746,4	-30027,27	-97127,83	-97070,21	-145364,1
Mole Flow [kmol/s]	0,18	0,18	0,06	0,06	1,16
Temperature [°C]	16,9	12,86	28	23,44	60
Pressure [barg]	18,7	16,5	18,8	16,5	18,9
Mole Fraction					
EDC	0	0	0,05	0,05	0,33
VCM	0,16	0,16	0,54	0,54	0,45
HCL	0,84	0,84	0,41	0,41	0,22

Table 91: Stream results from the process section without H1401 and H1406.

Stream	11401	11402	12301	12403	12404
Liquid Fraction	1	1	0,92	1	1
Vapor Fraction	0	0	0,08	0	0
Enthalpy [J/kmol]	-127320000	-127320000	-72419280	-288625700	-287347700
Entropy [J/kmol K]	-208049,9	-208049,9	-147340,2	-170972	-166637,8
Mole Flow [kmol/s]	0,01	0,03	0,5	24,67	24,67
Temperature [°C]	182,36	182,36	48,1	14	29,68
Pressure [barg]	19	19	12,5	5	4,9
Mole Fraction					
EDC	0,88	0,88	0,34	0	0
VCM	0,09	0,09	0,44	0	0
HCL	0,03	0,03	0,22	0	0
WATER	0	0	0	1	1

Table 92: Stream results from the process section without H1401 and H1406.

Stream	12405	12406
Liquid Fraction	1	1
Vapor Fraction	0	0
Enthalpy [J/kmol]	-289115500	-288666200
Entropy [J/kmol K]	-172695,7	-171112,4
Mole Flow [kmol/s]	2,93	2,93
Temperature [°C]	8	13,51
Pressure [barg]	5	4,9
Mole Fraction		
WATER	1	1

G   Plant Data

The measurement data which constitutes the basis for the simulation of the base case is presented in the following figures. All the measurement points through the period have been plotted to illustrate any fluctuations in the data.
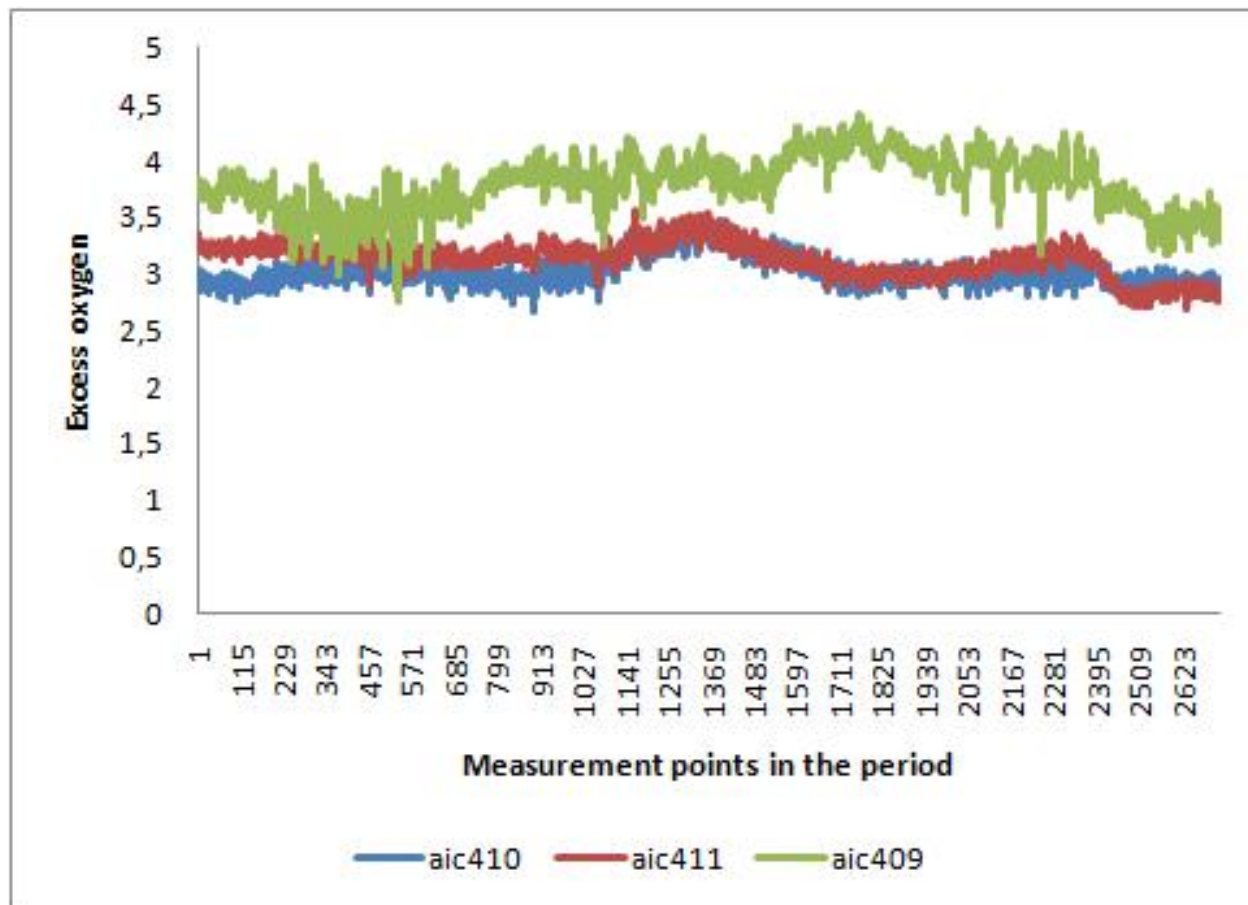
Figure 19: The analysis of oxygen in the flue gas from the three crackers.

G.1   Flow Measurements
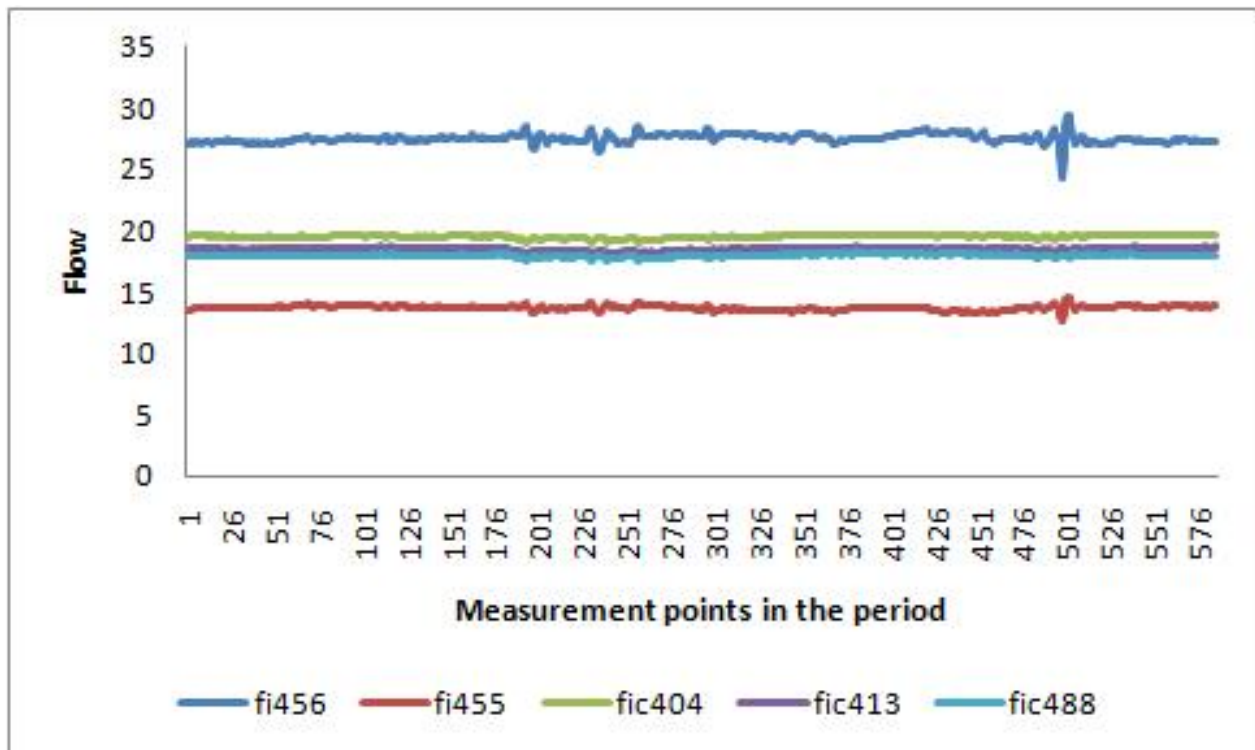
Figure 20: Fi456 and fi455 are the flows from the top and bottom of V1404 respectivly. The rest is flow measurements on the fuel gas to the crackers, measured in MW.
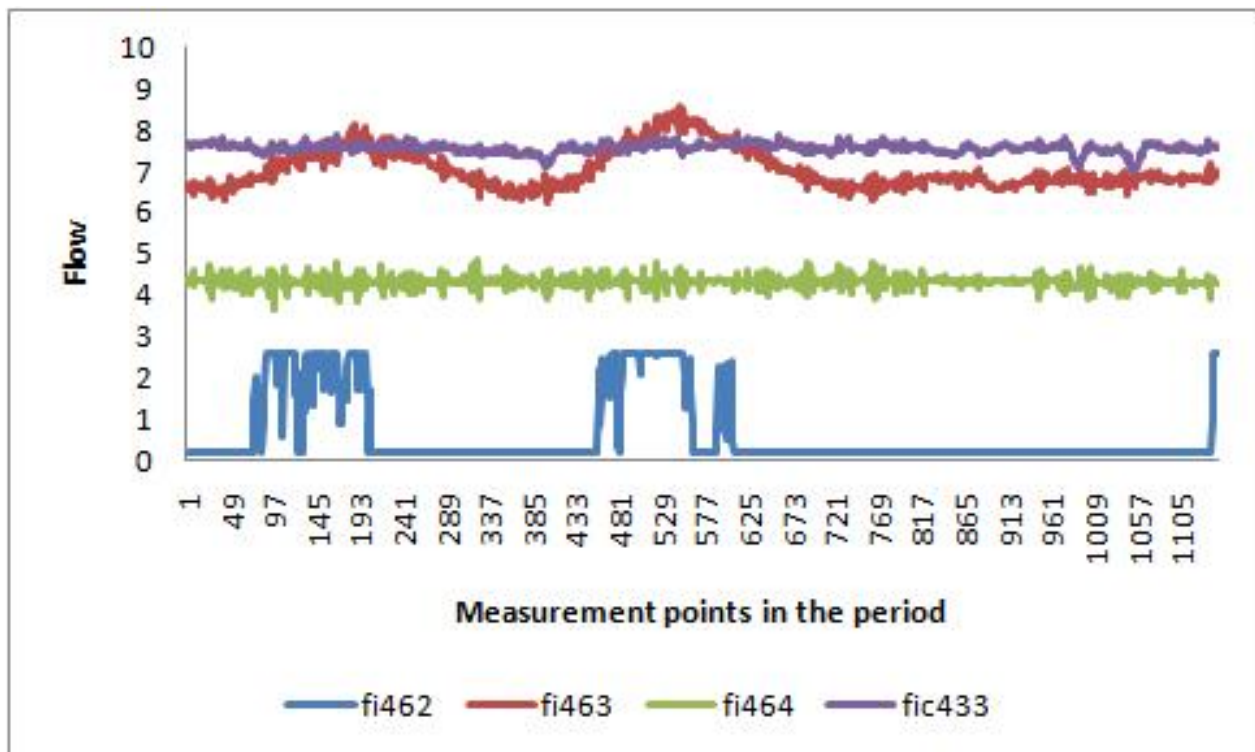
Figure 21: The flow measurements in the bottom system on the top stream of V1402 (fi462) and the top stream (fi463 and fi464) and bottom stream (fic433) of V1403
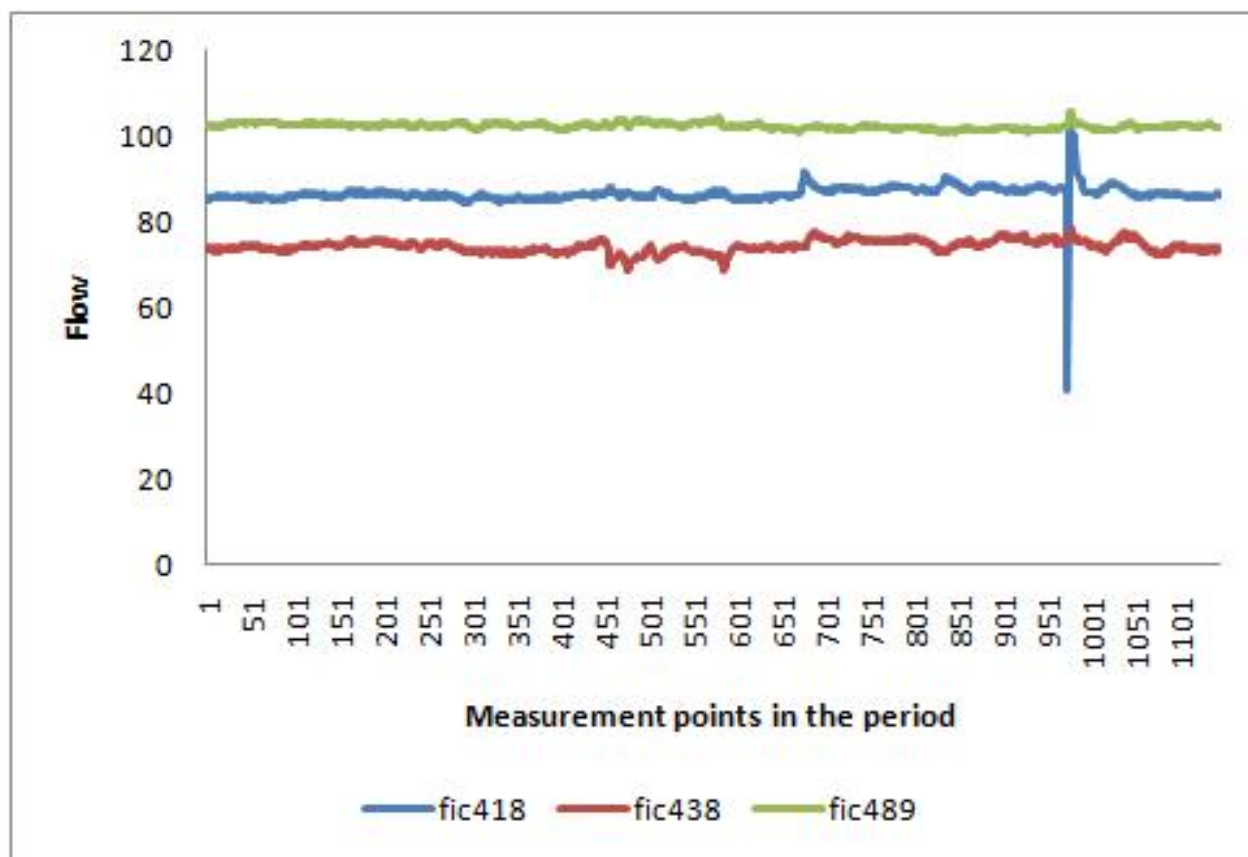
Figure 22: The reflux flow to C1401 A, B and C.
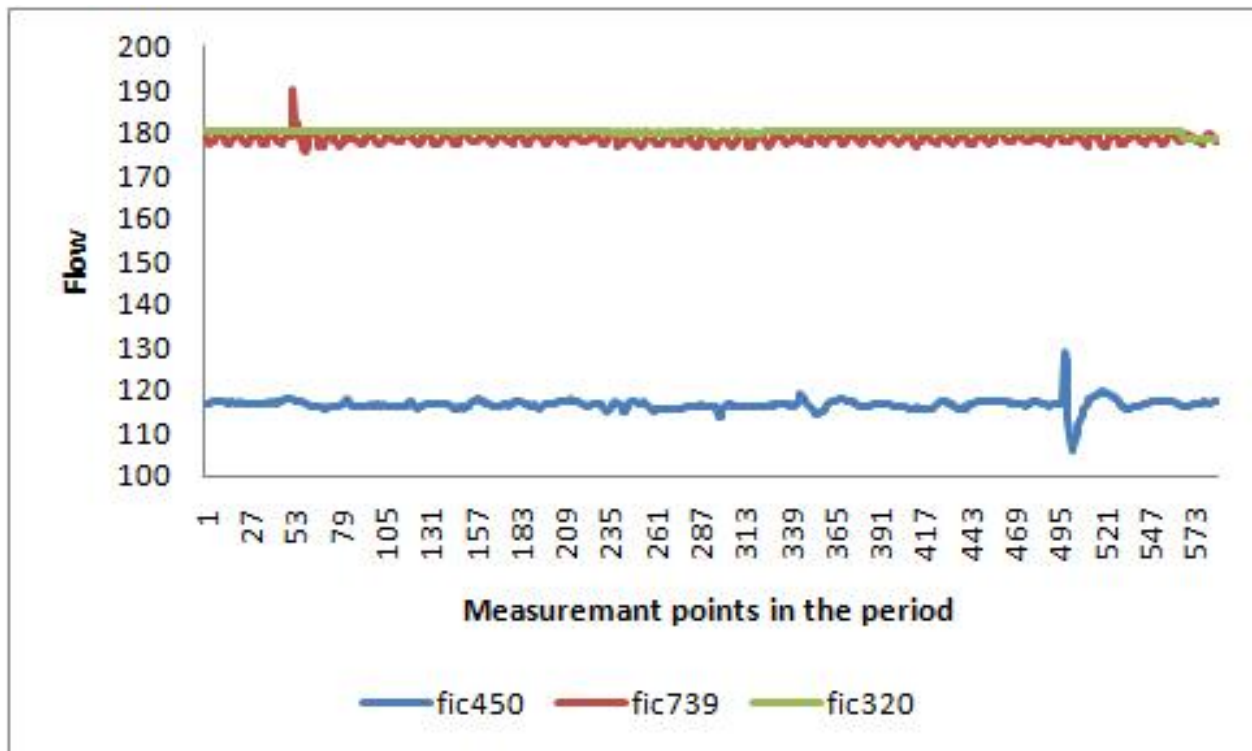
Figure 23: The flow measurement of the bottom stream of V1401 (fic450), the feed stream from T2702 (fic739) and the feed stream from V2704 (fic320)
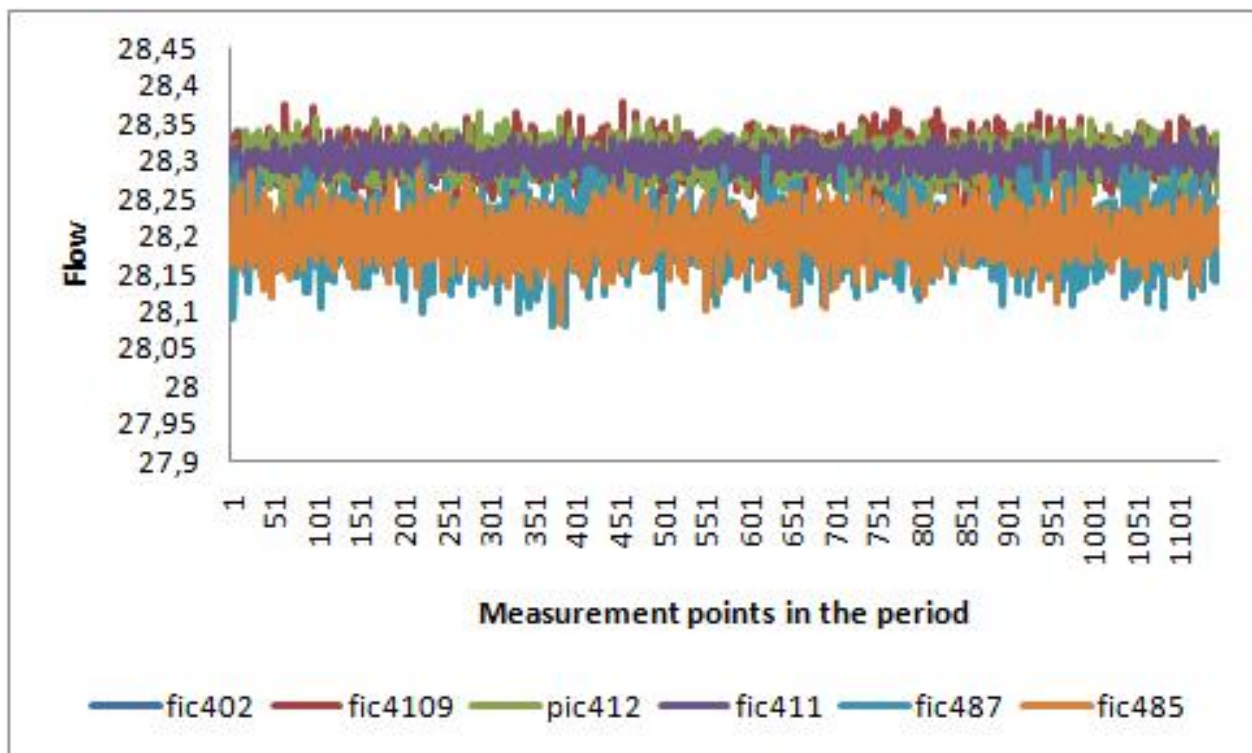
Figure 24: Flow measurements on the six feed streams to the crackers.
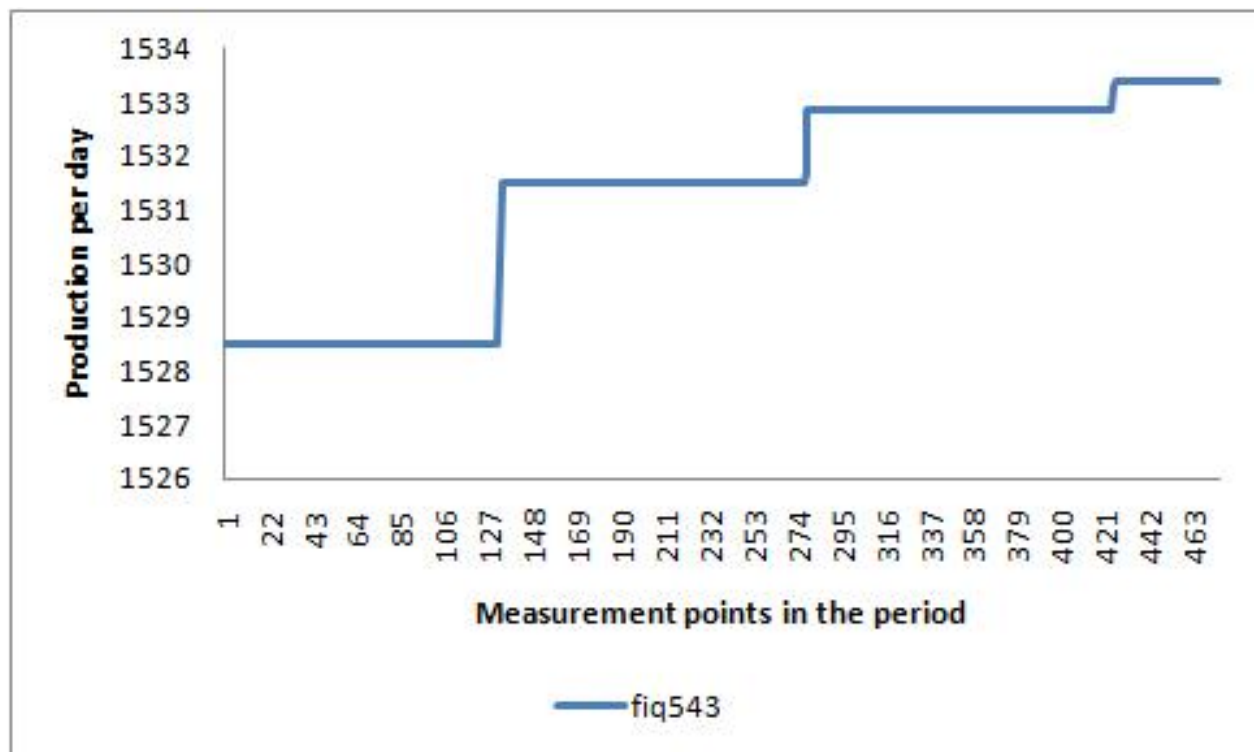
Figure 25: Total production of VCM per day

G.2   Pressure Measurements
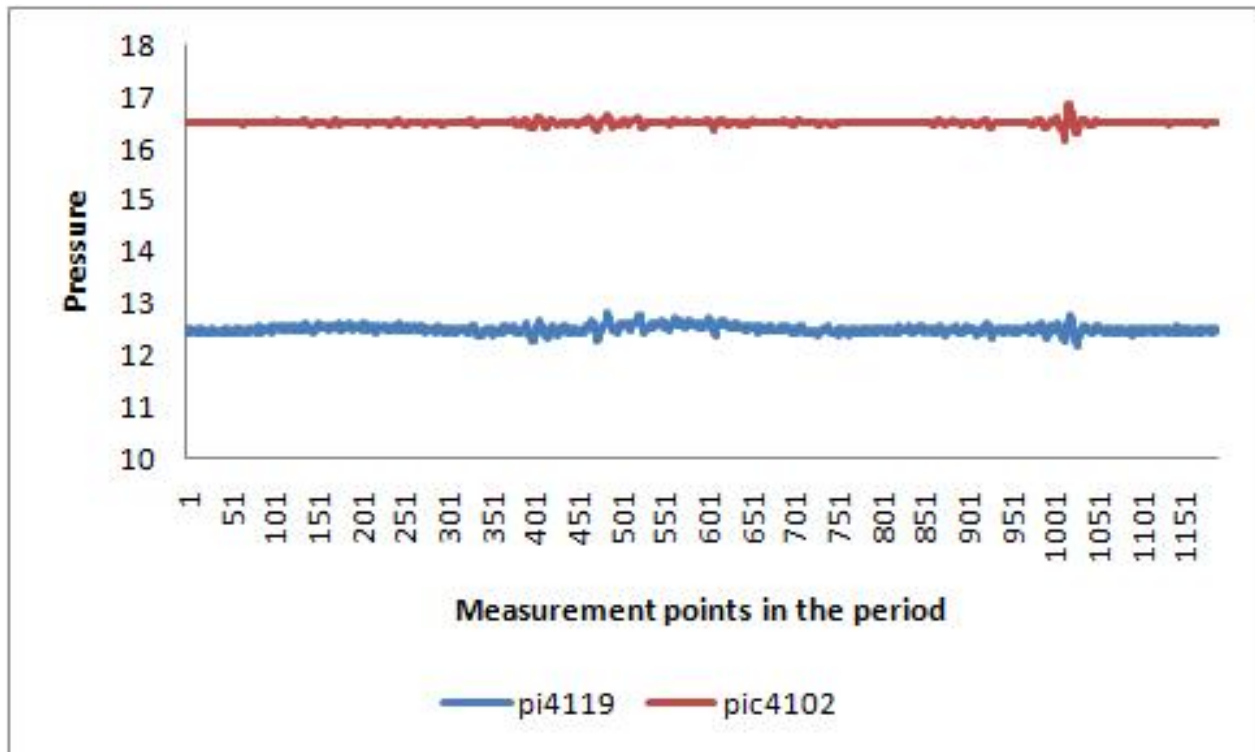
Figure 26: The pressure in V1402 (pi4119) and after H1403 (pic4102).
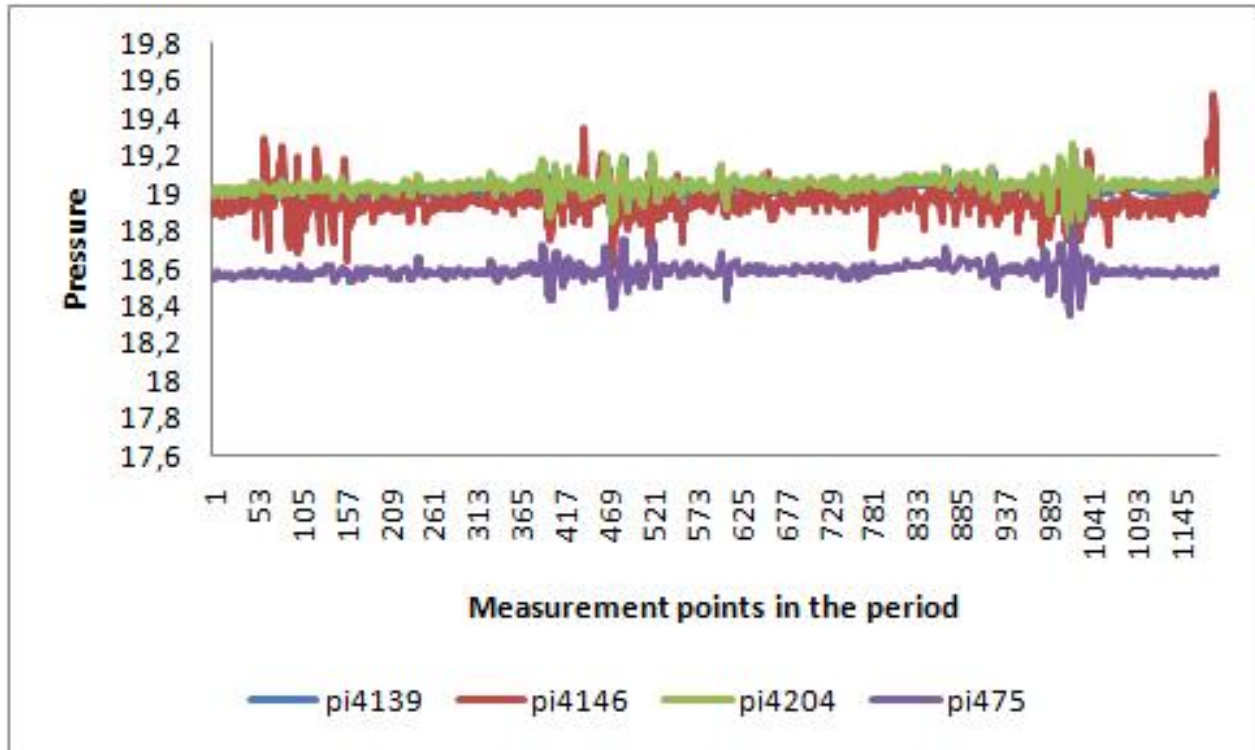
Figure 27: The pressure in the top stream of C1401 (pi4139, pi4146 and pi4204) and the outlet gas stream from H1401 (pi475).
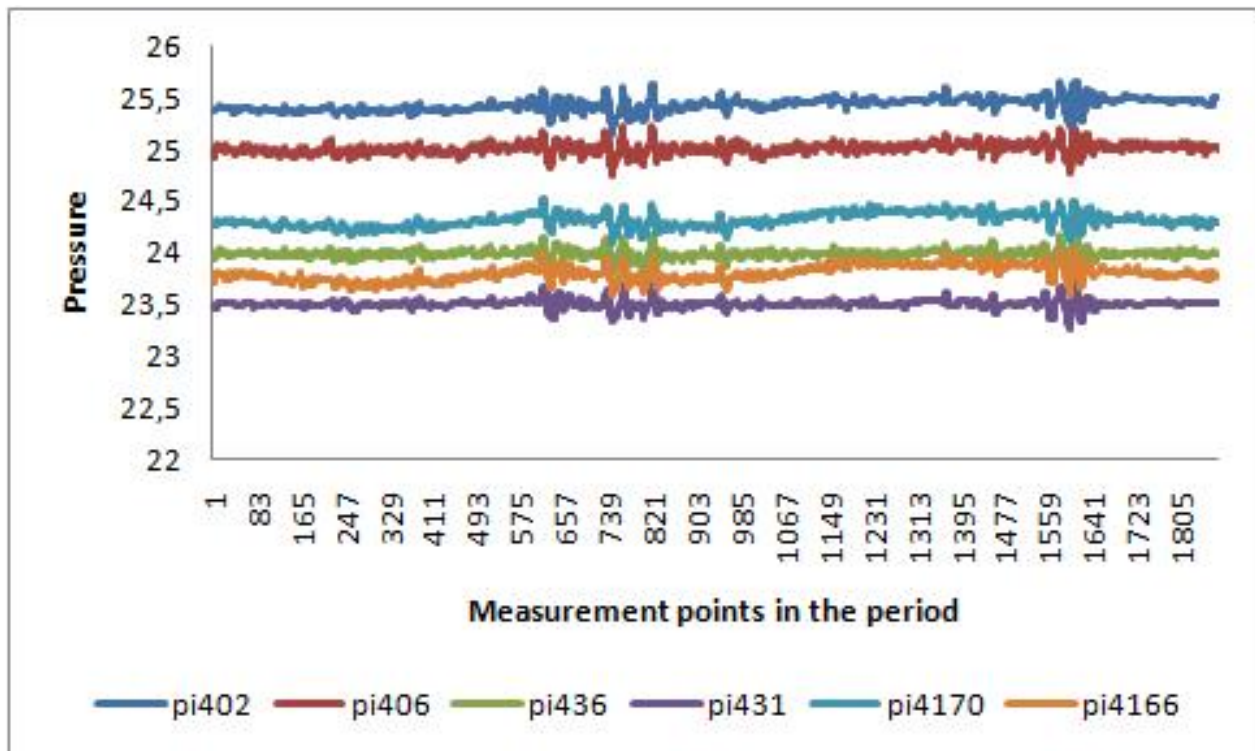
Figure 28: The pressure on the six feed streams to the crackers.
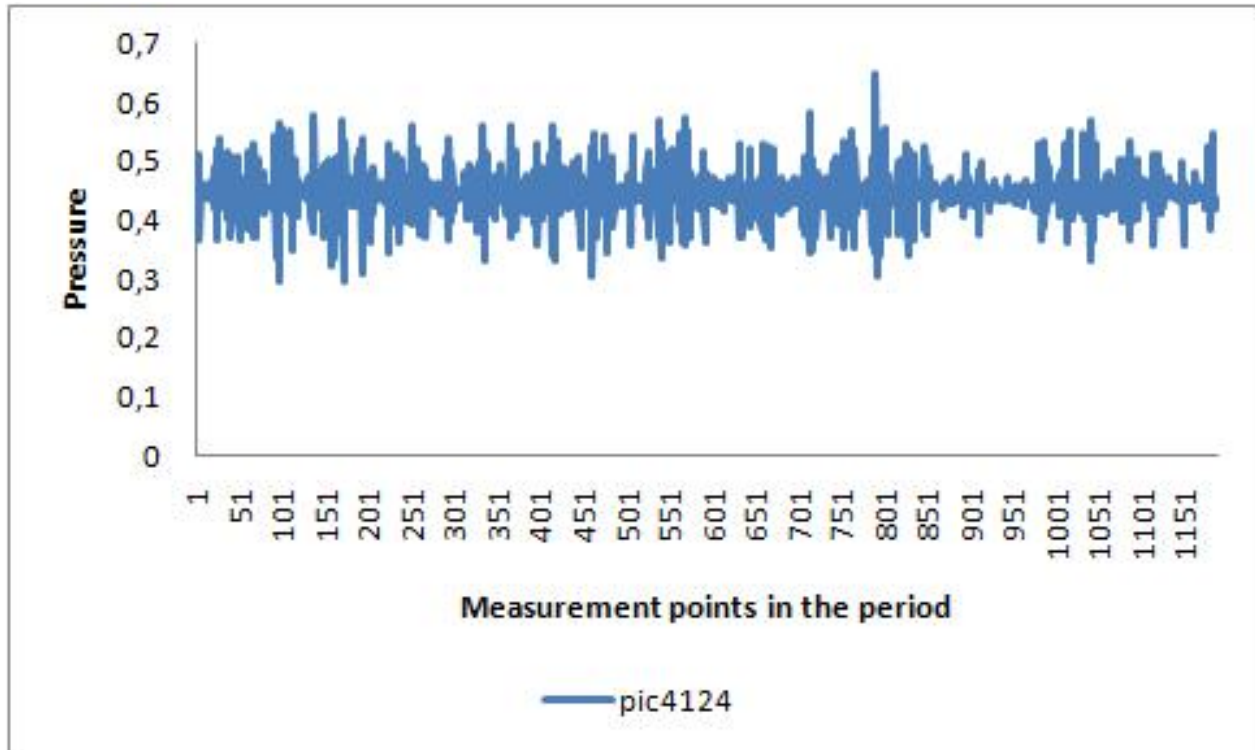
Figure 29: The pressure in V1403.
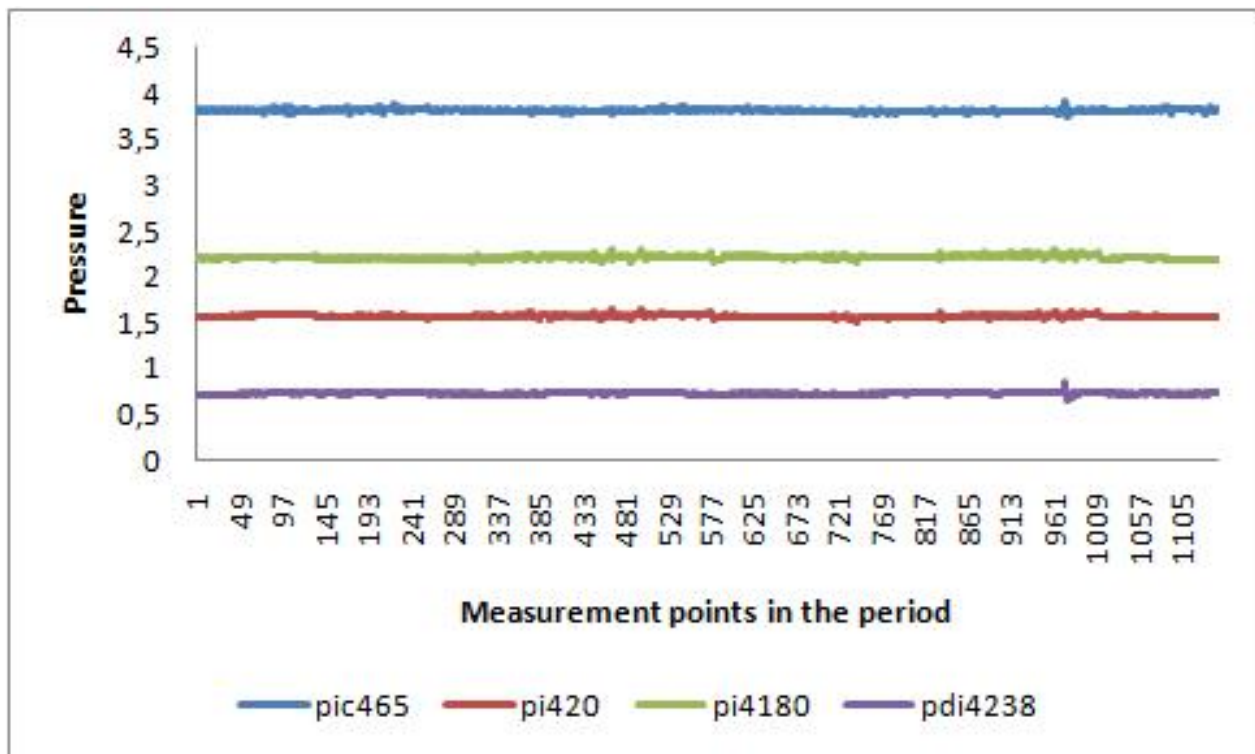
Figure 30: The pressure on the low pressure steam (pic465), the fuel gass pressure to cracker B and C (pi420 and pi4180) and the pressure difference over H1406 (pdi4238).

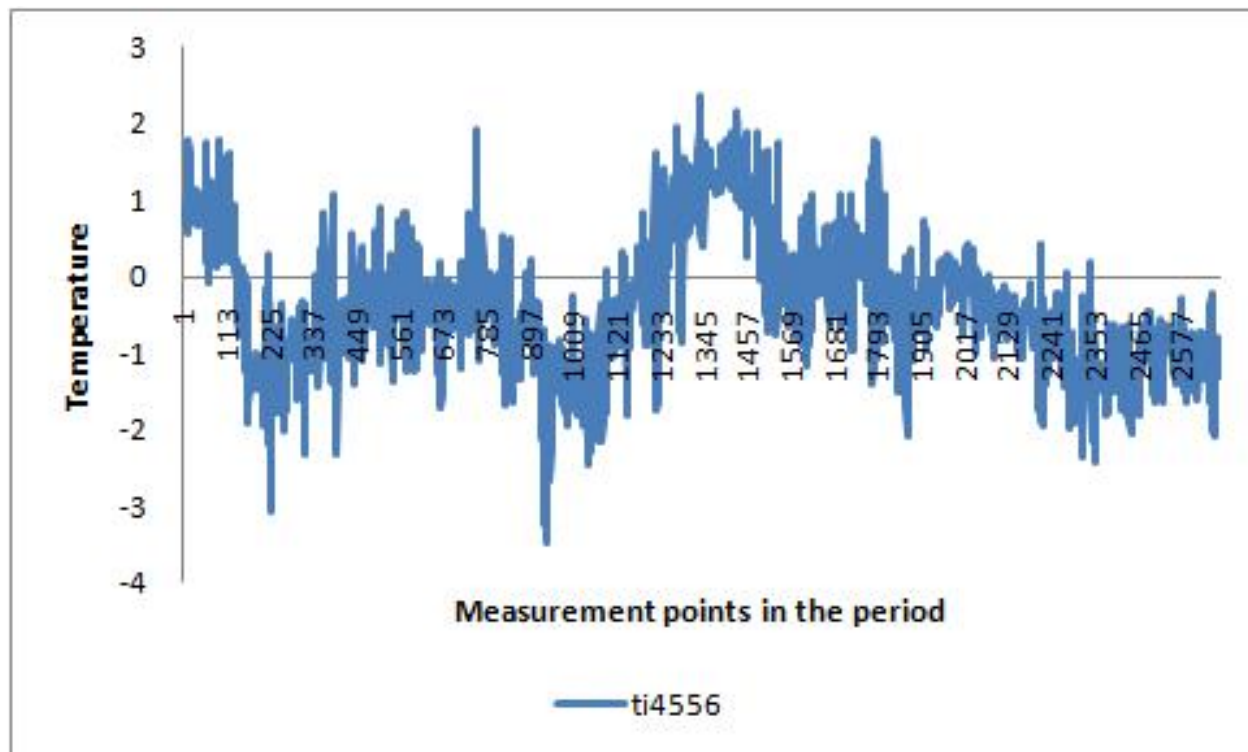## G.3   Temperature Measurements
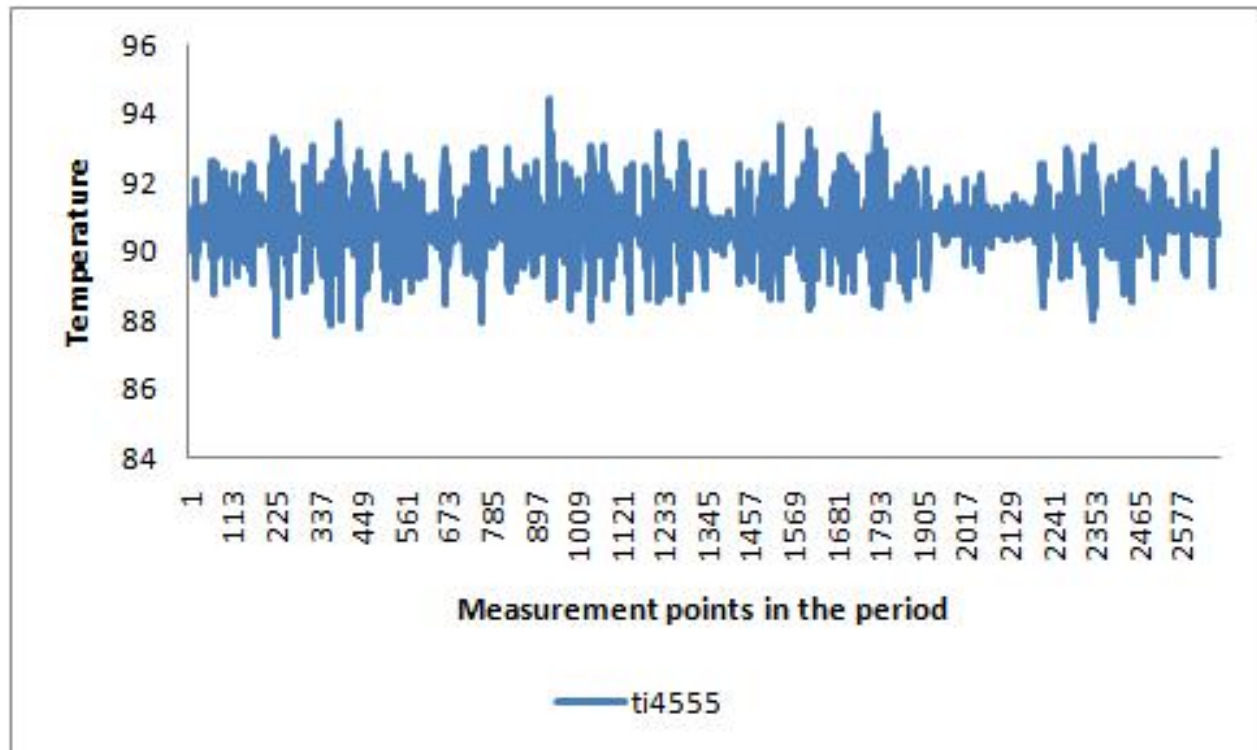
Figure 31: The temperature in V1403.

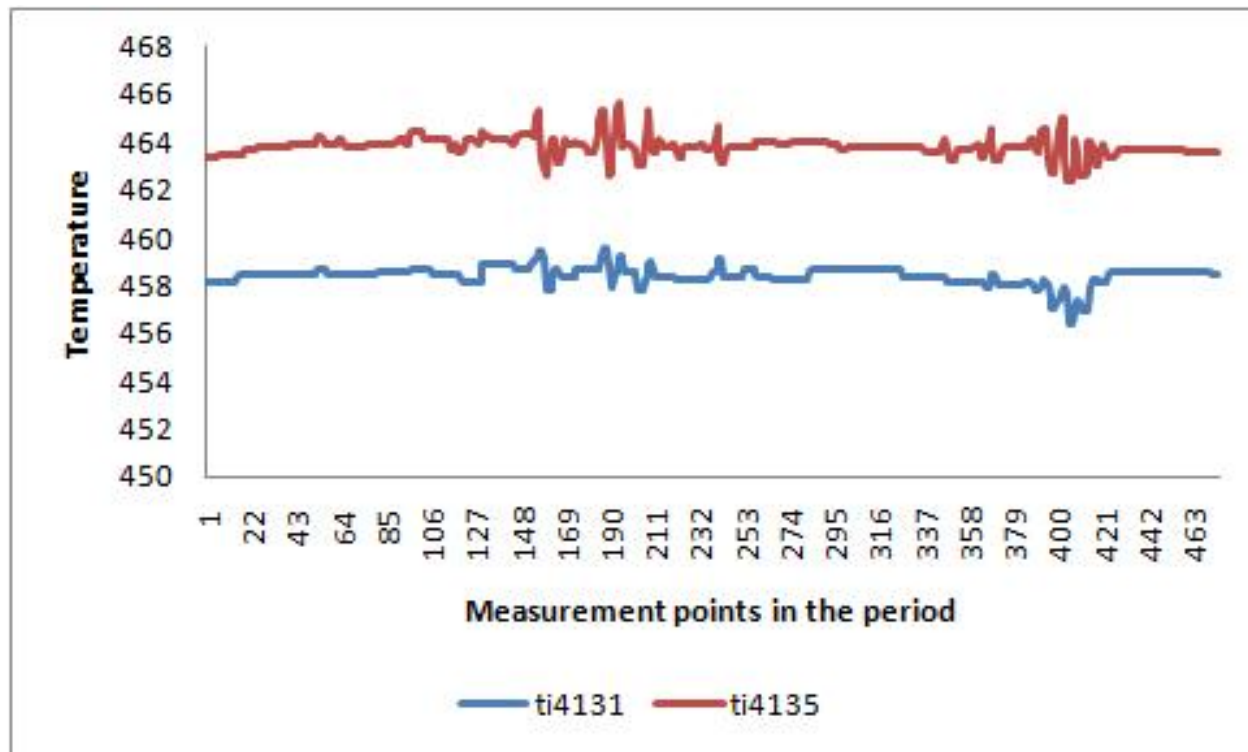Figure 32: The temperature after H1404.

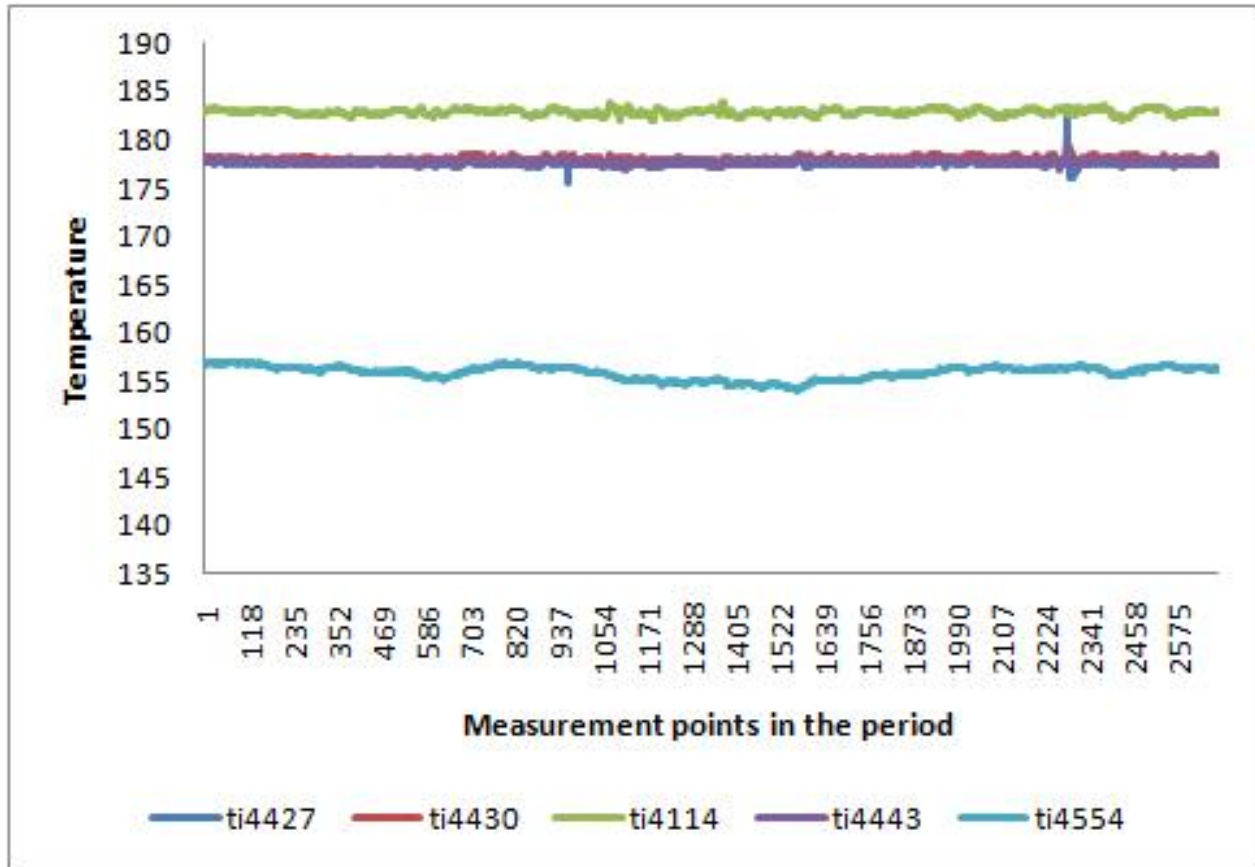Figure 33: The temperature on the outlef from adiabatic reactor A and B.

Figure 34: The temperature on the top stream from C1401 A, B and C (ti4427, ti4430 and ti4443), the temperature in C1401B (ti4114) and the temperature in V1402 (ti4554).
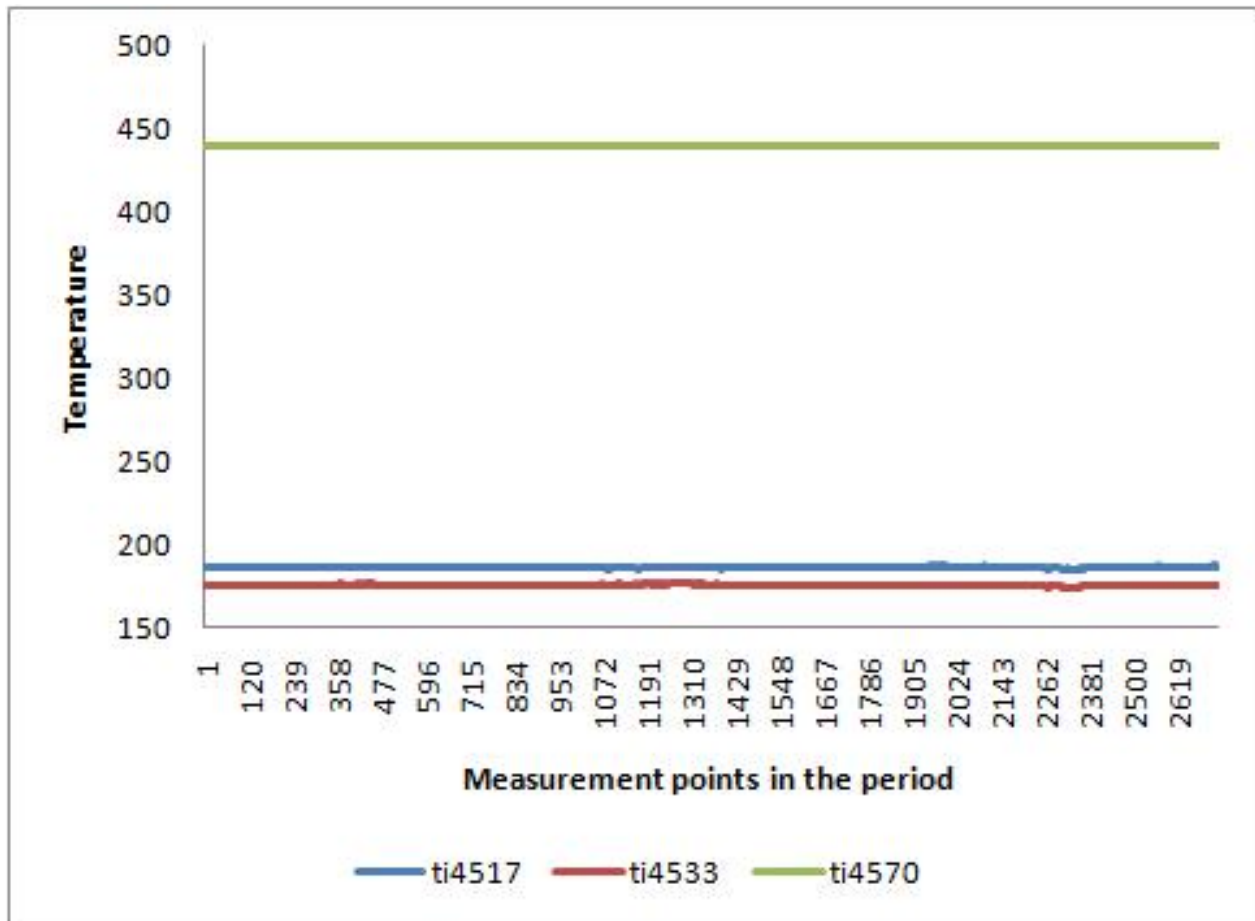
Figure 35: The flue gas temperature in the crackers. Notice that ti4570 has a defect and therefore shows a constant temperature of 440 ℃.
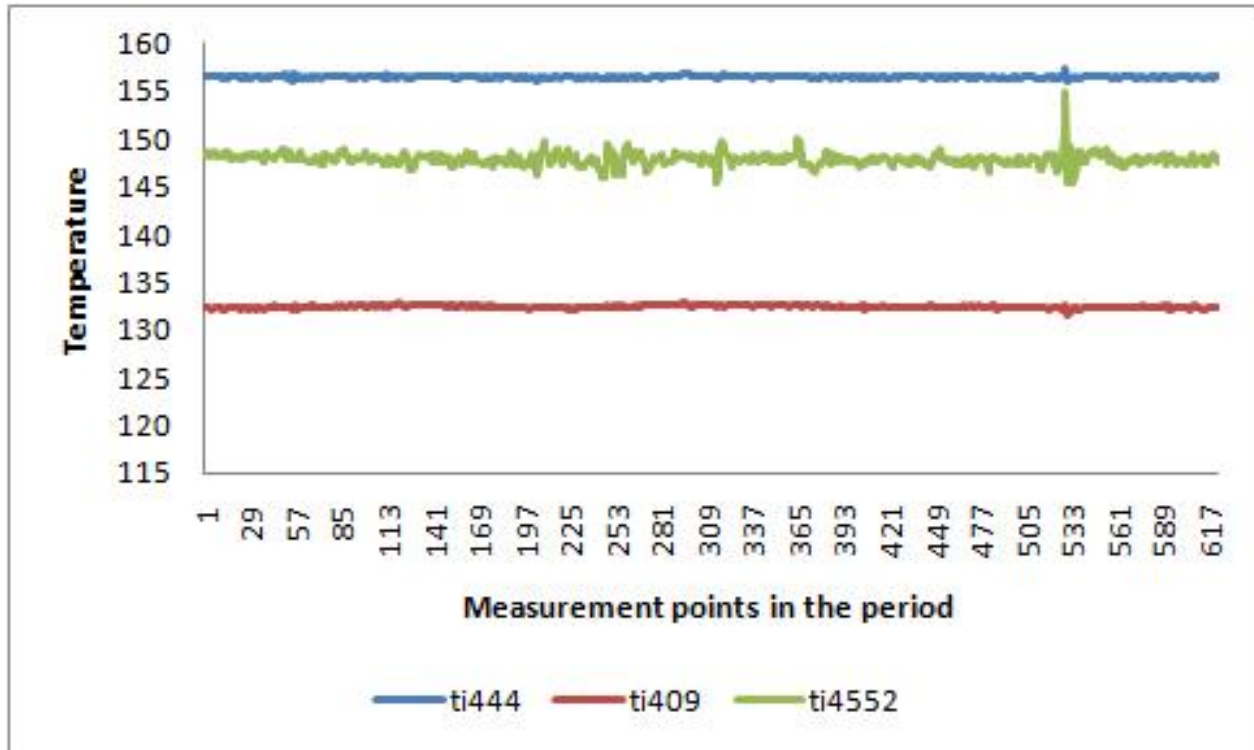
Figure 36: The temperature on the outlet gas from H1401 (ti444), the EDC feed outlet from H1406 (ti409) and in V1406 (ti4552).
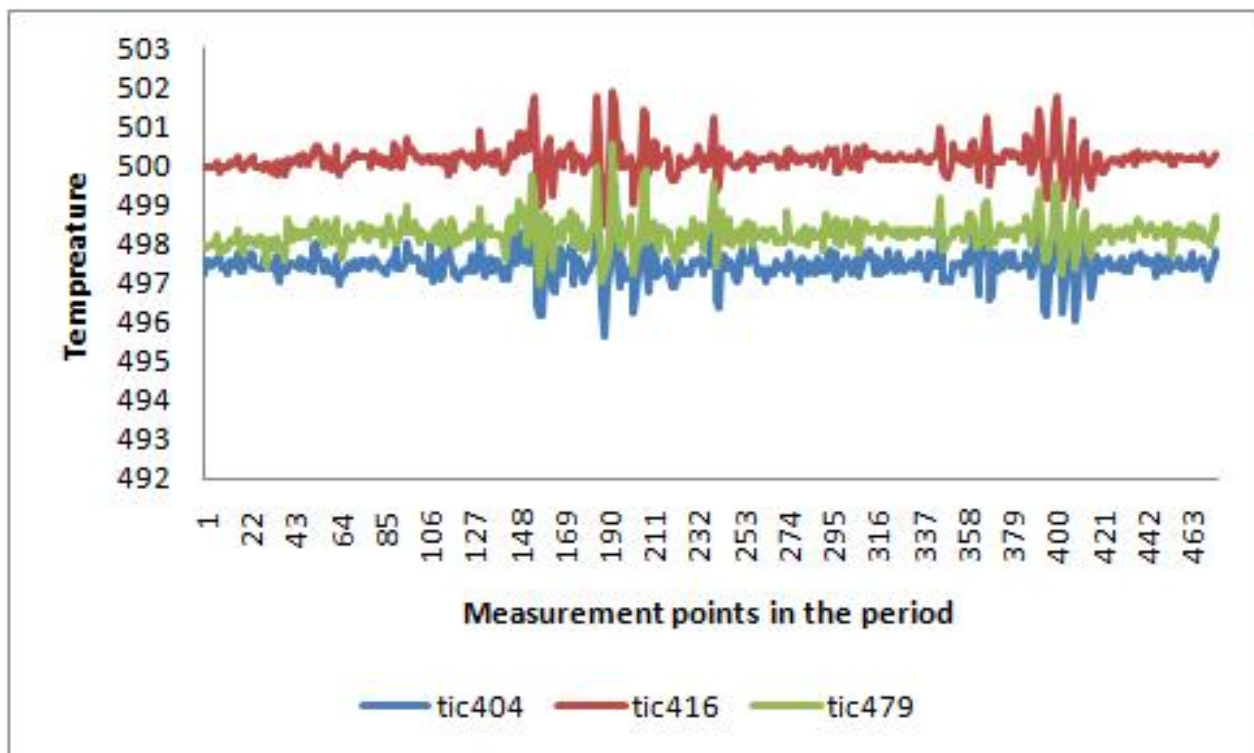

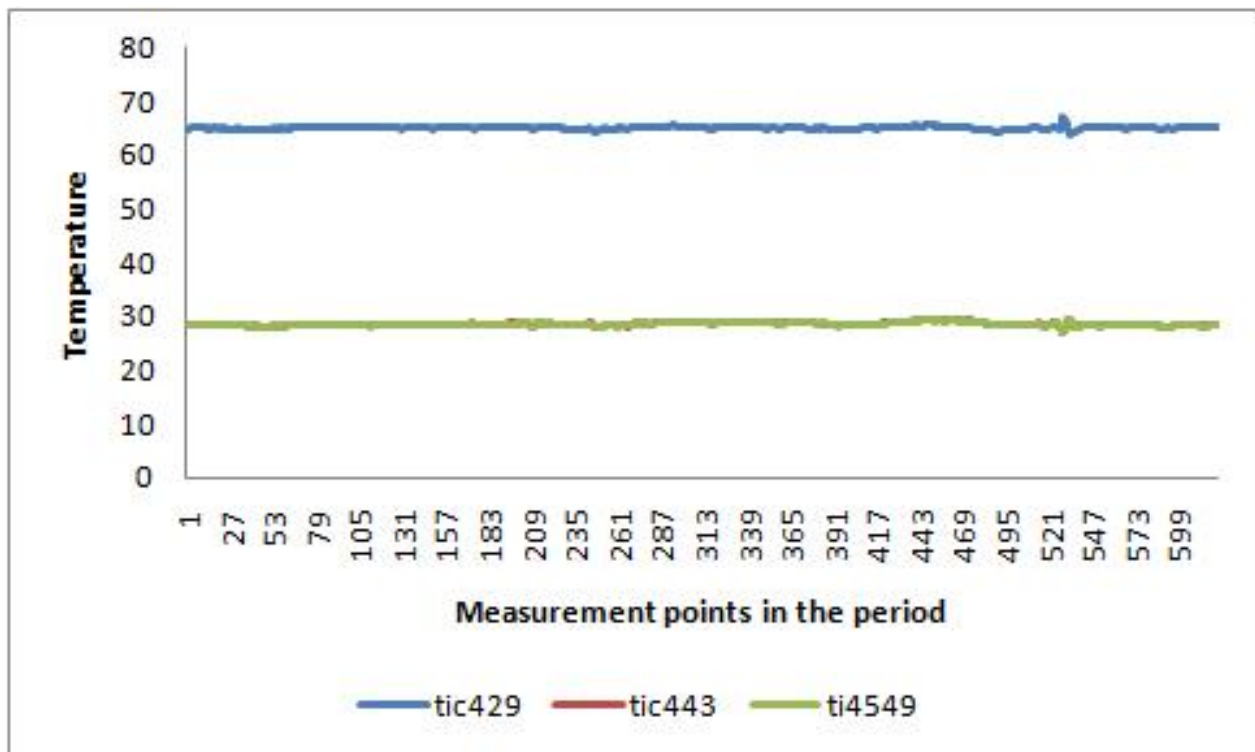Figure 37: The outlet temperature from the three crackers.

Figure 38: The temperature in V1401 (tic429), the outlet stream from H1405 (tic443) and the top strean from V1404 (ti4549).

NTNU			Utarbeidet av	Nummer	Dato
			HMS-avd.	HMSRV2601	05.03.2010
			Godkjent av		Erstatter
HMS			Rektor	Side 1 av 2	01.12.2006

Kartlegging av risikofylt aktivitet

Enhet: IKP **Dato:** 05.06.2011

Deltakere ved kartleggingen (m/ funksjon):
Stine Karlsen (Utførende)

Kort beskrivelse av hovedaktivitet/hovedprosess:
Datasimulering kun på lesesal

ID nr.	Aktivitet/prosess	Ansvarlig	Lov, forskrift o.l.	Eksisterende dokumentasjon	Eksisterende sikringstiltak	Kommentar
1	Datasimulering	-	-	NTNU HMS håndbok	-	Ingen risiko

NTNU	Kartlegging av risikofylt aktivitet	Utarbeidet av	Nummer	Dato
HMS		HMS-avd.	HMSRV2601	05.03.2010
		Godkjent av	Side	Erstatter
		Rektor	2 av 2	01.12.2006

Hva

Aktivitet/prosess

Kartlegging av aktiviteter/prosesser som inngår i risikovurderingen og som kan inneha risiko for skade på menneske eller miljø. Dette kan f.eks. være maskiner, labaktivitet, verkstedarbeid, bruk av visse kjemikalier osv. Bryt ned hele aktiviteten/prosessen i enkeltdeler, beskriv kort hver del.

Aktivitetene velges enten som gjennomgang av en prosess (aktivitet fra f.eks. innkjøp av materiale, via bearbeiding til ferdig produkt), eller alle aktiviteter som oppleves mulig risikofylte i et gitt område. Deltagerne må bli enige om omfanget av aktivitetene som skal risikovurderes,

Man må ta stilling til

- "Risiko for hvem" - for ansatte, for nabomiljø, for enkeltindivider eller en gruppe, for bedriften, for samfunnet
- "Risiko fra hva" - hvilket anlegg, hvilken aktivitet, fra hvilke ulykkeskategorier
- "For hvilket tidsrom"- risikonivået kan variere over tid

Risiko er et potensielt tap, ikke et oppstått tap. Aktiviteter/prosesser som i utgangspunktet blir vurdert som lite risikofylte, kan medføre økt risiko under gitte forhold.

Ansvarlig

Hvem er ansvarlig for de enkelte aktiviteter/prosesser? Er det noen andre enheter som har ansvar eller oppgaver for å redusere risiko? Organisasjonskart kan brukes for å avklare ansvarsforhold

Lov, forskrift o.l.

Hvilke lover, forskrifter og andre myndighetskrav gjelder for aktiviteten/prosessen? Se HMS-håndboka, HMSRV-20/01, www.lovdata.no, www.arbeidstilsynet.no, www.hmsetatene.no, kommunale bestemmelser (www.trondheim.kommune.no)

Eksisterende dokumentasjon

Enheten skal finne fram eksisterende sentrale og lokale retningslinjer, tegningsunderlag, sertifikater, kranførerbevis, truckførerbevis, gjennomført opplæring, serviceavtaler, bruksanvisninger, sjekklister osv. Se også tidligere risikovurderinger og HMS-runder, lokalt HMS-hefte, labhåndbok, NTNUs stoffkartotek osv.

Sikringstiltak

Hva finnes av eksisterende sikringstiltak for området/utstyret? Feks. ventilasjon, personlig verneutstyr, nødstopp, merking/ilting, skillevegger osv.

NTNU		
HMS/KS		

	utarbeidet av	Nummer	Dato
	HMS-avd.	HMSRV2603	4.3.2010
	godkjent av	side	Erstatter
	Rektor	1 av 2	9.2.2010

Risikovurdering

Enhet: IKP
Linjeleder: Professor Magne Hillestad
Deltakere ved risikovurderingen (m/ funksjon): Stine Karlsen

Dato: 05.06.2011

ID nr	Aktivitet fra kartleggings-skjemaet	Mulig uønsket hendelse/ belastning	Vurdering av sannsyn-lighet (1-5)	Vurdering av konsekvens: Menneske (A-E)	Ytre miljø (A-E)	Øk/ materiell (A-E)	Om-dømme (A-E)	Risiko-verdi	Kommentarer/status Forslag til tiltak
1	Datasimulering	Ingen	-	-	-	-	-	-	Ingen risiko knyttet til oppgaven

Sannsynlighet
1. Svært liten
2. Liten
3. Middels
4. Stor
5. Svært stor

Konsekvens
A. Svært liten
B. Liten
C. Moderat
D. Alvorlig
E. Svært alvorlig

Risikoverdi (beregnes hver for seg):
Menneske = Sannsynlighet x Konsekvens Menneske
Ytre miljø = Sannsynlighet x Konsekvens Ytre miljø
Økonomi/materiell = Sannsynlighet x Konsekvens Øk/materiell
Omdømme = Sannsynlighet x Konsekvens Omdømme

NTNU		utarbeidet av	Nummer	Dato
	Risikovurdering	HMS-avd.	HMSRV2603	4.3.2010
		godkjent av	side	Erstatter
HMS/KS		Rektor	2 av 2	9.2.2010

Sannsynlighet vurderes etter følgende kriterier:

Svært liten 1	Liten 2	Middels 3	Stor 4	Svært stor 5
1 gang pr 50 år eller sjeldnere	1 gang pr 10 år eller sjeldnere	1 gang pr år eller sjeldnere	1 gang pr måned eller oftere	Skjer ukentlig

Konsekvens vurderes etter følgende kriterier:

Gradering	Menneske	Ytre miljø Vann, jord og luft	Øk/materiell	Omdømme
E Svært Alvorlig	Død	Svært langvarig og ikke reversibel skade	Drifts- eller aktivitetsstans >1 år.	Troverdighet og respekt betydelig og varig svekket
D Alvorlig	Alvorlig personskade. Mulig uførhet.	Langvarig skade. Lang restitusjonstid	Driftsstans > ½ år Aktivitetsstans i opp til 1 år	Troverdighet og respekt betydelig svekket
C Moderat	Alvorlig personskade.	Mindre skade og lang restitusjonstid	Drifts- eller aktivitetsstans < 1 mnd	Troverdighet og respekt svekket
B Liten	Skade som krever medisinsk behandling	Mindre skade og kort restitusjonstid	Drifts- eller aktivitetsstans < 1 uke	Negativ påvirkning på troverdighet og respekt
A Svært liten	Skade som krever førstehjelp	Ubetydelig skade og kort restitusjonstid	Drifts- eller aktivitetsstans < 1 dag	Liten påvirkning på troverdighet og respekt

Risikoverdi = Sannsynlighet x Konsekvens

Beregn risikoverdi for Menneske. Enheten vurderer selv om de i tillegg vil beregne risikoverdi for Ytre miljø, Økonomi/materiell og Omdømme. I så fall beregnes disse hver for seg.

Til kolonnen "Kommentarer/status, forslag til forebyggende og korrigerende tiltak":

Tiltak kan påvirke både sannsynlighet og konsekvens. Prioriter tiltak som kan forhindre at hendelsen inntreffer, dvs. sannsynlighetsreduserende tiltak foran skjerpet beredskap, dvs. konsekvensreduserende tiltak.

NTNU		utarbeidet av	Nr.	dato
		HMS-avd.	HMSRV12/24	04.03.2010
		Godkjent av	Erstatter	
HMS		Rektor	side	01.12.2006
			1 av 1	

Handlingsplan for HMS

Enhet: IKP

Handlingsplan

ID.nr	Beskrivelse av tiltaket	Ansvarlig	Innen dato	Gjennomført/ Kontrollert, dato
1	Ingen tiltak nødvendig	-	-	-

Dato: 6/6 - 2011   Linjeleder: _Magne Hillestad_